DOES CARDIOPROTECTION BY AUTOPHAGY GO BEYOND ACUTE DOXORUBICIN CARDIOTOXICITY?

by

Itumeleng Chabaesele

Thesis presented for the Degree of

Master of Science

(Physiological Sciences)

At Stellenbosch University

Supervisor: Dr Balindiwe Sishi

Faculty of Science

Department of Physiological Sciences

March 2016

DECLARATION

By submitting this thesis electronically, I declare that the entirety of the work contained therein is my own, original work, that I am the sole author thereof (save to the extent explicitly otherwise stated), that reproduction and publication thereof by Stellenbosch University will not infringe any third party rights and that I have not previously in its entirety or in part submitted it for obtaining any qualification.

March 2016

SUMMARY

Introduction and Aim

The discovery of Doxorubicin (DOX) in the 1960s has drastically improved the survival rates of cancer patients; however, its success is limited by dose-dependent cardiotoxicity. While much of the literature has focused on acute cardiotoxicity which is generally reversible, chronic cardiotoxicity is irreversible and poses a serious threat since it can lead to congestive heart failure. The mechanisms that contribute to cardiotoxicity are still a matter of controversy; however, oxidative stress-induced myocardial damage and apoptosis are thought to be the major role players. One of the best understood and most widely studied processes is autophagy, an evolutionary conserved pathway of intracellular degradation. Although it has been attributed to various cardiac disorders, an increasing body of evidence corroborates the notion that autophagy may serve as a probable therapeutic target by providing cardioprotection in different contexts.

Materials

Autophagy was induced in H9c2 cardiomyoblasts by rapamycin treatment, starvation and siRNA (mTOR). This process was also inhibited by bafilomycin A1 treatment. Chronic DOX cytotoxicity was induced by treating cells daily with 0.2 µM DOX for 120 hrs. In an effort to determine whether autophagy upregulation or downregulation was beneficial, cell viability, apoptosis, oxidative stress and mitochondrial membrane function were assessed by utilizing various assays, western blotting, fluorescence microscopy as well as flow cytometry.

Results and Conclusion

Autophagy stimulation via siRNA (mTOR) and autophagy inhibition with bafilomycin did not decrease the detrimental effects associated with long-term DOX cytotoxicity. These effects were instead aggravated and became progressively worse. However, autophagy upregulation through rapamycin or starvation proved beneficial in this context as the amount of DOX that normally accumulates in the cells was reduced, and mitochondrial function and damage substantially improved. These observations also lead to improved cell survival. Therefore, based on the above results, autophagy induction in this context may be used as a plausible adjuvant treatment strategy for the mitigation of DOX-induced cardiac damage.

OPSOMMING

Inleiding en Doelwit

Die ontdekking van Doksorubisien (DOX) in die 1960s het oorlewingstempo van kankerpasiënte drasties verbeter; alhoewel die sukses hieraan beperk is tot ‘n dosis afhanklike kardiotoksisiteit. Menige literatuur fokus op akute kardiotiksisiteit wat oor die algemeen omkeerbaar is, terwyl chroniese kardiotiksisiteit onomkeerbaar is wat ‘n groot risiko inhou en kan tot die ontstaan van kongestiewe hartversaking lei. Die bydraende kardiotoksisiteitmeganismes is steeds kontroversiëel, maar oksidatiewe stres-geïnduseerde miokardiale skade en apoptose word as moontlike hoofrolspelers ondersoek. Een van die mees begrypte, en bestudeerde proses is outofagie, ‘n evolusionêr gekonserveerde intra-sellulêre degradasie padweg. Alhoewel dit bydraend is tot verskeie kardiale afwykings het ‘n toenemende hoeveelheid bewyse aangetoon dat outofagie moontlik as ‘n terapeutiese teiken in kardiale beskerming in verskeie kontekse kan dien.

Materiale

Outofagie is in H9c2 kardiomioblaste deur rapamisienbehandeling, nutrientweerhouding, en siRNA (mTOR) geïnduseer. Hierdie proses is ook geinhibeer deur bafilomisien A1 behandeling. Chroniese DOX sitotoksisiteit is verkry deur die selle daagliks met 0.2 µM DOX vir 120 uur te behandel. In ‘n poging om vas te stel of outofagie opregulering of afregulering voordelig was, is selvatbaarheid, apoptose, oksidatiewe stres en mitochondriale membraanfunksionering deur verskeie toetse, “western blotting”, fluoresensie mikroskopie sowel as vloeisitometrie ondersoek.

Resultate en Gevolgtrekking

Outofagie stimulasie *via* siRNA (mTOR) en outofagie inhibering met bafilomisien het nie die skadelike effekte wat met langtermyn DOX sitotoksisiteit gepaard gaan verlaag nie. Inteendeel het hierdie effekte toenemend vererger. Outofagie opregulering deur rapamisien of nutrientweerhouding was voordelig in hierdie konteks, omrede die hoeveelheide DOX wat normaalweg in die selle ophoop, verlaag was en die mitochondriale funksionering en skade betekenisvol verbeter het. Hierdie waarnemings het tot verbeterde seloorlewing aanleiding gegee. Die resultate van hierdie studie toon dat outofagie induksie in hierdie konteks moontlik

gebruik kan word as ‘n moontlike adjuvante behandelingstrategie vir die verligting van DOX-geïnduseerde kardiale beskadiging.

CONFERENCE PROCEEDINGS

I. Chabaesele and B. Sishi. Autophagy conundrum in cardiotoxicity. 43rd meeting of the Physiology Society of Southern Africa (PSSA). 6th -9th September 2015. University of Johannesburg and the University of the Witwatersrand, South Africa. Winner of the Wyndham best oral presentation award

“Tshimologo ya botlhale ke tshabo modimo”

“The beginning of wisdom is the fear of GOD”

Words of wisdom by my late grandmother

ACKNOWLEDGEMENTS

I firstly would like to acknowledge **GOD** for his ever growing presence, love and mercy in my life.

To my supervisor **Dr Balindiwe Sishi**, thank you for the guidance and support throughout this study for without you none of this would have been possible. Also, thank you for the conference experience, it will remain one the highlights of my MSc degree.

To **Rozanne Adams** and the entire CAF team, thanks for the help with flow cytometry analysis and fluorescent microscopy images. The results have truly added a value to my work.

I would also like to thank **Dr Theo Nell** on they excellent work done in translating my abstract to Afrikaans.

To **Andre Du Toit** and **Charlene Kimar**, words can't describe how thankful I am for your friendship, support and late night conversions about everything. You guys are the best. TEAM WORK.

My research group, **DSG** and the **Physiological Sciences Department** as whole. I am thankful for the constructive criticism, lab assistance and skills I have learned from you all.

I also would like to acknowledge the **NRF** for funding this study.

To my **Mama le Papa**, your daily sacrifices remain my greatest motivation. For without your love and support I don't think any of this would have been possible.

Lastly, but most importantly, to my best friend, partner and voice of reason for the past 3 years. **Oarabile Karabo Naledi Motumi**, thank you for listening to my "whining" because only you truly know how long this journey has been. I am forever thankful.

ABBREVIATIONS

3-MA	3-Methyladenine
AMPK	AMP-activated protein kinase
ATG	Autophagy related proteins
ATM	Ataxia telangiectasia mutated
ATP	Adenosine dinucleotide
BAX	Bcl-$_2$ associated protein
Bcl-x_L	B-cell lymphoma extra-large
Ca^{2+}	Calcium ions
CHF	Congestive heart failure
CO_2	Carbon dioxide
cTnT	Cardiac troponin T
CVDs	Cardiovascular diseases
DEX	Dexrazoxane
DNA	Deoxyribonucleic acid
DOX	Doxorubicin
FADD	Fas-Associated protein with Death Domain
Fe^{2+}	Ferrous iron
Fe^{3+}	Ferric iron
FOXO3	Foxhead box O3
GATA-4	GATA binding protein 4
GFP	Green fluorescent protein
IRP-1	Iron regulatory protein-1
LC3	Microtubule associated protein light chain 3
LVEF	Left ventricular ejection fraction
MDA	Malonyl dialdehyde
MHC	Myosin heavy chain
MLC	Myosin light chain
MPT	Mitochondrial permeability transition

mRNA	Messenger ribonucleic acid
mTOR	Mammalian target of rapamycin
NADH	Nicotinamide adenine dinucleotide
O_2	Oxygen
O_2^-	Superoxide
PARP	Poly-ADP ribose polymerase
PGC-1α	Peroxisome proliferator-activated receptor gamma co-activator 1 alpha
PUMA	p53 upregulated modulator of apoptosis
RA	Retinoic acid
ROS	Reactive oxygen species
SERCA	Sarco/endoplasmic reticulum calcium ATPase
siRNA	Silencing ribonucleic acid
SOD	Superoxide dismutase
TNFR	Tumour necrosis factor receptor
ULK1	Uncoordinated (unc-51) like kinase 1
XOD	Xanthine oxidase

UNITS

g	gram
mg	milligram
mM	millimolar
µM	micromolar
nM	nanomolar
M	molar
L	litre
mL	millilitre
µL	microlitre
° C	degrees Celsius
%	percentage
mol	moles

TABLES

FIGURES

CONTENTS

1 CHAPTER 1: LITERATURE REVIEW

1.1 INTRODUCTION

Cardiovascular diseases (CVDs) are a global problem affecting over 26 million individuals globally. CVDs account for 17.5 million deaths worldwide, representing 31% of the total global deaths observed in 2012. What is more alarming is that CVDs are expected to account for 23.6 million deaths worldwide by 2030 (Ambrosy *et al.*, 2014; Mozaffarian *et al*., 2015). This highlights the need for new and improved treatment regimens to better manage CVDs in an effort to reduce the large number of deaths (Mozaffarian *et al.*, 2015). Doxorubicin (DOX) cardiotoxicity is a key CVD that has become a threat to chemotherapy patients (Lefrak *et al.*, 1973; Ky *et al.*, 2014). DOX is a tetracyclic anthracycline that was discovered in the 1960s (Fig. 1.1). Since its discovery, it remains one of the most widely used chemotherapeutic drugs because of its ability to treat a wide spectrum of soft and solid tumours (Tacar *et al.*, 2013). However, its effective use is limited by its cumulative, dose-dependent cardiotoxic effects which lead to congestive heart failure (CHF) (Swain *et al.*, 2003). DOX cardiotoxicity is broadly classified as acute or chronic; where on the one hand the symptoms of acute DOX cardiotoxicity are generally temporary, clinically treatable and reversible (Octavia *et al.*, 2012). Chronic cardiotoxicity is on the other hand is untreatable primarily because it presents itself as irreversible cardiomyopathy which causes CHF (Lefrak *et al.*, 1973). CHF due to DOX cardiotoxicity has a poor prognosis, with a 50% mortality rate within the year of diagnosis (Van Hoff *et al.*, 1979; Chatterjee *et al.*, 2010). As there are currently no statistics available specifically for DOX-induced CHF, this type of cardiomyopathy also contributes to the economic and health burden of CVDs (Ambrosy *et al.*, 2014).

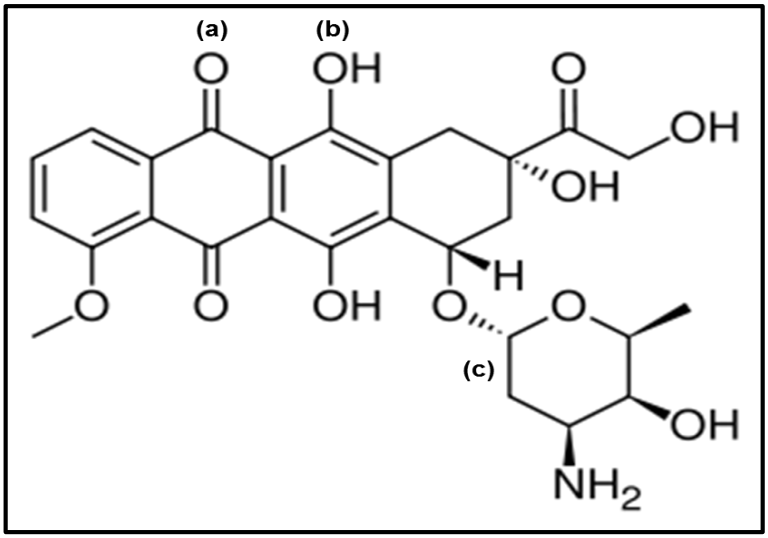

Figure 1.1: The tetracyclic structure of doxorubicin. DOX contains four tetracyclic ring, quinone (a), hydroquinone (b) and a sugar moiety (c) group. Adapted from Yacoub *et al.*, 2011.

1.2 CLASSIFICATION OF DOXORUBICIN CARDIOTOXICITY

1.2.1 Acute DOX cardiotoxicity

Acute DOX cardiotoxicity is a form of cardiotoxicity that occurs very early during chemotherapy treatment. It can occur within minutes, hours or even a few days following DOX administration (Hydock *et al.*, 2009). Although the literature utilizes the term early onset cardiotoxicity and acute DOX cardiotoxicity interchangeably, this current study will utilize the latter. Clinically, acute DOX cardiotoxicity presents itself as either pericarditis (inflammation of the pericardium) or myopericarditis (inflammation of pericardium and myocardium) syndrome (Bristow *et al.*, 1978). Furthermore, electrocardiograph examinations in patients with acute DOX cardiotoxicity show abnormal changes including prolonged QT intervals, T wave flattening, decreased QRS voltage and non-specific changes in ST and T waves (Lipshultz *et al.*, 2008). Arrhythmias, particularly tachycardia, atrial flutter and fibrillation have also been observed previously. As these symptoms are rare and clinically manageable, the overall incidence of acute DOX cardiotoxicity occurs within 0.7% of patients treated with DOX (Frishman *et al.*, 1997). In cases where these symptoms are recurrent DOX treatment is either decreased or terminated to avoid excessive cardiac damage or development of chronic DOX cardiotoxicity later in life (Hyodock *et al.*, 2009).

1.2.2 Chronic DOX cardiotoxicity

Chronic DOX cardiotoxicity is dose-dependent and occurs one or more years after the patient's last treatment dose (Alexieva *et al.*, 2014). This form of cardiotoxicity is most prevalent in individuals that have received DOX treatment in their early childhood years and in individuals who have survived cancer in their adult lives (Boucek, 1998; Greiner *et al.*, 1998; Goorin *et al*., 1999). The development of chronic DOX cardiotoxicity within a year is referred to as early-onset chronic cardiotoxicity, whereas its occurrence after a year is referred to as late-onset chronic DOX cardiotoxicity (Prezioso *et al.*, 2010). Clinically, early-onset chronic cardiotoxicity is characterised by the progressive diminishing contractility of the left ventricle (Harake *et al.*, 2012). This decrease in left ventricular contractility is caused by a reduction in the wall thickness of the left ventricle as a result of cardiomyocyte damage (Lipshultz *et al.*, 2006). This condition is nonetheless rare with a prevalence of 1.6 to 2.1 % in patients treated with DOX during their childhood years (Harake *et al.*, 2012). Late-onset chronic cardiotoxicity is characterised by an asymptomatic period which is followed by the development of heart failure (Pfeffer *et al.*, 2009). The asymptomatic period represents a phase of progressive cardiomyocyte death, that later leads to CHF as the remainder of functional cardiomyocytes cannot sustain normal heart function (Harake *et al.*, 2012). Although there is a clear distinction between early and late-onset chronic cardiotoxicity, both of these conditions will be referred to as chronic DOX cardiotoxicity from here onwards.

Chronic DOX cardiotoxicity remains clinically untreatable because of its cumulative dose-dependent nature. This characteristic has previously been shown to be directly proportional to the incidence of developing CHF (Goorin *et al*., 1999). Lefrak *et al* (1973) indicated that the incidence of developing CHF increased with each subsequent dose administered. For example in patients treated with cumulative doses of 500-550, 551-600 and 660 mg/m^2 of DOX, the incidence of developing CHF was determined to be 4, 18 and 36% respectively. It is for this reason that the lifetime cumulative dose of DOX is limited to 550mg/m^2 of body surface area in an effort to minimise the risk of developing cardiovascular complications. Unfortunately even with this adjustment of the cumulative dose, patients still develop DOX cardiotoxicity and later succumb to CHF (Gharib *et al.*, 2002). It should be noted, however, that other factors including age, underlying heart disease, hypotension and gender can influence the development of DOX cardiotoxicity (Grenier *et al.*, 1998; Lipshultz *et al.*, 1995). When considering age, pre-puberty children are at higher risk of developing CHF because DOX inhibits proper myocardial growth in these individuals (Greiner *et al.*, 1998). Young girls have also been

shown to have a four-fold risk of developing chronic DOX cardiotoxicity compared to males of the same age who receive the same cumulative dose. The latter is potentially influenced by factors such as differences in body composition and differential expression of multidrug-resistance genes (Lipshultz *et al.*, 1995). Older individuals (age > 65) have a greater incidence of CHF when compared to younger individuals (age < 65), potentially due to the decrease in anti-oxidant capacity with increasing age (Giergiel & Kankofer *et al.*, 2015). The damage induced by DOX toxicity can be observed from myocardial biopsies of these patients (Bristow *et al.*, 1978). Normal cardiomyocytes have a long, cylindrical and striated muscle fibre appearance (Fig. 1.2a), but in affected patients the myocardium becomes vacuolated, the sarcoplasmic reticulum is distended and a high level of interstitial fibrosis is present due to extensive myocardial loss (Fig. 1.2b) (Young *et al.*, 2006). What is alarming about these manifestations is that these changes were observed a year following the patients last DOX treatment, thus highlighting the very detrimental nature of DOX toxicity (Bristow *et al.*, 1978). Therefore if we are to successfully treat, prevent or delay this condition, it is vital that we fully understand the underlying mechanisms responsible for these unfavourable alterations to cardiac function and structure.

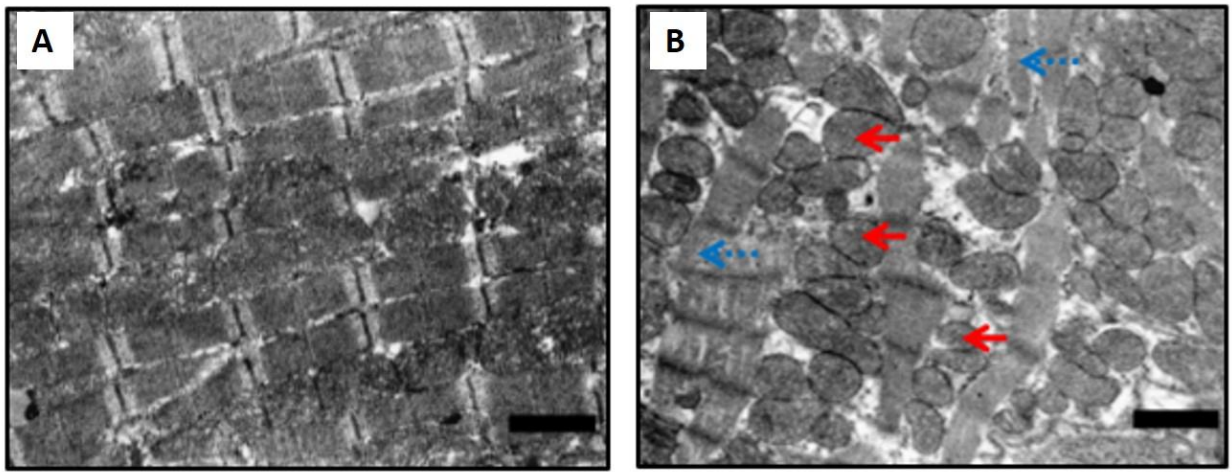

Figure 1.2: Endomyocardial biopsy and histological analysis of normal and DOX treated cardiomyocytes. Normal cardiomyocytes with their characteristic long, cylindrical and striated appearance (a). Endomyocardial biopsy and histological analysis of the heart tissue from DOX treated subjects. Changes in cell morphology such as vacuolization of cardiomyocytes (red normal arrow) and appearance of interstitial fibrosis (blue broken arrow) can be observed (b). Adapted from Takumera, 2007.

1.3 THE OXIDATIVE STRESS HYPOTHESIS AND ITS INVOLVEMENT IN DOX CARDIOTOXICITY

The most widely accepted mechanism by which DOX induces its damaging effects is oxidative stress of which there are two main mechanisms (Li *et al*., 20015; Šimùnek *et al*., 2009). Firstly, mitochondria are susceptible to DOX-induced oxidative stress because of DOX's high affinity for cardiolipin, a phospholipid that is enriched in the inner mitochondrial membrane and plays a crucial role in mitochondrial structural organization (Goormaghtigh *et al*., 1991; Ren *et al*., 2014). Reactive oxygen species (ROS) production in the mitochondria is initiated by the interaction of the DOX quinone form with nicotinamide adenine dinucleotide (NADH) dehydrogenase (Fig. 1.3). NADH dehydrogenase forms part of complex I of the electron transport chain and is responsible for transportation of electrons to complex III. DOX disrupts this chain of events by diverting these electrons to itself. The diverted electrons are consequently used to convert the DOX quinone group into a semiquinone radical. This newly formed semiquinone radical convert molecular oxygen to superoxide (O_2^-) and subsequently gets reduced back to its quinone form which can further generate more ROS. This is termed redox cycling (Vergely *et al.*, 2006; Davies *et al.*, 1986). Other enzymes such as NAD phosphate (NADPH) and xanthine oxidase (XOD) also have the ability to convert DOX to a semiquinone form which will ultimately be converted to O_2^- (Cross *et al.*, 1991; Vergely *et al.*, 2006). In the presence of naturally occurring anti-oxidants such as superoxide dismutase (SOD), the O_2^- is converted to hydrogen peroxide (H_2O_2) which interacts with iron. This gives rise to hydroxyl ions and hydroxyl radical which further aggravate the already elevated oxidative stress (Vergely *et al.*, 2006; Torres *et al.*, 2012).

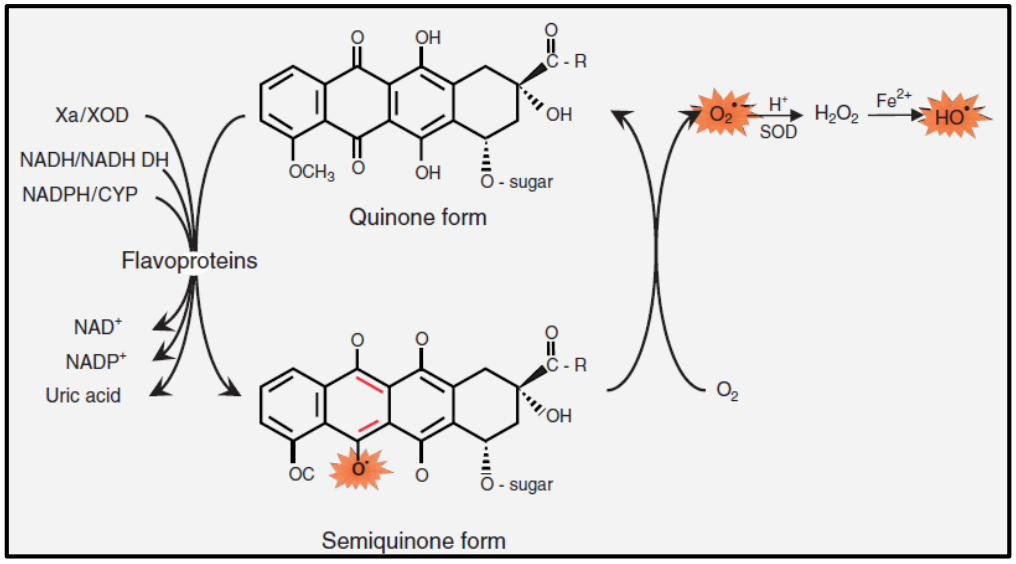

Figure 1.3: The DOX cycling process and the production of stress inducing radicals and ions. The DOX molecule gets converted to a semiquinone form by multiple enzymes. This form of DOX produces O_2^- and other stress inducing radicals such as H_2O_2, hydroxyl radicals and ions. Abbreviations: NADH: nicotinamide adenine dinucleotide, $NADP^+$/NADPH: nicotinamide adenine dinucleotide phosphate and XOD: xanthine oxidase. Adapted from Vergely *et al.*, 2006.

Secondly, DOX induces oxidative stress through the utilization of iron. Cytoplasmic DOX interacts with free circulating iron molecules in the cytoplasm to form DOX-ferric iron (Fe^{3+}) complexes (Torres *et al.*, 2012). This Fe^{3+} on the complex is further reduced to ferrous iron (Fe^{2+}) by NADPH cytochrome P450 reductase, glutathione and cysteine reductase. The Fe^{2+} component of the complex produces O_2^- through its interaction with free oxygen molecules (Halliwell & Gutteridge, 2007; Torres *et al.*, 2012). As mentioned previously, O_2^- can be dismutased to H_2O_2 or it can promotes the release of more Fe^{2+} from ferritin, an iron storing molecule (Minotti *et al.*, 1999; Xu *et al.*, 2008). The dismuated H_2O_2 forms hydroxyl radicals which are highly unstable, and are not recognised by anti-oxidants. These radicals form lipid oxides, conjugated dienes and malonyl dialdehyde (MDA), which are byproducts of lipid peroxidation (Halliwell & Gutteridge, 2007; Torres *et al.*, 2012; Ichikawa *et al.*, 2014).

Iron is regulated by two key molecules: ferritin and transferrin. Ferritin is a cytoplasmic protein that stores iron, whereas transferrin is a membrane bound receptor which binds and triggers iron uptake by cells (Wang *et al.*, 2011). The regulation of these key proteins is performed by a cytoplasmic enzyme known as the iron regulatory protein-1 (IRP-1). During times of low iron levels in the cytoplasm, IRP-1 binds to the transferrin messenger ribonucleic acid (mRNA)

to increase its transcription in an effort to upregulate iron uptake. Similarly, IRP-1 also binds to ferritin mRNA, however, when this binding occurs the expression of ferritin decreases, subsequently decreasing iron storage and elevating unbound cytoplasmic iron (Cairo *et al.*, 2000). Literature has indicated that DOX targets IRP-1 as a means to disrupt iron regulation and increase oxidative stress (Minotti *et al.*, 2001). The mechanism by which DOX achieves this is when cytoplasmic DOX is converted to DOXol by NADPH carbonyl reductase. DOXol binds the active site of IRP-1 and disrupts its iron regulatory functions. The loss in IRP-1 function leads to unregulated iron uptake by transferrin and unregulated iron release by ferritin (Forrest *et al.*, 1991; Minotti *et al.*, 1998). This disruption in iron homeostasis results in a build-up of high iron concentrations in the cytosol which are toxic to cardiomyocytes. Moreover, much of this iron is taken up by mitochondria which creates a vicious cycle of further ROS production (Ichikawa *et al.*, 2014). The high oxidative stress level in cardiomyocyte is among some of the key upstream triggers that lead to cell death (Zhang *et al.*, 2009). As cardiomyocytes are known to be susceptible to the damaging effects of ROS due to their inferior defence systems as well as their inability to regenerate, oxidative stress-induced death is a downstream contributor to the progression of cardiotoxicity and ultimately CHF (Yoshida *et al.*, 2009).

1.4 DOXORUBICIN-INDUCED CELL DEATH

1.4.1 Apoptosis

It is common knowledge that DOX enters cardiomyocytes through passive diffusion where it primarily localizes to the nucleus in addition to mitochondria (Kiyomiya *et al.*, 2001; Goormaghtigh *et al.*, 1991). On the one hand, DOX is proposed to intercalate nuclear deoxyribonucleic acid (DNA) to induce cell death in a similar manner to which it kills cancerous cells (Minotti *et al.*, 2004). On the other hand, DOX inhibits the expression of anti-oxidant genes as a mechanism to elevate overall oxidative stress and thus trigger apoptosis (Li *et al.*, 2002). The damaged DNA in addition to elevated oxidative stress levels stimulates the activation of ataxia telangiectasia mutated (ATM) kinase (Yoshida *et al.*, 2009). ATM kinase phosphorylates nuclear p53 and leads to transcription of p53 upregulated modulator of apoptosis (PUMA). PUMA promotes the dissociation of cytosolic p53 from b-cell lymphoma 2-extra-large (Bcl-X_L) and consequently activates it (Follis *et al.*, 2013). Cytosolic p53 acts as a transcriptional activator of Bcl-2 associated X protein (BAX), a pro-apoptotic protein that

translocates from the cytosol to the mitochondrial membrane and induces opening of the mitochondrial permeability transition (MPT) pore where cytochrome C leaks (Deniaud *et al.*, 2008). The released cytochrome C reacts with other mitochondrial proteins such as apoptosis activating factor-1 and apoptosis inducing factor (AIF) to form the apoptosome (Zou *et al.*, 1997). This complex induces caspase activation, a characteristic hallmark of apoptosis induction (Green *et al.*, 1998). Caspases are also known to cleave essential cardiac myofibrils such as troponin, alpha actin, actinin and myosin light chain. This cleavage of key structural proteins may account for the abnormal structural damage often observed in histological samples of cardiomyocytes treated with DOX (Coummonal *et al.*, 2002).

The dysregulation of calcium ion (Ca^{2+}) handling is another mechanism that has been suggested to induce intrinsic apoptotic cell death in cardiomyocytes (Zhang *et al.*, 2009). The sarco/endoplasmic reticulum (Ca^{2+})-ATPase (SERCA), Na^{+}/Ca^{2+} pumps and activator of calcium (Rossini *et al*., 1986) are important proteins that are responsible for transporting Ca^{2+} into the sarcoplasmic reticulum and sarcolemma respectively. Normally, the activator of calcium is intricately involved in the electrical excitation within the sarcoplasmic reticulum (Rossini *et al*., 1986) and its function is consequently controlled by the activity of both SERCA and the Na^{+}/Ca^{2+} pumps (Carafoli, 1985; De Beer *et al*., 2001). During DOX treatment however, these pumps become dysfunctional resulting in the accumulation of Ca^{2+} in the cytosol (Arai *et al.*, 2000). Moreover, the activator of calcium cannot perform its function of initiating the interaction between actin and myosin, which influences the force of contraction (Rossini *et al*., 1986). Therefore, this excessive Ca^{2+} accumulation hinders the cardiac contraction and relaxation processes, and thereby disturbs pulmonary circulation which limits nutrient supply to the heart and thus promotes apoptosis (Bennet, 2002). This disruption of Ca^{2+} homeostasis also activates Ca^{2+}-sensitive calpains which active caspases, further increasing signals that promote intrinsic induction of apoptosis and the cleavage of structural proteins (Jang *et al.*, 2004).

The extrinsic apoptotic pathway is a less commonly observed mechanism of cardiomyocyte death in the context of DOX-induced cardiotoxicity. This pathway can be activated mainly through cell surface receptors, namely the FAS receptor (FASR) and the tumour necrosis factor receptor (TNFR) which have a death domain attached to them (Ryu *et al*. 2000). Activation of these receptors leads to downstream activation of caspase-8 and -3 and ultimately apoptosis (Chinnaiyan et al 1996; Zhang *et al.*, 2009). In an acute *in vivo* model of DOX cardiotoxicity, Nakamura *et al* (2000) indicated an overexpression of the FASR without any significant change

in p53 expression. This observation implied that the extrinsic pathway of apoptosis was responsible for the cell death observed. Furthermore, injection of an anti-FAS ligand into these DOX treated animals appeared to improve functional parameters of the myocardium and the reduction of apoptosis. Animals with a double knockout of TNFR1 and TNFR2 showed a higher susceptibility to DOX-induced apoptosis when compared to their respective wild type (Lien *et al.*, 2006), however, it remains unclear which receptor offers protection against DOX-induced apoptosis or if both are necessary to achieve the latter (Xu *et al.*, 2008).

1.4.2 Necrosis

Necrotic cell death represents another mechanism by which cells can die. Although this mechanism is very common, very little is known about the molecular controls of this process particularly in the context of DOX cardiotoxicity (Zhang *et al.*, 2009). This form of cell death is typically characterized by mitochondrial swelling, lysis of the plasma membrane and unorganised DNA fragmentation (Edinger *et al.*, 2004). Physical insult such as membrane leakage (Wallace, 2007) and adenosine triphosphate (ATP) depletion (Zhou *et al.*, 2001) appear to be the main triggers of necrosis. The key cause of ATP depletion during DOX treatment could possibly be mitochondrial damage as a result of DOX binding, ROS production or Ca^{2+} dysregulation (Lebrecht *et al.*, 2007; Nakayama *et al.*, 2007). Interestingly, poly-ADP ribose polymerase (PARP), a repair enzyme that makes use of nicotinamide adenosine dinucleotide (NAD^+) during the DNA repair process, plays a crucial role during ATP production (Edinger *et al.*, 2004). Therefore, in the context of DOX cardiotoxicity the constant utilization of NAD^+ by PARP as a result of ROS-induced DNA and mitochondrial damage, lowers ATP production and as consequence, necrosis is induced (Wallace, 2007; Zhou *et al.*, 2001). Another potential cause for necrosis induction is the degradation of titin, a protein in striated muscle that acts as a template for sarcomere assembly, but also provides elasticity during cardiac diastole (Lim *et al.*, 2004; Castro-Ferreira *et al.*, 2011). The degradation of titin by Ca^{2+}-sensitive calpians is suggested to be one of the early steps in necrosis induction during DOX cardiotoxicity, nevertheless the exact mechanism as to how this occurs remains relatively unknown. It is, however, clear that the inhibition of titin degradation significantly decreases cardiomyocyte necrosis (Lim *et al.*, 2004). Based on the above, this data suggest that the inhibition of titin and restoration of ATP production could be a potential therapeutic or cardioprotective mechanisms against cardiomyocyte necrosis.

1.5 POTENTIAL CARDIOPROTECTIVE INTERVENTIONS AGAINST DOX CARDIOTOXICITY

1.5.1 Anti-oxidants treatment as a means to attenuate the detrimental effects of DOX cardiotoxicity

Anti-oxidants are among the most widely investigated compounds in terms of disease treatment because a large majority of diseases have an oxidative stress component (Steven *et al.*, 2008). Thus, it comes as no surprise that anti-oxidant therapy is a highly investigated niche area in the field of DOX cardiotoxicity, as this condition is primarily mediated by oxidative stress (Angsutararux *et al.*, 2015; Simunek *et al*., 2009). The fact that cardiomyocytes are susceptible to oxidative stress due to their low anti-oxidant capacity and high mitochondrial content further motivates the interest in anti-oxidant therapy as a mechanism of cardioprotection (Shi *et al.*, 2011; Berthiaume *et al*. 2005). Carvedilol (Coreg) is one such anti-oxidant that has been evaluated as a potential cardioprotective intervention against DOX cardiotoxicity. Clinically, patients who received DOX treatment in conjunction with carvedilol displayed improved left ventricular ejection fraction (LVEF) in comparison to patients who only received DOX treatment (Kalay *et al.*, 2006). In DOX treated animals, carvedilol decreased ROS levels and subsequently improved mitochondrial dysfunction. This is effect is achieved by partially inhibiting the electron transport chain by carvedilol, thus lowering the amount of ROS produced by DOX interaction with the mitochondrial complexes (Carreira *et al*., 2006). Similar beneficial effects have also been observed in an *in vitro* setting of acute DOX cytotoxicity (Oliveira *et al.*, 2004). Another anti-oxidant, Probucol (Lorelco) also demonstrated improved LVEF and overall reduced DOX cardiotoxicity *in vivo* (Singal *et al*., 1995). This lipid-lowering agent with known anti-oxidant properties and a reasonably high dissemination within the myocardium due to its binding capability to cardiolipin (Li *et al*., 2000), is thought to provide cardioprotection due to its inference with DOX binding to cardiolipin in the mitochondria.

A number of other commonly used anti-oxidants such as vitamins (C and E), enzymes (SOD) and phytochemical anti-oxidants (carotenoids) have also been shown to offer cardioprotection against DOX toxicity *in vivo* (Viswanatha Swamy *et al.*, 2011; Wahab *et al.*, 2000; Yen *et al.*, 1996; Indu *et al.*, 2014). Despite these promising results, many clinical studies utilizing various anti-oxidants have either failed or produced mixed results (Steven *et al.*, 2008). Although it is remains speculative as to why anti-oxidants are not as successful clinically, a number of hypothesis have been proposed. Firstly, it is suggested that anti-oxidants fail because oxidative stress is not the primary or only cause for disease progression. Secondly, the time (before,

during or after DOX treatment), duration (once off or continues) and possibly dose translation from animal models to humans may not be optimal. Lastly, there is also the possibility that not all patients benefit equally from the anti-oxidant therapy (Firuzi *et al.*, 2008; Steven *et al.*, 2008). Therefore, there is a need to review the administration of anti-oxidants and to look beyond only targeting oxidative stress as a means to prevent or treat DOX cardiotoxicity.

1.5.2 Iron chelators and their role in cardioprotection against DOX-induced cardiotoxicity

As mentioned earlier iron interaction with DOX produces O_2^-, H_2O_2, hydroxyl radicals and hydroxyl ions which all contribute to the condition of oxidative stress (Torres *et al.*, 2012). Iron chelators represent another area of research toward the prevention and treatment of DOX cardiotoxicity. (Speyer *et al.*, 1992). Iron chelators mediate cardioprotection by decreasing the amount of free iron available to form complexes with DOX. The decrease in DOX-iron complexes decreases overall oxidative stress levels in cardiomyocytes. (Frishman *et al.*, 1997). Clinically, iron chelators have had more success than anti-oxidants. The first randomised, controlled clinical study using Totect (dexrazoxane) as a cardioprotective agent was undertaken by Speyer and colleagues (1992). Breast cancer subjects who received dexrazoxane (DEX) pre-treatment prior to DOX administration showed mild or no cardiomyocyte damage when compared to patients who did not receive DEX treatment. A significant reduction in LVEF was observed and the incidence of CHF was reduced in these patients (Speyer *et al.*, 1992). Interestingly, other clinical studies that have since followed have also reported on the efficacy of DEX as a cardioprotective agent (Swain *et al.*, 1997a; Swain *et al*. 1997b). The efficiency of iron chelators such as DEX is attributed to their ability to be able to substantially decrease the accumulation of iron not only in the cytosol but also in the mitochondria. This particular attribute decreases overall mitochondrial dysfunction and thus limits DOX-induced cardiotoxicity (Ichikawa *et al.*, 2014). DEX, however, has adverse side effects which includes the development of neutropenia and thrombocytopenia, which are blood related conditions characterised by a decrease in the number of neutrophils and thrombocyte levels respectively (Langer *et al.*, 2014). In addition, DEX treated patients are also at risk of developing myelodysplastic syndrome, a serious condition characterised by an inadequate production of red blood cells. Furthermore, there is a risk of developing a secondary cancer such as acute myeloid leukaemia, which is characterised by the rapid growth of cancerous/abnormal white blood cells (Tebbi *et al.*, 2007). It is therefore recommend that the use of iron chelators be

administered with great caution considering the vast side effects associated with their use (Langer *et al.*, 2014; Tebbi *et al.*, 2007).

1.5.3 Doxorubicin nanoparticles as a possible mechanism to reduce DOX cardiotoxicity

A relatively recent undertaking in the field of DOX cardiotoxicity is the usage of DOX nanoparticles. Nanoparticles are sphere-like, microscopic structures that contain a core structure made of a variety of materials such as liposomes (Lotrionte *et al.*, 2012.), polysaccharides (Janes *et al.*, 2001) and proteins (Bae *et al.*, 2012) (Fig. 1.4). The drug is usually confined within the core of the nanoparticle in an aqueous or lipid form (Brigger *et al.*, 2002). Most nanoparticle also have targeting moieties such as anti-bodies, peptides, nuclei acids, vitamins or carbohydrates (Yu *et al.*, 2012; Petrelli *et al.*, 2010; Davis, 2009). The main attraction about nanoparticles in the context of cardiotoxicity and oncology is that they minimize DOX exposure to the cardiomyocytes while maximizing drug exposure to the cancer cells (Kanter *et al.*, 1993). The mechanism by which this is achieved is mainly based on the controlled release of DOX (Park *et al.*, 2009). During normal intravenous administration of DOX, the heart and liver are the main receipts of venous blood, therefore the majority of DOX ends up in the liver and heart before it even reaches its intended cancer site. However, unlike the liver, the heart is susceptible to oxidative damage and is therefore highly affected by DOX production of reactive species, hence the development of cardiotoxicity (Wanga *et al.*, 2004). When DOX nanoparticles are administered intravenously there is far less DOX that enters cardiac tissue because the drug is entrapped in nanosphere and the target moieties on the nanoparticle ensure that it is released at the cancer target site, therefore further minimizing cardiac tissue exposure to DOX (Yu *et al.*, 2012). Studies have also demonstrated that the concentration of DOX nanoparticles in circulation is much lower post administration when compared to normal intravenously administered DOX, further limiting cardiac exposure to the drug (Park *et al.*, 2009). Moreover, DOX nanoparticles attenuate the severity of DOX cardiotoxicity-related parameters such as LVEF and DOX-induced ROS production (Yuan *et al.*, 2012). The histological changes associated with DOX cardiotoxicity such as cardiomyocyte vacuolization, sarcoplasmic reticulum distension and fibrosis are also significantly reduced in subjects treated with liposomal DOX nanoparticles (O'Brien *et al.*, 2004). Notwithstanding the potential benefits of DOX nanoparticles, they do, however, have their own set of drawbacks. DOX nanoparticles can be taken up by the mononuclear phagocyte system which significantly

limits their anti-neoplastic efficiency (Immordino *et al.,* 2006). Other studies have indicated that even with the use of DOX nanoparticles, cardiotoxicity still arises (Harris *et al.,* 2002; Swarnakar *et al.,* 2014). Liposomal nanoparticles also lead to the development of hand foot syndrome characterised by redness, pain and swelling of the palms, soles, elbows and knees. Literature further suggests that the incidence of hand-foot syndrome increases up to 50% in patients receiving DOX nanoparticles (Lorusso *et al.,* 2007). This syndrome greatly decreases the quality of life in patients that already have cancer and are undergoing DOX treatment. Based on the above, more research into DOX nanoparticles and other therapeutic avenues against DOX cardiotoxicity are required and urgently needed.

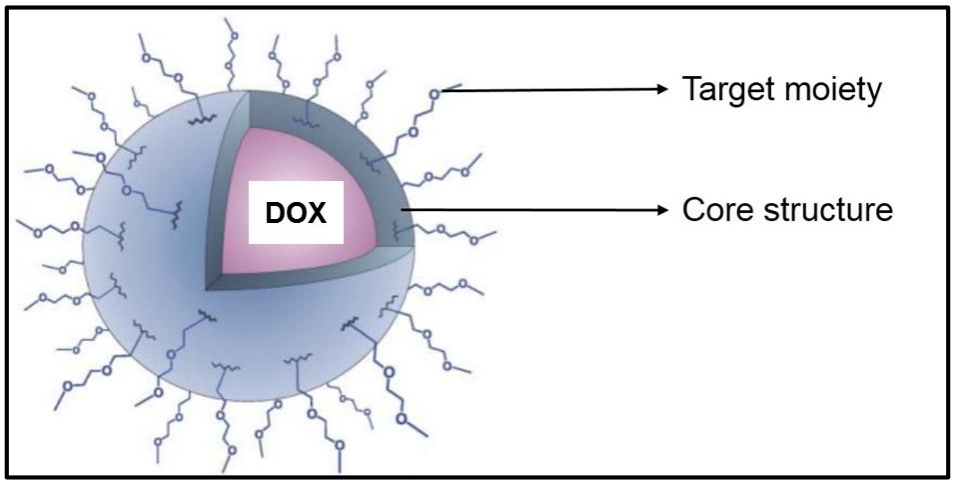

Figure 1.4: Basic structure of a nanoparticle. The nanoparticle contains a core structure which encapsulates a drug core and has target moieties on its surface. Adapted from Bertin *et al.,* 2005.

1.6 AUTOPHAGY MANIPULATION AS A POTENTIAL THERAPEUTIC ADJUVANT FOR DOX CARDIOTOXICITY

Autophagy is an intrinsic cellular process that is responsible for the degradation of cellular organelles and proteins as a means to generate energy in the form of adenosine triphosphate (ATP) (Mizushima, 2007). Although there are different types of autophagic processes namely: macroautophagy, microautophagy and chaperone mediated autophagy, this study will focus on macroautophagy which will be referred to as autophagy. Autophagy is best described as the direct uptake and degradation of cellular cargo by a double layered lipid membrane (Glick *et al.,* 2010). It is induced by a series of upstream signals involving nutrient deprivation, stress or

hypoxia; these lead to inhibition of the mammalian target of rapamycin complex 1 (mTORC1) which will be referred to as mTOR from here onwards (Fig. 1.5) (Laplante & Sabatini, 2009). Inhibition of the latter leads to activation of the Unc51 like kinase 1 (ULK1) complex and the formation of the pre-autophagosomal structure which then elongates to form a phagophore. The phagophore sequestrates cellular material during the elongation process and Sequestome 1 (p62) and microtubule-associated protein light chain 3 (LC3) are attached to the surface of the membrane. Once sequestration is completed, the phagophore closes and the attached LC3 molecule is lipidated from LC3-I to LC3-II by a series of catalytic reactions mediated by autophagy related genes (Atg). The final structure that is formed is known as an autophagosome. The autophagosome which contains cellular cargo is then targeted to lysosomes to form an autophagolysosome and the end result is the degradation and removal of the sequestrated cellular cargo (Mizushima, 2013).

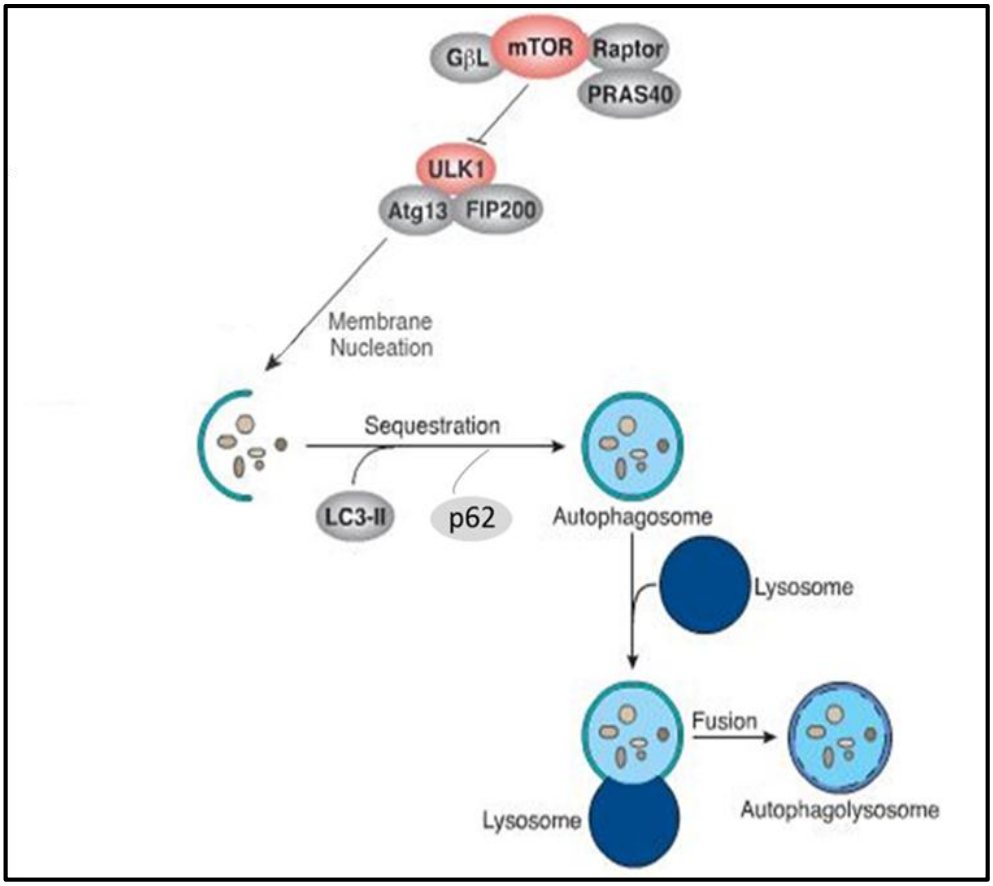

Figure 1.5: The macroautophagy process. Macroautophagy begins as a pre-autophagosomal structure which elongates to form a phagophore. The phagophore takes in cellular cargo and subsequently forms an autophagosome which is targeted to lysosomes for the degradation of cellular cargo. Abbreviations: mTOR: mammalian target of rapamycin**,** PRAS40: proline-rich Akt substrate of 40 kDa, GβL: G-protein Beta-subunit-

like protein, RAPTOR: Regulatory Associated Protein of mTOR, ULK1: Unc51 like kinase 1, Atg: autophagy related genes, FIP200: FAK family kinase-interacting protein of 200 kDa, p62: sequestome 1 and LC3: microtubule-associated protein light chain 3 (LC3). Adapted from Zhang, 2013.

Autophagy has been previously shown to participate in cardiomyocyte death in multiple disease states, including hypertrophy, dilated cardiomyopathy, hypertension and chronic ischemia (Lin *et al.*, 2005; Shimomura *et al.*, 2001; Hein *et al.*, 2003). As autophagy was upregulated in these diseases states, it remains unclear whether autophagy was elevated to prevent or induce cell death. Literature has indicated that as a result of mitochondrial damage, ATP production drastically declines and as a consequence autophagy is induced (Lu *et al.*, 2009; Wang *et al.*, 2014). The link towards cardiomyocyte death is said to involve Atg 5 which binds to fas-associated protein with death domain (FADD) to stimulate the extrinsic form of apoptosis (Chen *et al.*, 2011). Atg 5 can also be cleaved into truncated Atg5 by calpains, which then inhibits the anti-apoptotic protein Bcl-X_L to promote cell death (Su *et al.*, 2013). Similarly, Atg12 prevents the activity of Bcl_2, an anti-apoptotic protein, to further encourage apoptosis (Rubinstein *et al.*, 2001). DOX has previously been shown to have negative effects on the expression of GATA binding protein-4 (GATA-4) which regulates Bcl_2, a negative modulator of beclin-1 (Kobayashi *et al.*, 2010). Therefore under the influence of DOX, GATA-4 and Bcl_2 expression levels decline resulting in an increased expression of beclin-1 and consequently heighted autophagic activity which becomes detrimental when uncontrolled (Kobayashi *et al.*, 2010; Rubinstein *et al.*, 2009).

Autophagy upregulation as a means to counteract DOX cardiotoxicity is a relatively new and exciting prospect in the field of cardio-oncology (Dirks-Naylor, 2013). Studies focusing on autophagy as an adjuvant therapy to reduce the detrimental effects of DOX in an acute setting have produced very interesting and promising results. One of the key observations made by these studies was that DOX mediates its cardiotoxic effects by autophagy inhibition, and therefore upregulating autophagy is a viable option that could be utilized to attenuate the detrimental effects associated with the use of DOX (Kawaguchi *et al.*, 2012; Sishi *et al.*, 2013). Kawaguchi and colleagues (2012) demonstrated autophagy induction through starvation significantly improved left ventricular function and myocardial ATP content *in vivo*. Moreover, DOX-induced cardiac pathology such as fibrosis and cardiomyocyte atrophy were also significantly reversed. Another common mechanism often used to stimulate autophagic activity is rapamycin treatment. The advantage of rapamycin is that it is an already approved treatment regimen for renal cancer and is currently in clinical trials for various other cancers

(Kwiatkowskia & Wagel., 2015). In a tumour bearing mouse model, Sishi *et al* (2013) illustrated that treatment with rapamycin before DOX administration prolonged survival and preserved body weight when compared to only DOX-treated animals. On a cellular level, rapamycin treatment reduced ROS production and apoptosis substantially. Based on the evidence above, autophagy manipulation could potentially be used as a preventative strategy to limit the damaged caused during DOX treatment.

1.7 RATIONALE FOR STUDY

The beneficial effects of autophagy manipulation within this context provided by the literature is quite controversial, although some studies have concluded that autophagy induction is beneficial in this context (Sishi *et al*., 2013; Kawaguchi *et al*., 2012), others have concluded that inhibition of autophagy is more beneficial (Lu *et al.*, 2009; Kobayashi *et al*., 2010). It is also not clear whether DOX induces or inhibits autophagy as contradictory results have been reported, furthermore it is unknown whether DOX modulation of autophagy is a pro-apoptotic or anti-apoptotic mechanism (Dirks-Naylor. 2013). It is also important to note that these studies made use of different models, DOX concentration and treatment duration which could account for some of the contradictory results (Table 1). However, even more importantly these latter studies made use of an acute cytotoxicity models though acute cardiotoxicity is clinically manageable. Therefore, there is a need for studies investigating autophagy modulation in the chronic DOX setting, particularly since it is life threatening and culminates in CHF (Lefrak *et al.*, 1973).

Table 1.1: A summary of studies that have investigated the function of autophagy in the context of DOX cytotoxicity.

Author	Model	DOX (µM)	Duration (hours)	Mode of autophagy modulation	Conclusion
Sishi *et al.*, 2013	H9c2 cardiomyoblasts	3	24	Rapamycin	Beneficial

Kawaguchi *et al*., 2012	Neonatal GFP-LC3 mice cardiomyocytes	0.1	6	Starvation	Beneficial
Kobayashi *et al*., 2010	Sprague Dawley neonatal rat cardiomyocytes	1	18	3-MA	Beneficial
Lu *et al*., 2009	Sprague Dawley neonatal rat cardiomyocytes	1.8	24	3-MA	Beneficial
Kobayashi *et al*., 2010	Sprague Dawley neonatal rat cardiomyocytes	1	18	Rapamycin	Detrimental
Wang *et al*., 2014	H9c2	10	24	n/a	n/a
Chen *et al*., 2011	Sprague Dawley neonatal rat cardiomyocytes	1	16	n/a	n/a
Xu *et al*., 2011	Sprague Dawley neonatal rat cardiomyocytes	1	24	n/a	n/a
Dimitrakis *et al*., 2012	Adult rat cardiomyocytes	10	48	n/a	n/a

1.8 HYPOTHESIS

Autophagy upregulation before chemotherapy treatment reduces the detrimental side effects associated with DOX treatment in an *in vitro* model of chronic DOX cytotoxicity.

1.9 AIMS

- To differentiate H9c2 cardiomyoblast into cardiomyotubes and assess differentiation by looking at:
    - H9c2 morphology
    - Myosin light chain and cardiac troponin expression
    - Oxidative phosphorylation capacity
- To successfully modulate autophagy in a cell model by:
    - Rapamycin (inducer)
    - Starvation (inducer)
    - mTOR silencing (inducer)
    - Bafilomycin treatment (inhibitor)
- To elucidate which mechanisms of autophagy modulation are beneficial in this context
- To investigate the therapeutic benefits of autophagy modulation in a chronic model of DOX cytotoxicity by assessing:
    - Cell viability and apoptosis
    - Mitochondrial morphology
    - Mitochondrial lipid peroxidation and membrane potential

2 CHAPTER 2: METHODS AND MATERIALS

2.1 PILOT STUDY: H9c2 DIFFERENTIATION

2.1.1 Culturing of H9c2 myoblasts

H9c2 cardiomyoblast cells were cultured in Dulbecco's modified eagle's medium (DMEM) (Gibco, 41965-039) supplemented with 10% fetal bovine serum (FBS) (Biocom Biotech, FBS-G1-12A), 1% penicillin/streptomycin (ThermoFisher Scientific, 15140-122) at 37 ^{o}C under 95% humidified oxygen (O_2) and 5% carbon dioxide (CO_2). Culture medium was refreshed every second day and the cells were maintained until they reached 70% confluency. Once confluent, culture medium was discarded and the cells were trypisinized (0.25% Trypsin-EDTA, Gibco, 25200-012) and then counted to determine the appropriate seeding densities for each experiment.

2.1.2 Induction of H9c2 differentiation

H9c2 myoblasts have been used for a number of years to represent various models of cardiac disease. However, the use of these cells as cardiovascular models has come under scrutiny as recent studies suggest that they are not representative of cardiomyocytes. Hence current literature has suggested that H9c2 cardiomyoblast should be differentiated into cardiomyotubes, which is a more representative model of cardiomyocytes (Pereira *et al.*, 2011). One of the key features that make H9c2 cardiomyoblast different from cardiomyocytes is their reliance on glycolysis as a means of producing ATP (Lopaschuk *et al.*, 1991). This is in contrast to cardiomyocytes which make use of oxidative phosphorylation (Kolwicz *et al.*, 2013). Furthermore, H9c2 cardiomyoblast expression of cardiac troponin T (cTnT) and myosin light chains (MLC) is significantly lower than that of cardiomyocytes (Lopaschuk *et al.*, 2010), thus increased expression of the latter genes is an ideal indicator of H9c2 differentiation in cardiomyotubes (Branco *et al.*, 2012). H9c2 cardiomyoblast differentiation was induced according to a protocol provided by Pereira *et al.*, (2011), where serum was dropped to 1% and cells were supplemented daily with 10 nM of retinoic acid (RA) (Sigma, R2625) for 11 days. For comparison, some cells were maintained with either 10% FBS or 1% FBS for the same number of days. In an effort to determine differentiation, MLC (Cell Signalling, D511C) and cTnT (Abcam, ab11C11) was assessed by western blotting and immunocytochemistry respectively at day 6 and day 11 of differentiation.

2.1.3 Western blot analysis

2.1.3.1 Preparation of cell lysates

At the end of the treatment protocol, culture medium was discarded and the cell monolayer was washed twice with ice cold phosphate buffered saline (PBS). The cells were incubated in approximately 60 µl of radio-immunoprecipitation assay (RIPA) buffer for a period of 10 minutes on ice. The cells were then scrapped off using a cell scraper, transferred into chilled microfuge tubes and then sonicated for ±4 seconds at an amplitude of 4 units using an Ultrasonic Liquid Processor (Misonix). The cell homogenate was then placed on ice to allow the entire cell contents to settle. The homogenate was centrifuged, whereafter the supernatant (cell lysate) was transferred into a clean microfuge tube and stored at -80^{o}C until needed.

2.1.3.2 Determination of protein concentration

The cell lysate was thawed on ice and protein concentration was determined using the Bradford method (Appendix B, protocol 8, pg. 92-93). Briefly, equal volumes of protein (5 µL) were mixed with Bradford reagent and distilled water. Increasing concentrations of bovine serum albumin (BSA) (Roche, 10735078001) were used to a produce standard curve. The absorbance of the sample was plotted against that of the standard curve to determine protein concentration of the sample. Protein samples were prepared at the correct concentration in Laemmli's loading buffer and stored at -80 until needed.

2.1.3.3 Sodium dodecyl sulphate-polyacrylamide gel electrophoresis (SDS-PAGE)

Samples that had already been prepared were thawed, followed by a 5 minute boiling process at 95 ^{o}C. Protein separation was performed on a 12% stain free, fast cast gel (Bio-rad, 161-0184) which was prepared according to the manufacturer's instructions. The gel was run to completion at a 180 mV and then activated on the Chemi Doc™ XRS system (Bio-rad). The proteins were then transferred on to a polyvinylidene fluoride (PVDF) membrane (Bio-rad, 170-4156) for 10 minutes at 25 V and 1.3 A. Following transfer, the membrane was placed in methanol and then left to dry. This was followed by a wash in Tris-buffered saline-tween (TBST) and a 1 hour blocking process in 5% fat free milk. The membrane was then incubated at 4 ^{o}C overnight with primary anti-body (1:1000) followed by three, ten minute washes in TBST and then placed in anti-rabbit secondary anti-body (1: 5000) for 1 hour at room

temperature. The membrane was washed again and treated with a 1:1 ratio of ECL western blot substrate (Bio-rad, 170-5061) for 5 minutes. The Chemi Doc™ system was used to image and analyse the protein bands. All bands were normalized to β-actin.

2.1.4 Fluorescence microscopy

Cells were seeded onto coverslip and grown to 70% confluency. Cell differentiation was induced for 11 days as described previously. At the end of the treatment period medium was removed and cells were washed with ice cold PBS and fixed in cold 4% paraformaldehyde (Sigma, 158127) for 10 minutes. Cells were washed again in cold PBS, blocked in 1% BSA, permeated with 0.1% triton solution (Sigma, X-100) and incubated at 4 ^{O}C with cTnT anti-body (1: 100) (Abcam, 11C11) overnight. The cell were then washed with cold PBS and incubated with an anti-mouse secondary anti-body (1: 400) (ThermoFisher Scientific, A11029) for 1 hour in the dark. This was followed by staining with Hoescht (5 µM) (ThermoFisher Scientific, H1399), where after the slide was left to air dry. Once dry, the coverslip was mounted on a glass slide using Dako fluorescent mounting medium (Diagnostech, S302380). Images were acquired using a Nikon eclipse E400 fluorescent microscope equipped with a DMX1200 CCD Camera 200. Images were acquired using the Nikon plan Flour 10x and 20x objective lens. The slide was divided into 9 equal blocks using a 1 cm x 1 cm grid and four images were taken at 10x magnification per block, for a total of 36 images per slide (n=1) and 108 (36 x 3) images per experimental group (n=3). One image was take at 20x magnification as a representative image of the differentiated cells in each group. All data was done in triplicate and the number of differentiated cells were not quantified.

2.1.5 Oxygraph analysis

The change from glycolysis to oxidative phosphorylation is a fundamental characteristic observed in differentiated cells. The assessment of respiration rate is an ideal measure for oxidative phosphorylation capacity in cells. The Hansatech oxygraph system was used to determine respiration rate in differentiated cells; assessment was only performed at day 6 in this experiment. The oxygraph was also calibrated beforehand according to the manufacture's protocol. Following treatment, the cells were trypsinizesd and 1 million cells were transferred into the oxygraph respiration chamber containing Hedly's intracellular buffer, thereafter, saponin (1 µM) (Sigma, 47036) was used to permeate them. The mitochondrial complex I

substrates, malate (5 µM) (Sigma, M1000) and glutamate (10 µM) (Sigma, G1251) and the mitochondrial complex II substrate succinic acid (100 µM) (Sigma, S3674) were added. This was process was allowed to continue for 5 minutes. Active respiration was induced by the addition of adenosine dinucleotide (ADP) (Sigma, 01905). Respiration rate was then measured for 60 minutes. The average respiration rate during this period was determined and compared between groups. Carbonyl cyanide-p-trifluoro-methoxy-phenyl-hydrazone (FCCP) (Sigma, C2920), a mitochondrial un-coupler was used to confirm that mitochondria were actively respiring at the end of the experiment.

2.2 MAIN STUDY

2.2.1 Doxorubicin treatment

Since this study aimed to stimulate chronic DOX cytotoxicity, a 3.4 mM stock of DOX (Sigma, D1515) was prepared in sterile DMEM and stored in light protected microfuge tubes at -20 ^{0}C. At confluency, the cells were treated daily with 0.2 µM for five days, resulting in a cumulative dose of 1.0 µM. Cumulative in this study indicates the total amount of DOX used to treat the cells for the duration of the treatment protocol. Clinically, DOX is often administered intravenously at a dose that varies between 60 mg/m^2 and 75 mg/m^2, where it peaks within the plasma at concentrations between 5 - 15 µM (Mross *et al*., 1988). Considering that the majority (± 75%) of the DOX is bound to plasma proteins (independently of its plasma concentration) (Greene *et al*., 1983), the amount of DOX available to act on actively replicating cells ranges between 1.25 µM and 3.75 µM (Liu *et al*., 2008). In addition, Minotti *et al*., (2004) indicated that several *in vitro* studies are conducted with concentrations of DOX that are too high compared to peak (± 5 µM) and steady-state (25 - 250 nM) plasma concentrations that are observed following standard bolus infusions in patients. It was thus suggested that *in vitro* studies utilizing concentrations > 1 to 2 µM should be re-evaluated. Based on these recommendations, the cumulative dose of DOX (1.0 µM) chosen for this study is clinically relevant and appropriate for a cell based study.

2.2.2 Rapamycin treatment

Rapamycin treatment is a common method used to upregulate autophagy. The cells were grown and maintained as previously described. Once confluent, cells received 25 nM of rapamycin

(Sigma R8781) pre-treatment for an hour at day 1, 3 and 5 (Fig 2.1). The medium was discarded following pre-treatment and fresh rapamycin medium contain DOX was added. The cells were treated with culture medium at day 2 and 4.

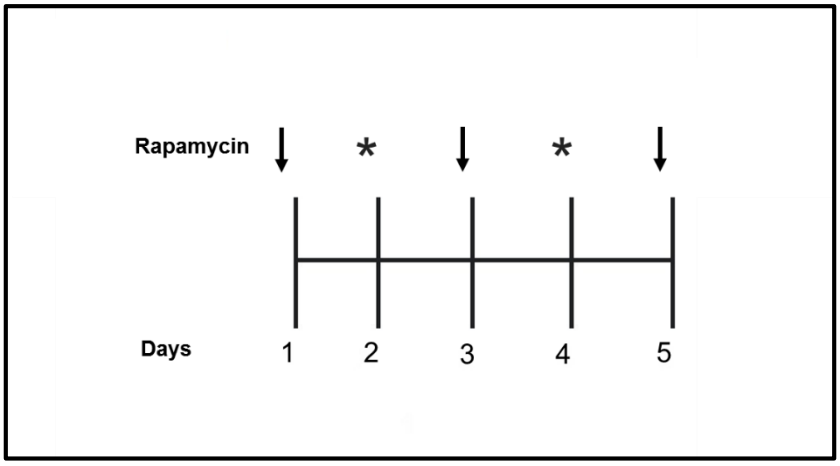

Figure 2.1: Experimental setup of autophagy induction by rapamycin. On days 1, 3 and 5, cells were pre-treated with rapamycin for an hour before DOX was introduced (arrow). On days 2 and 4, cells were only treated with DOX (asterix).

2.2.3 Amino acid starvation to induce autophagy

To upregulate autophagic activity starvation medium was used. This medium was prepared by combining equal volumes of amino acid free medium and culture medium (FBS free). (ThermoFisher Scientific, 24020-117). The cells were pre-treated with starvation medium for an hour at day 1, 3 and 5 as indicated by the arrows on figure 2.2. After pre-treatment, the medium was discarded and fresh starvation medium containing DOX was added. Autophagy was not induced at day 2 and 4 thus the cells were only treated with culture medium as indicated by the asterix of the figure below.

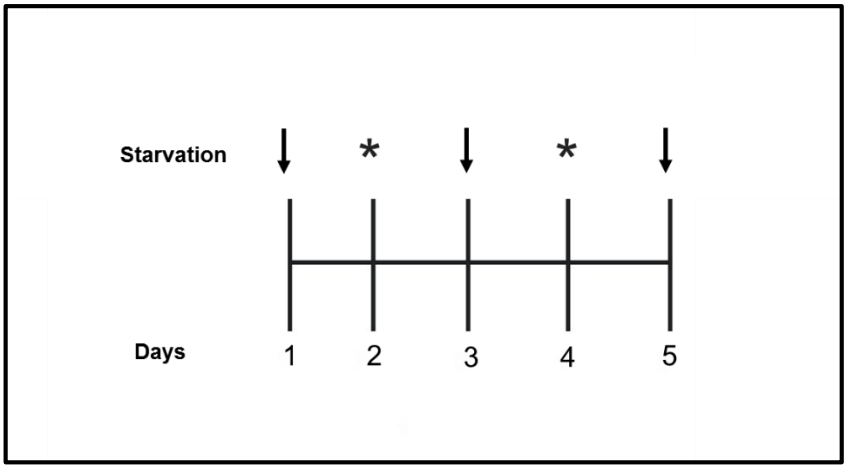

Figure 2.2: Experimental setup of autophagy induction by starvation. On days 1, 3 and 5, cells were pre-treated with starvation medium for an hour before DOX was introduced (arrow). On days 2 and 4, cells were only treated with DOX (asterix).

2.2.4 mTOR silencing RNA treatment

Cells were seeded and grown to 60% confluency, where after mTOR was silenced using mTOR silencing ribonucleic acid (siRNA) at days 1, 3 and 5 (Fig. 2.3). mTOR silencing medium was prepared by adding 5 nM of mTOR silencing RNA (siRNA) (Cell Signalling, 63815) and 0,75 µl of HiPerfect transfection reagent (Qiagen, 301705) per 100µl of serum free medium. The medium was made fresh daily and incubated for 15 minutes at room temperature prior to use. Once ready for use, DOX was added and the medium was administered in a dropwise manner. Cell received culture medium at day 2 and 4 as mentioned in previous sections.

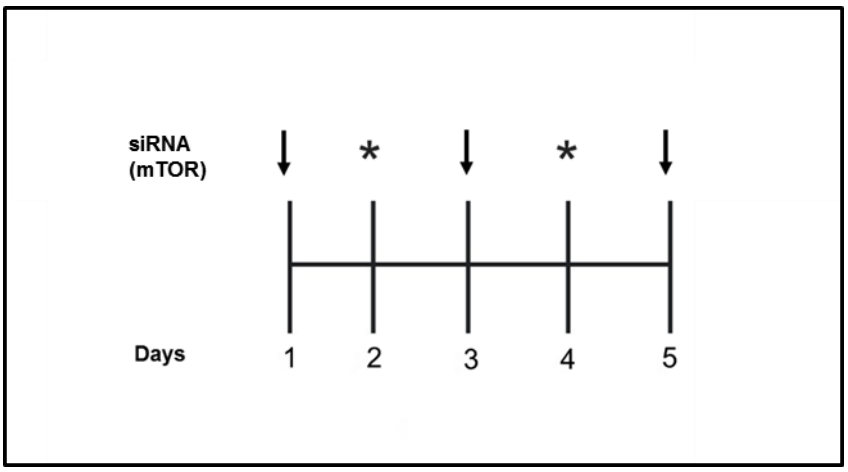

Figure 2.3: Experimental setup of autophagy induction by siRNA (mTOR). On days 1, 3 and 5, cells were treated with siRNA mTOR (arrow). On days 2 and 4, cells were only treated with DOX (asterix).

2.2.5 Bafilomycin treatment

The cells were maintained and grown to 70% confluency as described previously, where after they were pre-treated for an hour with 1 nM or 5 nM of bafilomycin (LKT laboratories, BOO25) as described in figure 2.4. After the pre-treatment, the medium was discarded and fresh medium containing only DOX was administered to the respective groups. The cells received normal culture medium at day 2 and 4.

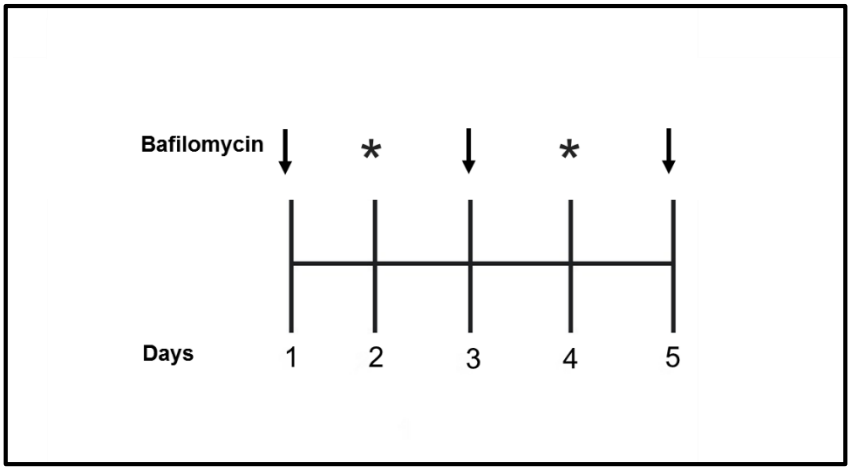

Figure 2.4: Experimental setup of autophagy inhibition by bafilomycin. On days 1, 3 and 5, cells were pre-treated with bafilomycin for an hour before DOX was introduced (arrow). On days 2 and 4, cells were only treated with DOX (asterix).

2.2.6 Cell viability (WST-1 assay)

The WST-1 cell viability assay allows the precise measurement of cell viability by assessing mitochondrial function. The tetrazolium salt (WST-1) is cleaved into soluble formazan by mitochondrial dehydrogenase in viable cells. The absorbance of formazan can therefore be used as an indirect measurement of metabolically active cells.

Following treatment, the culture medium was discarded and 200 µl of fresh medium and 10 µl of WST-1 reagent (Abcam, ab155902) was added to each well. The plates were covered in foil and incubated for 2 hours at 37 ^{o}C, where after absorbance was measured at 440 nm using the EL800 Universal Microplate Reader (Bio-Tek instruments, Vermont, USA). Wells containing only medium and WST-1 reagent were used as blank to compensate for false signal.

2.2.7 Cellular apoptosis (caspase-glo 3/7® assay)

The caspase-Glo 3/7® assay (Promega, G8091) measures the level of apoptosis by assessing the caspase 3 and 7 activity. The assay contains an amino acid substrate (DEVD tetrapeptide sequence) which is recognised and cleaved by caspase 3 and 7. The cleaved product is recognised by luciferase resulting in luminescence production which can be measured by a luminometer. The amount of light signal produced is directly proportional to the amount of caspase activity.

Following treatment, 100 µl of caspase-Glo 3/7® reagent was added to each well containing 100 µl of culture medium. The culture plate was then covered with foil, incubated for an hour at room temperature with gentle mixing process and luminescence was measured in a plate-reading luminometer (GloMax® 96 microplate luminometer, Promega, Winsconstin, USA). The average luminescence from the blank reaction (caspase-Glo 3/7® reagent, culture medium only) was subtracted from the luminescence of the treated samples to remove any background noise.

2.2.8 Mitochondrial morphology (Mito tracker® green FM)

Approximately 10 000 cells were seeded and grown to 70% confluency in an Nunc™Lab-Tek™ 8 well chamber plates (ThermoFisher Scientific, 154534). An Olympus IX81 inverted fluorescent microscope (Olympus) was used to acquire images at 60x magnification using an OLYMPUS PlanApo N60x/1.4 oil objective. The images were acquired through multi-colour Z-stack acquiring software. The upper and lower focal points of the z-stack were carefully selected prior to acquiring images and the cell R system was used for imaging optimization.

Mito tracker® green FM (ThermoFisher Scientific, M-7514) is a green fluorescent protein that localizes and binds to free sulfhydryl proteins in mitochondria irrespective of mitochondrial membrane potential state. The fluorescent probe was used to assess mitochondrial morphology and network organization often used as indicators of mitochondrial health. At the end of treatment period, the cells were stained with Mito tracker® green FM (25 µM) and Hoechst 33342 (5 µM) (ThermoFisher Scientific, H1399) and then images were acquired. Unstained cells were used as controls to account for non-specific signal.

2.2.9 Assessment of mitochondrial lipid peroxidation (MitoPerOX)

The mitochondrial permeable dye (4, 4-diflouro-5-(4-phenyl-1, 3-butadienyl)-4-bora-3a, 4a-diaza-*s*-indacene-undecanoic acid) (ThermoFisher Scientific, D-3861) commonly known as MitoPerOX, was used to assess mitochondrial lipid peroxidation since it is only taken up by functional mitochondria. This dye has two key characteristics: a boron-dipyrromethene (BODIPY) $^{581/591}$ fluorophore and an undecanoic acid portion allowing for anchoring into the inner mitochondrial membrane. Upon production of lipid peroxyl radicals the BODIPY$^{581/591}$ fluorophore fluorescence shifts from a wavelength of 590 nm to 510 nm. This shift in wavelength is used to measure mitochondrial lipid peroxidation state in cells.

The cells were maintained and treated as previously described. MitoPerOX was then prepared according to the manufacturers' instructions and 5 µM of the dye was added to each cell mixture followed by a 15 minute incubation period. Utilizing a BD FACS Aria I flow cytometer, a minimum of 10 000 cells were analysed using the 488 nm laser and the 515-545 and 575-625 fluorescence detectors. The geometric mean of the intensity histogram was then used to measure fluorescence intensity. Additionally, images were also acquired at 60x magnification using an Olympus IX81 inverted fluorescence microscope as previously discussed in section 2.2.8. An unstained control and DOX group were used as negative controls for unspecific auto-fluorescent signal from cells and DOX respectively.

2.2.10 Mitochondrial membrane potential assessment (JC-1)

Mitochondrial membrane potential was assessed using 5, 5, 5, 6-tetracholo-1, 3, 3 tetra-ethyl-benzimidazolyl-carbocyanine (ThermoFisher Scientific, T3168) commonly known as JC-1. This fluorescent probe enters the cell membrane via passive diffusion and accumulates in functional mitochondria producing an orange/reddish signal. Upon mitochondrial depolarization, the fluorescent probe exists and produces a green signal. This ratiometric change between the green and orange/reddish signal is used as an indicator of mitochondrial function.

Cells were maintained and treated as previously described. At the end of the treatment protocol, 5 µM of JC-1 was added to the cell mixture followed by a 15 minute incubation period. Utilizing a flow cytometer, a minimum of 10 000 cells were analysed using a 488 nm laser and

the 515-545 and 575-625 fluorescence detectors. The geometric mean of the intensity histogram was then used to measure fluorescence intensity. Furthermore, images were acquired using an Olympus IX81 inverted fluorescence microscope as previously explained. Unstained DOX and control cells were used as negative controls, and cells with FCCP depolarized mitochondria were used as a positive control.

2.2.11 DOX accumulation and co-localization

DOX is auto-fluorescent and its accumulation in cells can be assessed by flow cytometry. Cells were seeded and grown to 70% confluency as mentioned previously. At the end of the treatment protocol medium was discarded and cells were trypisinized and pelleted. The supernatant was discarded and the cells were resuspended in 1 ml warm sterile PBS and then vortexed. DOX fluorescent signal was measured in a minimum of 10 000 cells using a 488 nm blue laser and a 575-625 fluorescence detector. To determine DOX co-localization, images were acquired using an Olympus IX81 inverted fluorescent microscope as previously described. An unstained control group was used as a negative control to compensate for unspecific auto-fluorescent signals.

2.2.12 Statistical analyses

All experiments were performed in triplicate (n=3), unless otherwise stated. GraphPad Prism version 5.0.0 (GraphPad Inc., San Diego, CA) was used for statistical analysis of all the data. The data was first normalized to a percentage of control and a one way analysis of variance (ANOVA) with a Bonferroni's post-hoc test was used to assess differences between groups. Results were presented as mean ± standard error of the mean (SEM) and were considered significant if $p < 0.05$.

3 CHAPTER 3: RESULTS

3.1 PART 1: H9c2 DIFFERENTIATION

3.1.1 Morphological assessment

The differentiation of H9c2 cells was induced by decreasing the percentage of FBS from 10% to 1%, followed by supplementation with 10 nM of RA for 11 days. Normal undifferentiated H9c2 cardiomyoblasts are mononucleated and spindle shaped, whereas differentiated H9c2 cells form long, thin and multinucleated cardiomyotubes. After six days of differentiation, very few cells had displayed the desired cardiomyotube morphology. Furthermore, there were no obvious differences between the serum starved group (Fig. 3.1**B**) and the combination group (serum starved plus RA) (Fig. 3.1**C**) when compared to control (Fig. 3.1**A**). By day 11 of the cells being maintained in differentiation medium, there were relatively more cells that had differentiated in both groups (Fig. 3.1**D** and **E**) versus control. These cells appeared elongated and displayed a shrunken width indicative of differentiation. Unfortunately this study was unable to detect major differences between the two differentiation groups.

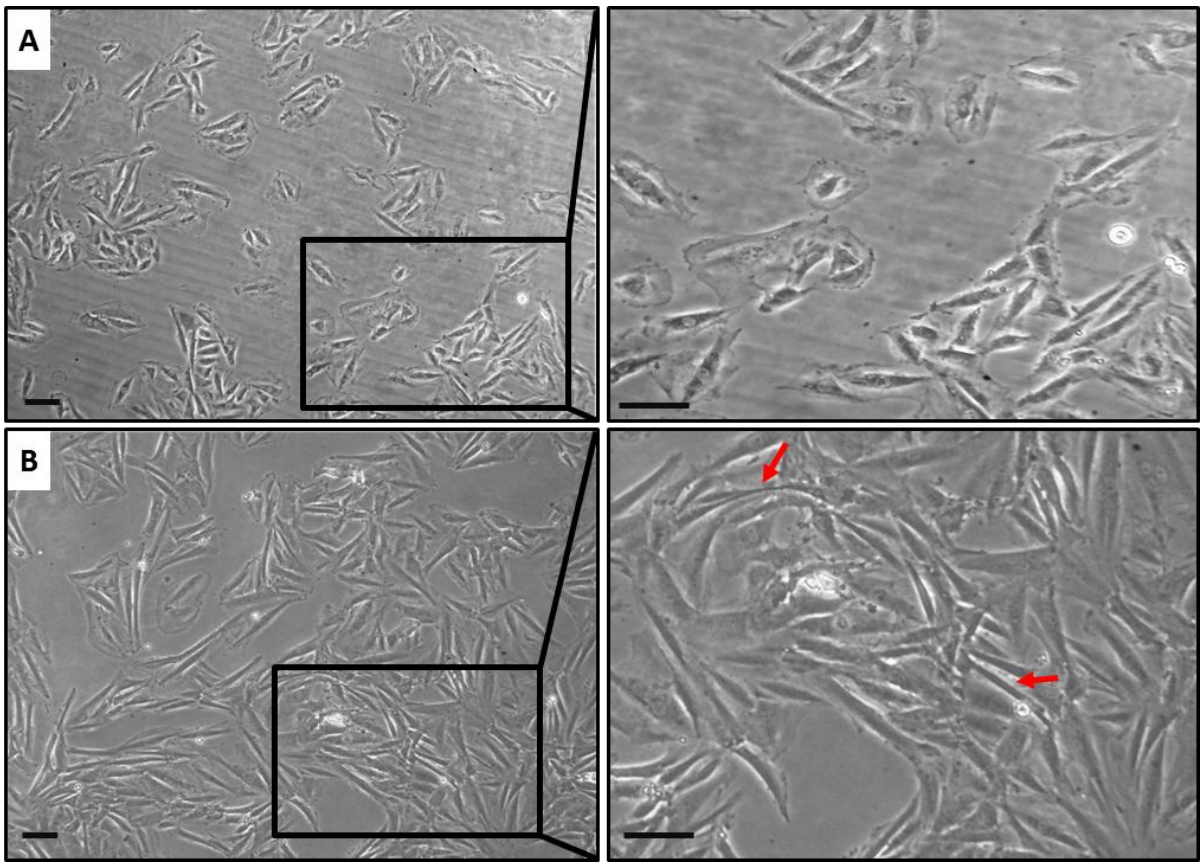

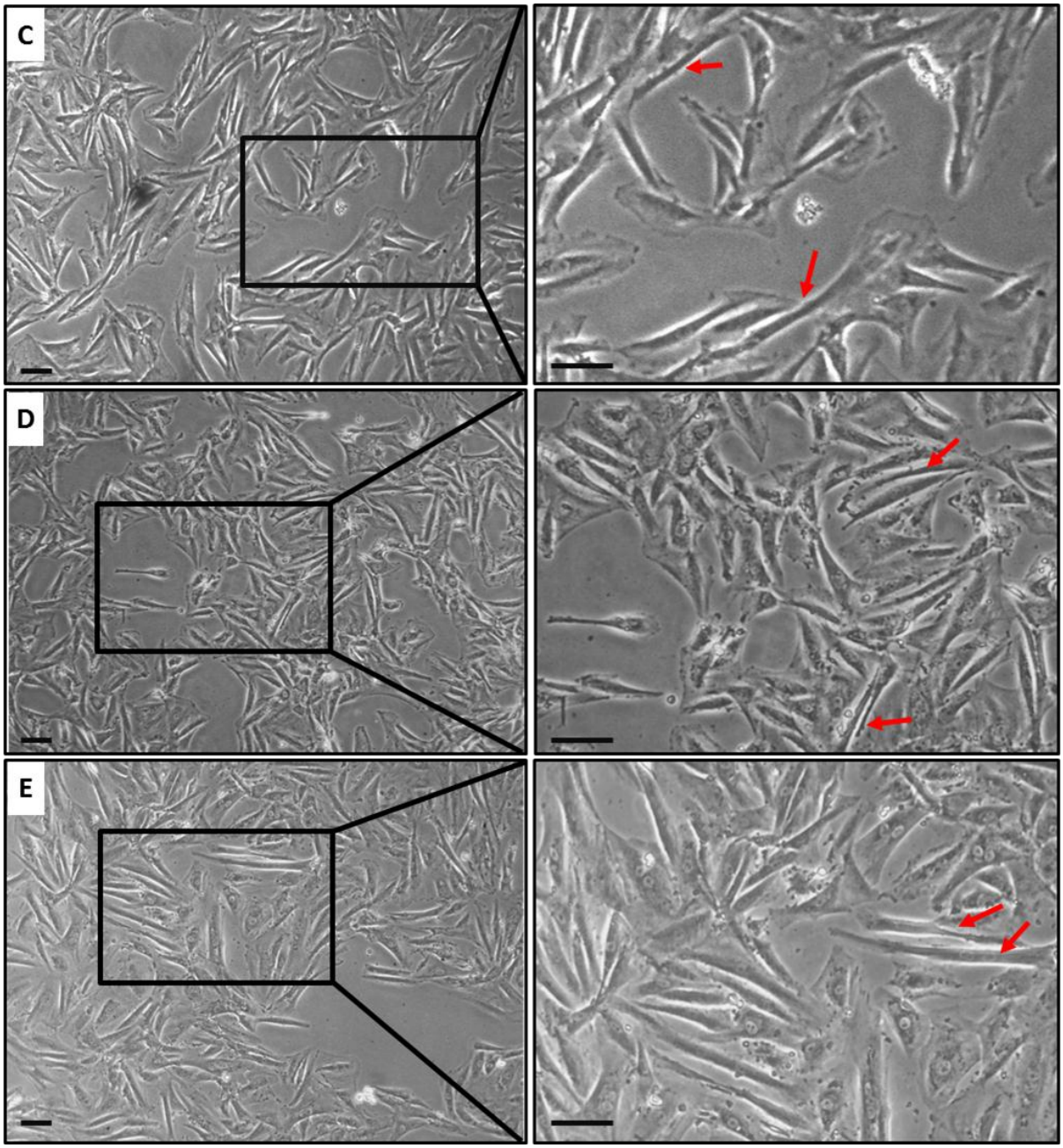

Figure 3.1: Morphological assessment of H9c2 differentiation. Cell differentiation was induced by either reducing the serum, or by reducing the serum and supplementing daily with 10 nM retinoic acid (RA) for a total period of 11 days. Morphological changes were analysed by bright field microscopy on days 6 and 11. (n=3). **A**: control, **B**: 1% FBS (6 days), **C**: 1% FBS plus RA (6 days), **D**: 1% FBS (11 days) and **E**: 1% FBS plus RA (11 days). Arrows indicate cardiomyotubes. Magnification = 5x. Scale bar = 0.1 mm.

3.1.2 Cardiac troponin T (cTnT) protein expression

To further analyse H9c2 differentiation, this study assessed the expression of cTnT by immunocytochemistry. In addition, the number of nuclei per cell was noted. Cells were

regarded as cardiomyotubes when they displayed more than two nuclei as well as by expressing cTnT. As observed in Fig. 3.2**B**, merely reducing serum for six days did not result in substantial expression of cTnT. However, by supplementing with RA, in addition to reducing the serum (Fig. 3.2**C**), more cells were able to express this protein at this time point compared to the control (Fig. 3.2**A**). By day 11, the serum starved group (Fig. 3.2**D**) demonstrated increased cTnT expression, compared to day 6 (Fig. 3.2**B**) and more cardiomyotubes contained multiple nuclei. A similar observation was made in the combination group (Fig. 3.2**E**), albeit to a greater extent at this time**.** Furthermore, the combination group at day 11 showed a greater capacity to induce formation of multinucleated cardiomyotubes when compared to the serum starved group at the corresponding day.

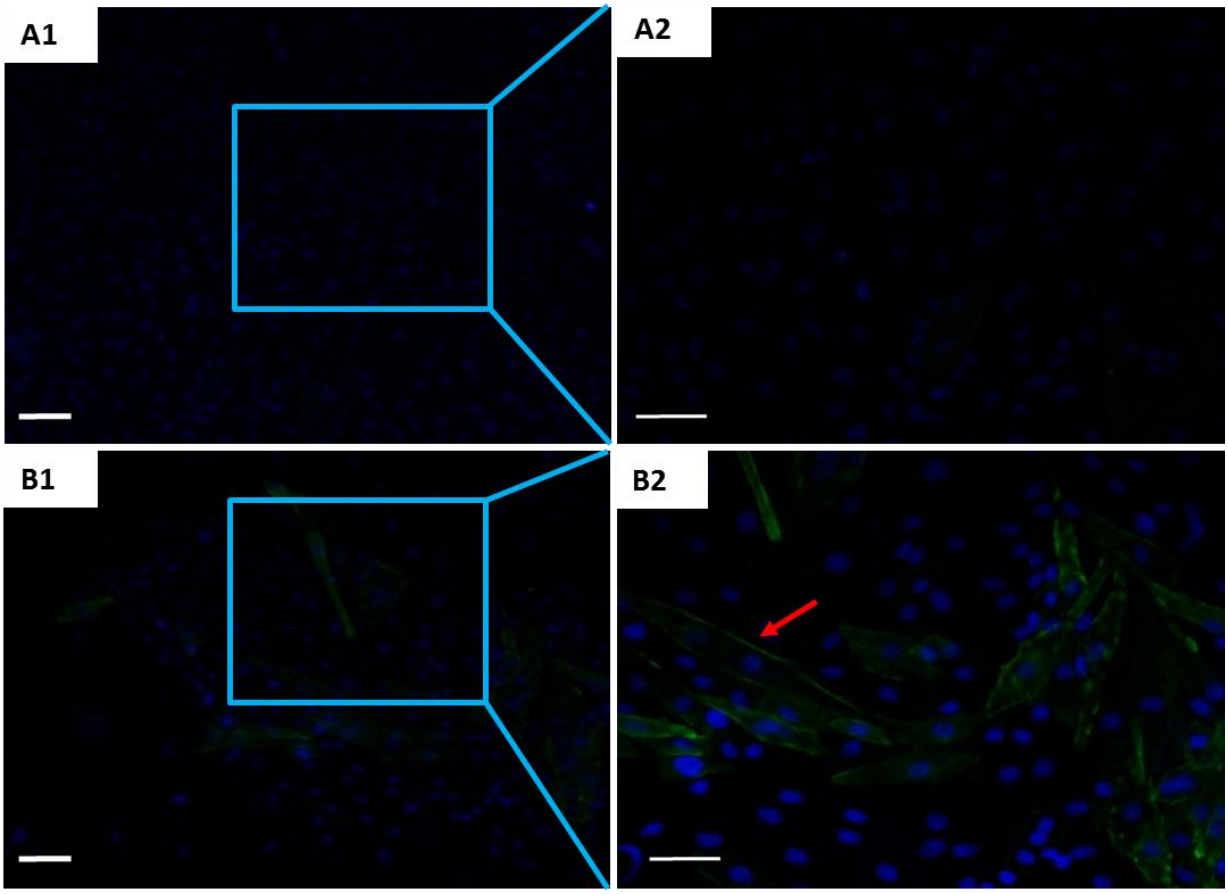

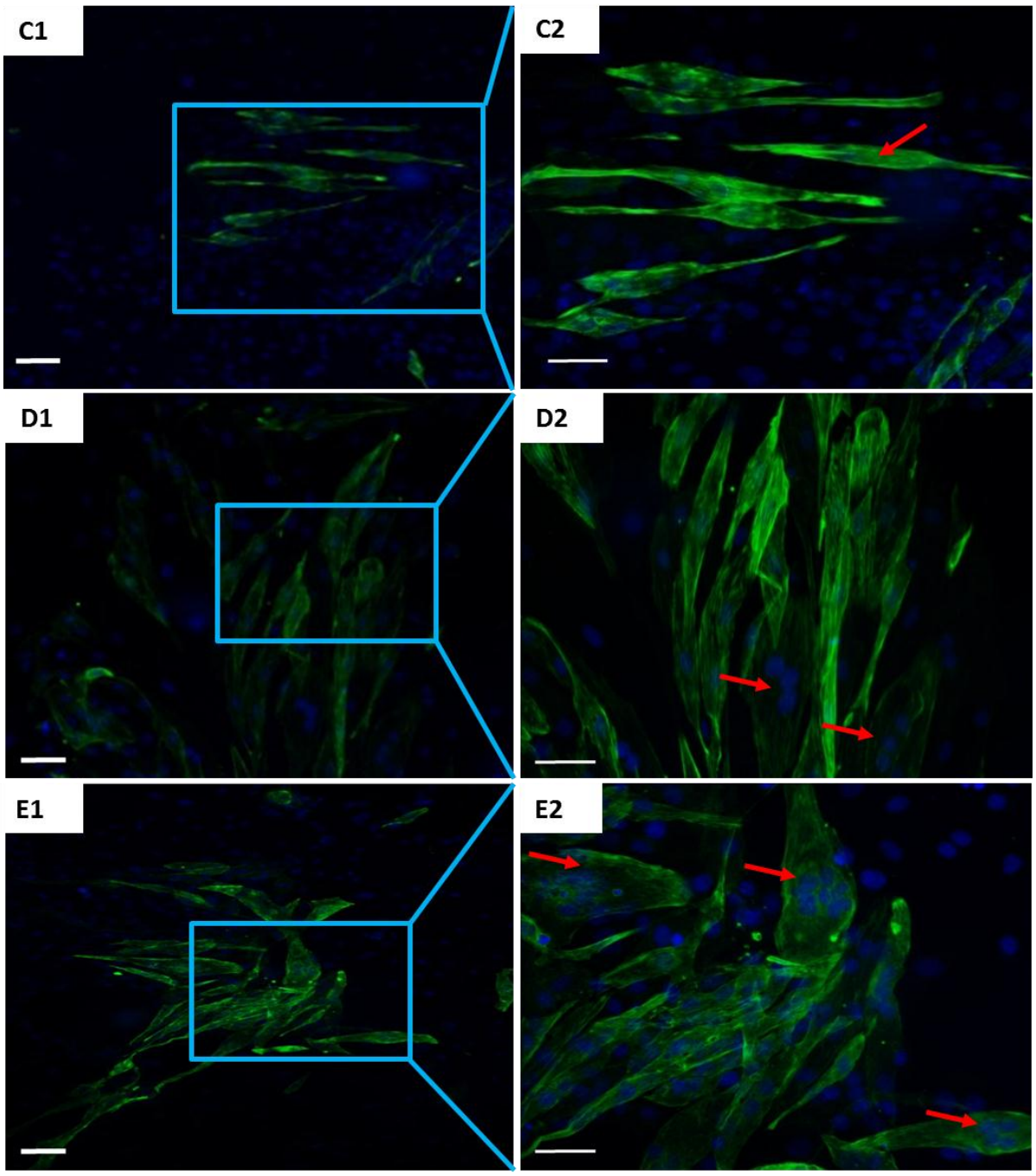

Figure 3.2: Analysis of cardiac troponin T (cTnT) expression following H9c2 differentiation. Cell differentiation was induced by either reducing the serum, or by reducing the serum and supplementing daily with 10 nM retinoic acid (RA) for a total period of 11 days. Changes in cTnT expression were analysed by immunocytochemistry analysis on days 6 and 11. (n=3). **A**: control, **B**: 1% FBS (6 days), **C**: 1% FBS plus RA (6 days), **D**: 1% FBS (11 days) and **E:** 1% FBS plus RA (11 days). Arrows indicate cardiomyotubes. **Green**: cardiac troponin expression. **Blue**: nuclei. **A1-E1**: Magnification = 10x. Scale bar = 0.1 mm and **A2-E2**: Magnification = 20x. Scale bar = 0.05 mm.

3.1.3 Myosin light chain (MLC) protein expression

In an effort to further distinguish between myoblasts and cardiomyotubes, MLC expression was investigated by western blotting. MLC is often used as an indicator of myoblast differentiation into cardiomyotubes (Comelli *et al*., 2011). As indicated in Fig. 3.3**A** and **B**, the addition of RA with the reduced serum significantly increased expression of MLC (209.5±7.4%, $p<0.001$) when compared to the serum only (118.4±9.9%) and control (100.0±9.8%) group on day 6. By day 11, a substantial increase in the expression of MLC was observed in both the serum only (236.9±16.6%, $p<0.001$) and combination group (244.4±9.2%, $p<0.001$) compared to the control. Major differences were also observed between day 6 and day 11 in the serum only groups. These results may possibly suggest that it takes much longer for cardiac specific markers to be expressed when only serum is reduced, compared to the addition of RA. However, RA appeared to lose its effects on the expression of cardiac markers when the duration of treatment is extended.

A)

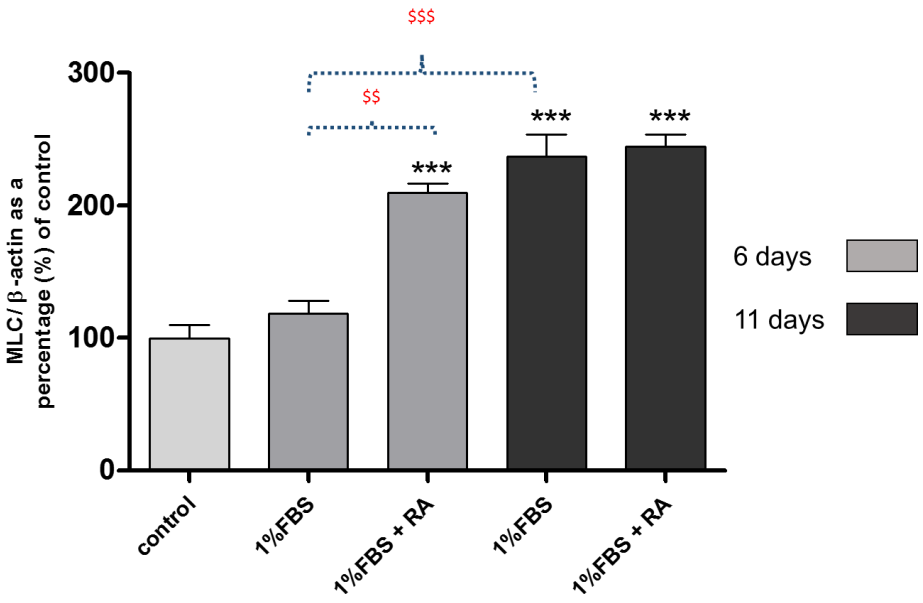

B)

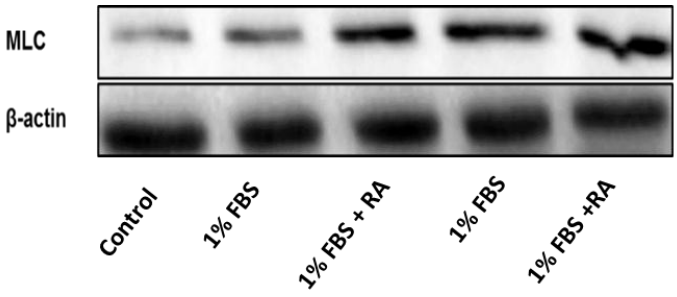

Figure 3.3: Myosin light chain (MLC) protein expression following cardiomyoblast differentiation. Cell differentiation was induced by either reducing the serum, or by reducing the serum and supplementing daily with 10 nM retinoic acid (RA) for a total period of 11 days. **(A)** Bar graph and **(B)** western blot representation of MLC expression. Result are presented as mean ± SEM (N=3). ***P < 0.001 vs control. $^{\$\$\$}$P < 0.001, $^{\$\$}$P < 0.01 vs 1%FBS (6 days).

3.1.4 Oxidative Phosphorylation analysis

The switch in substrate utilization from glucose (glycolysis) to fatty acids (oxidative phosphorylation) is a fundamental characteristic observed in differentiated cardiac cells. Cardiomyotubes, like primary cardiomyocytes prefer to utilize fatty acids as their source of energy rather than glucose preferred by cardiomyoblasts (Lopaschuk *et al*., 2010). Therefore, the determination of oxygen respiration rate is an ideal measurement for oxidative phosphorylation in these differentiated cells. It should be noted, however, that analysis in the results was only conducted for 6 days and no oxidative substrates were included. The rationale behind this was to merely establish whether a change in oxygen consumption would be evident following the differentiation process. As expected, a significant increase in the respiration rate was observed in both groups versus the control (100.0 ± 6.1 nM O_2/ million cells) suggestive of differentiation (Fig. 3.4). What was also interesting to note was the major difference between the serum only group (131.9 ± 5.2 nM O_2/ million cells, $p<0.05$) compared to the combination group (230.7 ± 15.8 nM O_2/ million cells, $p<0.001$).

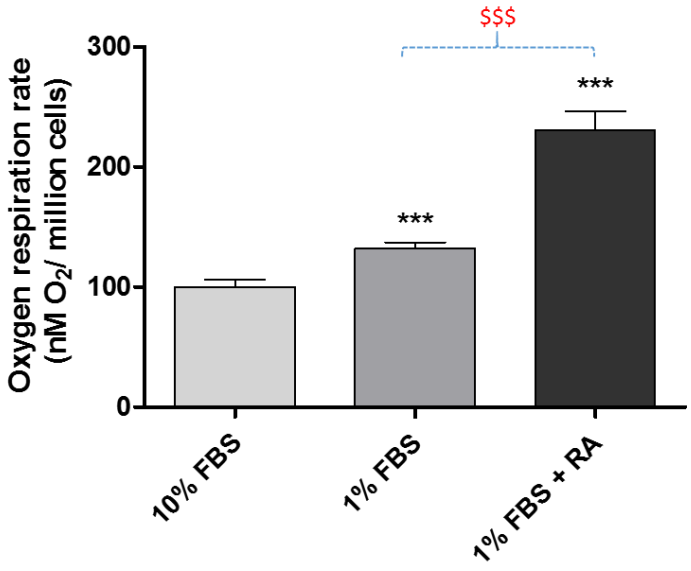

Figure 3.4: Oxygen respiration rate following differentiation. Cell differentiation was induced by either reducing the serum, or by reducing the serum and supplementing daily with 10 nM retinoic acid (RA) for a total period of 6 days. Result presented as mean ± SEM (N=4). ***P < 0.001 vs control. $^{\$\$\$}$P < 0.001 vs 1% FBS.

Based on the above results indicated in part I, it is clear that daily supplementation with RA in addition to serum reduction, has a positive effect on cardiomyoblast differentiation and cardiac specific protein expression. What was also evident with RA supplementation was the promotion of a switch in substrate utilization during the process of differentiation. Although reducing serum also produced similar characteristics, the effects were less pronounced. Since the differentiation of H9c2 represented a better *in vitro* model than undifferentiated cells, this study was not able to establish a homogenous cell population. Even though many cells were differentiated, the majority of them did not. It is therefore for this reason that further experimentation was conducted with undifferentiated H9c2 cardiomyoblast cells.

3.2 PART II: AUTOPHAGY MODULATION DURING CHRONIC DOX CYTOTOXICITY

3.2.1 The effect of autophagy modulation on cell viability

Autophagy is often described as a double edged sword because its stimulation could produce either beneficial or detrimental effects depending on the context. As there are numerous ways in which autophagic activity could be induced, this study used a physiological (starvation), pharmacological (rapamycin) and genetic (siRNA-mTOR) approach. All of the above are recognised scientific methods for stimulation of autophagy. In addition to stimulation, autophagy was inhibited by using bafilomycin A1. Considering that treatment with DOX continued for five consecutive days, this study aimed to maintain upregulated or downregulated autophagy throughout the treatment duration. The best way to do this was to modulate autophagy on days 1, 3 and 5 which coincided with refreshing media.

To determine cell viability in response to the different treatment regimens, this study employed the WST-1 assay. According to the results, autophagy induction by rapamycin and starvation was not detrimental to cells, in fact a trend towards an increase was observed in the starvation group. However, the down regulation of mTOR by siRNA was detrimental, as was DOX treatment (75.6±2.5%, $p<0.001$) and autophagy inhibition by bafilomycin (36.1±2.0%, $p<0.001$) (Fig. 3.5). In combination with DOX, however, bafilomycin (30.6±2.0%, $p<0.001$) and siRNA-mTOR (44.7±3.3%, $p<0.001$) treatment reduced cell viability even further when compared to DOX alone. When DOX was introduced during increased autophagic activity either by rapamycin or starvation treatment, a substantial improvement in cell viability was observed. These results indicate that promoting autophagy before chemotherapy treatment improves cell viability.

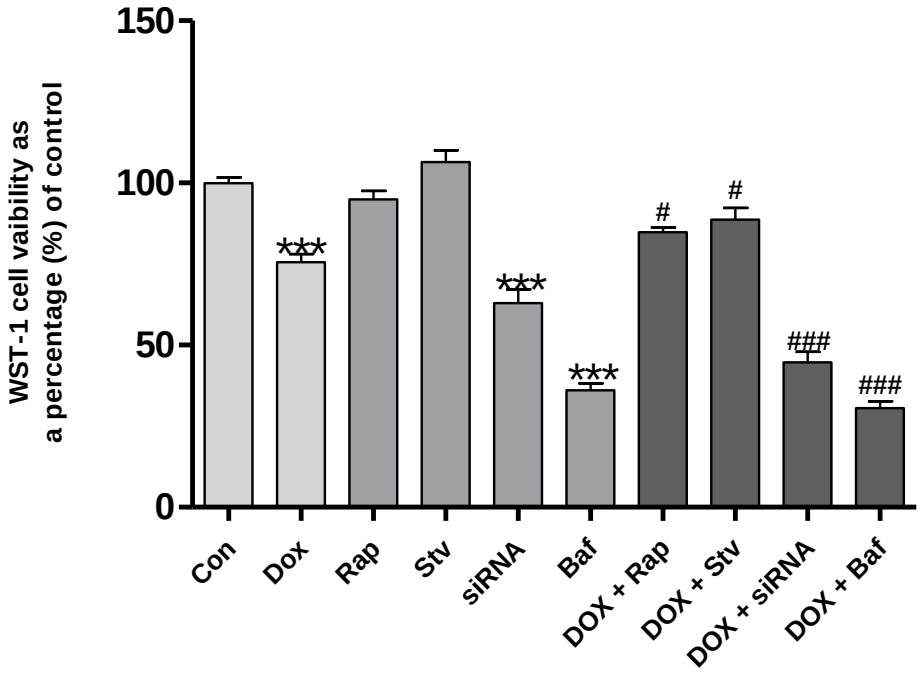

Figure 3.5: Analysis of cell viability following autophagy modulation: Cells either received 25 nM rapamycin, or 50% reduction in amino acid (starvation), or mTOR-siRNA (5 nM) or 1 nM bafilomycin treatment. Additionally, cells were treated daily for 5 days with a 0.2 µM DOX (1 µM cumulative dose). Result presented as mean ± SEM (N=3). ***P < 0.001 vs control. $^{###}$P < 0.001; $^{#}$P < 0.05 vs DOX. Abbreviations: **Con**: Control, **DOX**: doxorubicin, **Rap**: rapamycin, **Stv**: starvation. **siRNA**: siRNA (mTOR), Baf: bafilomycin.

3.2.2 Analysis of cellular apoptosis following autophagy modulation

Depending on the context, autophagy can play different roles when accompanied by other cell death modes. For example autophagy can act together with apoptosis to induce cell death, or autophagy can act against apoptosis to promote survival. Autophagy can also facilitate apoptosis by allowing apoptotic cell death to occur without the cell dying from autophagic cell death (Eisenberg-Lerner *et al*., 2009). Thus to determine apoptotic cell death during autophagy modulation the caspase-glo assay was employed. As expected, DOX treatment significantly increased (138.4±4.962, p<0.001) apoptosis versus the control (100.0±6.2) (Fig. 3.6). Similar results were observed when mTOR alone was downregulated (176.8±2.5%, p<0.001) or in combination with DOX (197.3±9.9%, p<0.001) when compared to the control and DOX groups respectively. Surprisingly, bafilomycin treatment alone (35.5±2.9%, p<0.001) or in combination (23.0±2.3%, p<0.001) produced significantly low apoptotic activity. This does not suggest that autophagy inhibition is beneficial in this context, but rather as a result of low

cell numbers observed during analysis in these groups. Rapamycin treatment alone (57.1±2.5%, p<0.001) or in combination (46.2±0.7%, p<0.001) significantly reduced apoptosis, whereas the combination of starvation with DOX also reduced (70.7±9.1%, p<0.001) apoptotic activity. Therefore based on the results obtained from the cell viability analysis (Fig. 3.5) as well as from the caspase-glo assay (Fig. 3.6), it is evident that stimulating autophagic activity using a genetic approach is detrimental as inhibiting autophagy in the context of DOX-induced cytotoxicity. Thus, for the duration of this study the siRNA and bafilomycin groups will be discontinued.

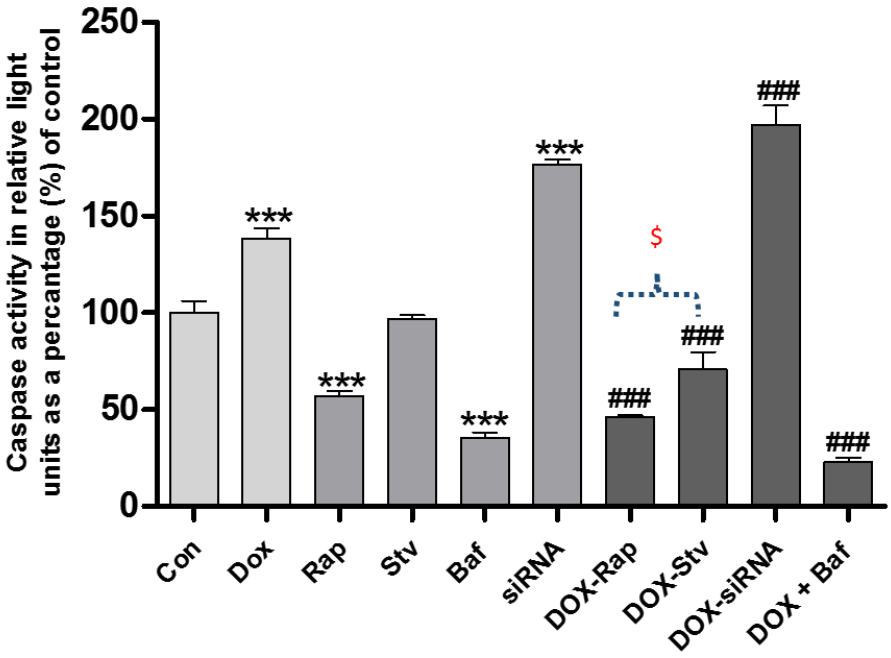

Figure 3.6: Analysis of apoptosis following autophagy modulation: Cells either received 25 nM rapamycin, or 50% reduction in amino acid (starvation), or mTOR-siRNA (5 nM) or 1 nM bafilomycin treatment. Additionally, cells were treated daily for 5 days with a 0.2 µM DOX (1 µM cumulative dose). Result presented as mean ± SEM (N=3). ***P < 0.001 vs control. ###P < 0.001 vs DOX. $P < 0.05 vs DOX-Rap. Abbreviations: **Con**: Control, **DOX**: doxorubicin, **Rap**: rapamycin, **Stv**: starvation, siRNA: siRNA (mTOR), **Baf**: bafilomycin.

3.3 PART III: ASSESSMENT OF AUTOPHAGIC ACTIVITY IN THE CONTEXT OF DOX

3.3.1 Mammalian Target of rapamycin (mTOR) protein expression

Rapamycin and starvation are potent inducers of autophagy and both induce this process through downregulation of mTOR, an upstream inhibitor of autophagy and its dephosphorylation stimulates autophagic activity which leads to the degradation of p62 and increased lipidation of LC3-I to LC3-II. To evaluate the protein expression of the above mentioned markers, western blotting was employed.

Chronic DOX treatment significantly reduced (71.7±3.7%, $p<0.05$) the phosphorylation of mTOR when compared to the control (101.3±11.8%) (Fig. 3.7**A** and **B**). A similar effect was observed when the stimulators of autophagy were used. Although expected, this effect was more pronounced than the DOX group. In the combination groups, mTOR phosphorylation remained downregulated and significance was observed in both the DOX-Rap (50.8±5.0%, $p<0.05$) and DOX-Stv (61.5±1.0%, $p<0.05$) groups.

A)

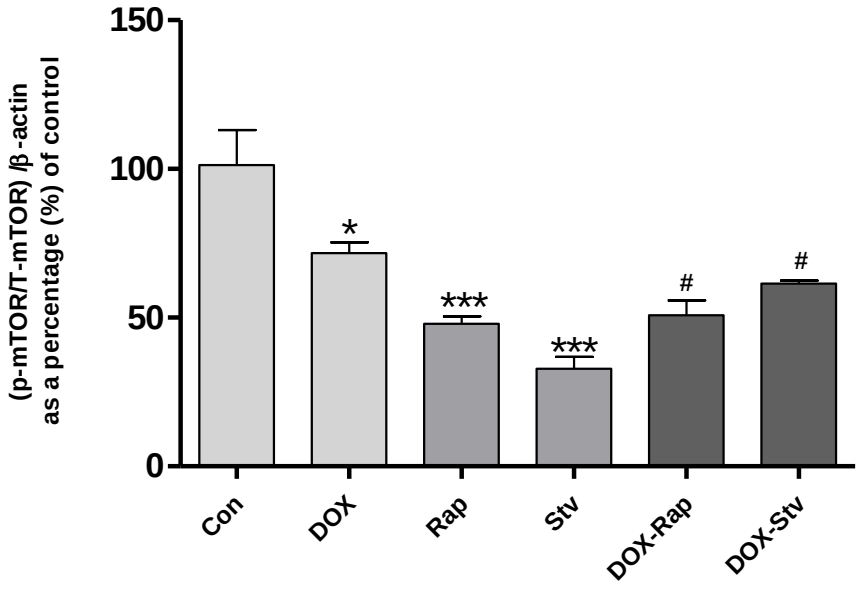

B)

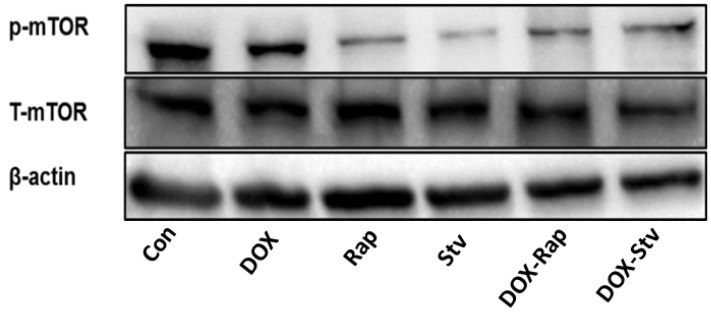

Figure 3.7: The expression of mTOR protein phosphorylation following autophagy induction during chronic DOX treatment. Autophagy was induced using rapamycin (25 nM) and starvation (50% amino acid reduction). Cells were treated with 0.2 µM DOX daily, for 5 days (1 µM cumulative dose). Graph representation **(A)** and western blot image **(B)** for mTOR expression. Result presented as mean ± SEM (N=3) ***P < 0.001;*P < 0.05 vs control. $^{\#}$P < 0.05 vs DOX. Abbreviations: **Con**: Control, **DOX**: Doxorubicin, **Rap**: Rapamycin; **Stv**: starvation

3.3.2 p62/SQSTM 1 protein expression

When autophagic activity is upregulated, p62 is degraded along with the waste material. p62 plays a vital role during autophagy as it acts as an adaptor protein for LC3 to the autophagosome (Itakura & Mizushima, 2011). The degradation of p62 is often used as an indicator of autophagic flux and activity. As seen on Fig. 3.8, DOX treatment resulted in accumulation (132.2±9.9%, $p<0.05$) of p62 suggestive of autophagy inhibition. All other groups in this experiment displayed significantly lower levels of p62 expression when compared to the control or DOX group. The degradation of this protein in these groups indicates autophagic activity.

A)

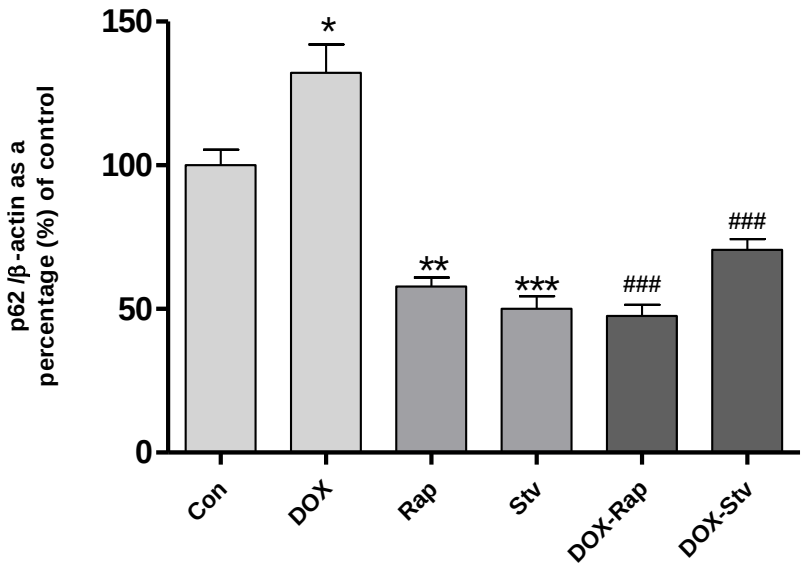

B)

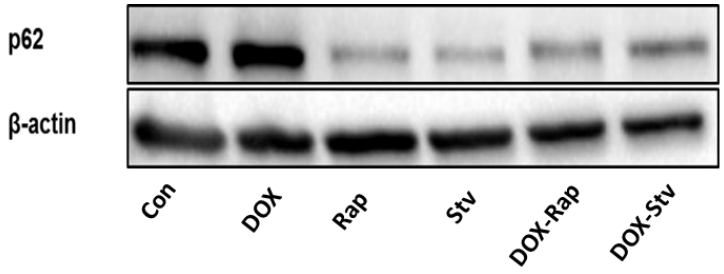

Figure 3.8: The expression of p62 following autophagy induction and chronic DOX treatment. Autophagy was induced using rapamycin (25 nM) and starvation (50% amino acid reduction). Cells were treated daily with 0.2 µM DOX daily, for 5 days (1 µM cumulative dose). Graph representation **(A)** and western blot image **(B)** for p62 expression. Result presented as mean ± SEM (N=3). ***P < 0.001, **P < 0.01; *P < 0.05 vs control. $^{###}$P < 0.05 vs DOX. Abbreviations: **Con**: Control, **DOX**: Doxorubicin, **Rap**: Rapamycin; **Stv**: starvation.

3.3.3 LC3-I and LC3-II protein expression

The culmination of autophagy occurs when LC3-I becomes lipidated into LC3-II. Analysis of this change, is by far the most common method used to determine autophagic activity. Literature indicates two main ways to assess LC3 bands by western blotting: (i) the quantification of LC3-II only or (ii) the quantification of the ratiometric change between LC3-

I and LC3-II. This study chose the latter method as this is regarded more accurate than the former. When evaluating Fig. 3.9**A** it appears as if the DOX group is increasing autophagy in much the same way as rapamycin and starvation groups are. However, when scrutinizing the western blot image (Fig. 3.9**B**), it is clear that there is accumulation of both LC3-I and LC3-II in the DOX group. In the rapamycin and starvation groups, however, there is a clear conversion of LC3-I to LC3-II. In other words, there is less of LC3-I and more of LC3-II. This implies that in the DOX group, flux through the autophagy system is increasing but little or no degradation occurs, when compared rapamycin and starvation groups where degradation is taking place. The DOX-Stv group resulted in significantly less LC3 protein expression than the DOX group and no difference was observed between the DOX-Rap and DOX group.

A)

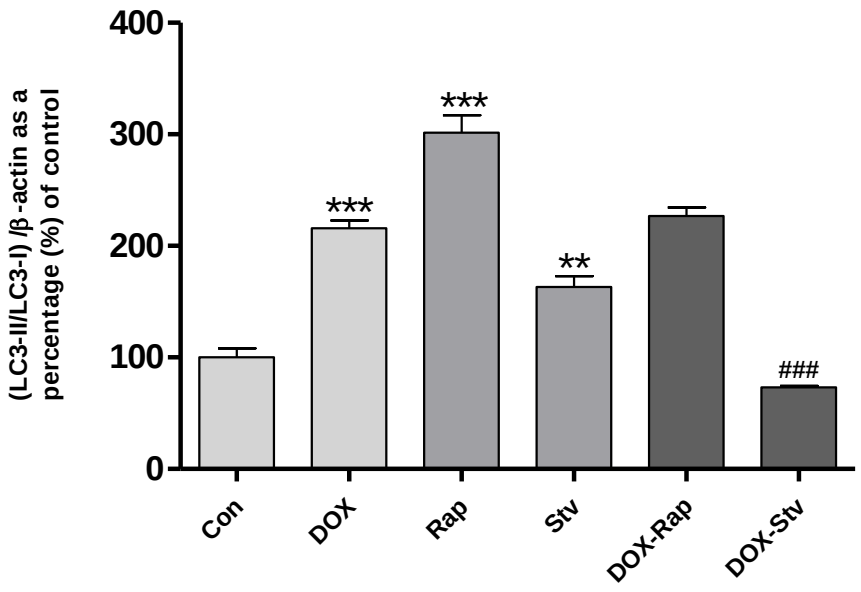

B)

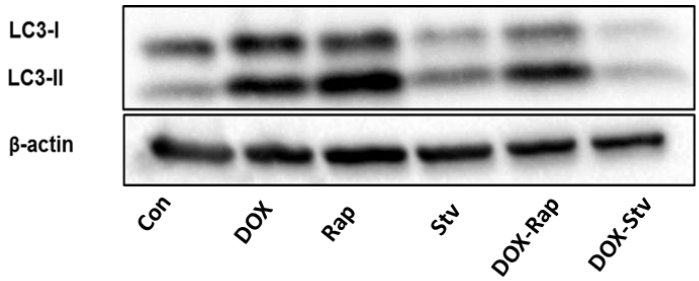

Figure 3.9: The expression of LC3 following autophagy induction and chronic DOX treatment. Autophagy was induced using rapamycin (25 nM) and starvation (50% amino acid reduction). Cells were treated daily with 0.2 µM DOX daily, for 5 days (1 µM cumulative dose). Graph representation **(A)** and western blot image **(B)** for LC3 expression. Result presented as mean ± SEM (N=3). ***P < 0.001, **P < 0.01 vs control. $^{###}$P < 0.001 vs DOX. Abbreviations: **Con**: Control, **DOX**: Doxorubicin, **Rap**: Rapamycin; **Stv**: starvation.

3.4 PART IV: ASSESSING THE THERAPEUTIC POTENTIAL OF AUTOPHAGY INDUCTION IN THE CONTEXT OF CHRONIC DOX CYTOTOXICITY

3.4.1 Mitochondrial morphology

Mitochondria are known as the powerhouses of the cells and their morphology is directly linked to the life and death signals. Considering the amount of mitochondria present in cardiac cells and the affinity that DOX has for these organelles, the preservation of their structure is vital. Normal, "healthy looking" mitochondria are elongated, tubular in structure and consist of an interconnected network, as observed in the control group of Fig. 3.10. Similar results were also observed in the rapamycin and starvation groups. When cells are treated with DOX, the mitochondria appear to have lost their tubular elongated structure and were shortened. Their network seems disrupted and congested suggesting damage. In the groups where autophagy was upregulated in the presence of DOX, a certain degree of damaged mitochondria was observed but this was substantially lower than that observed in the DOX only group.

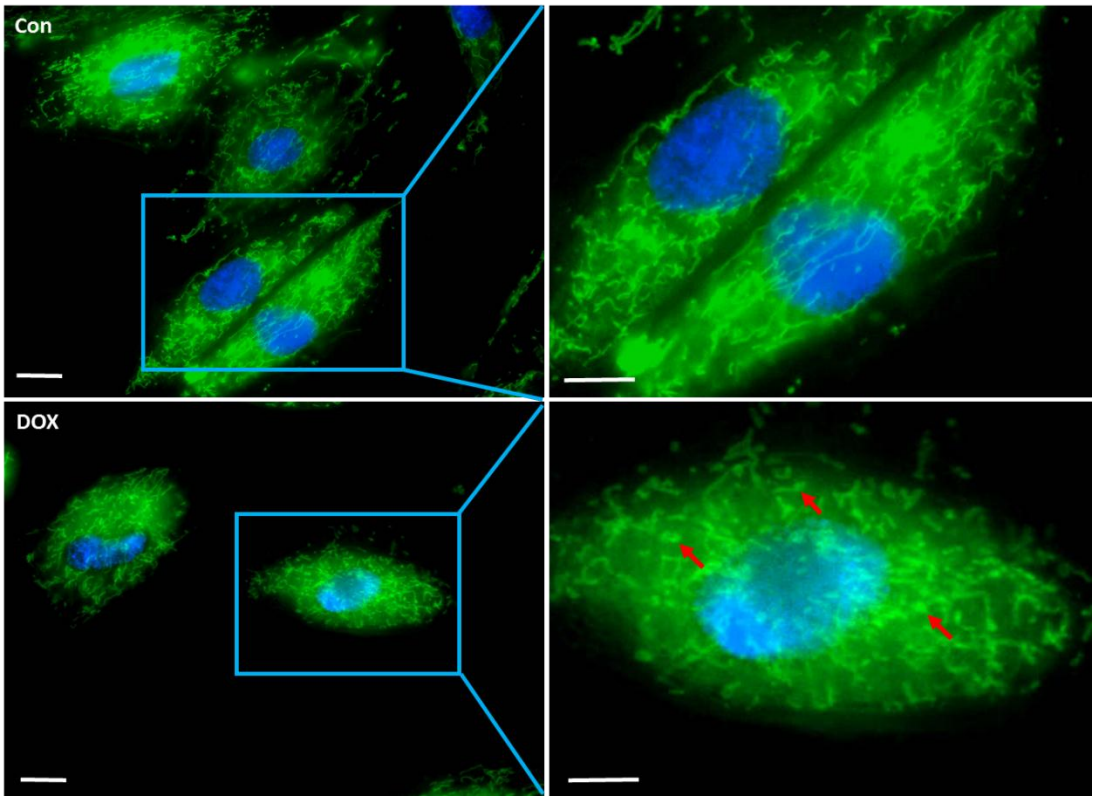

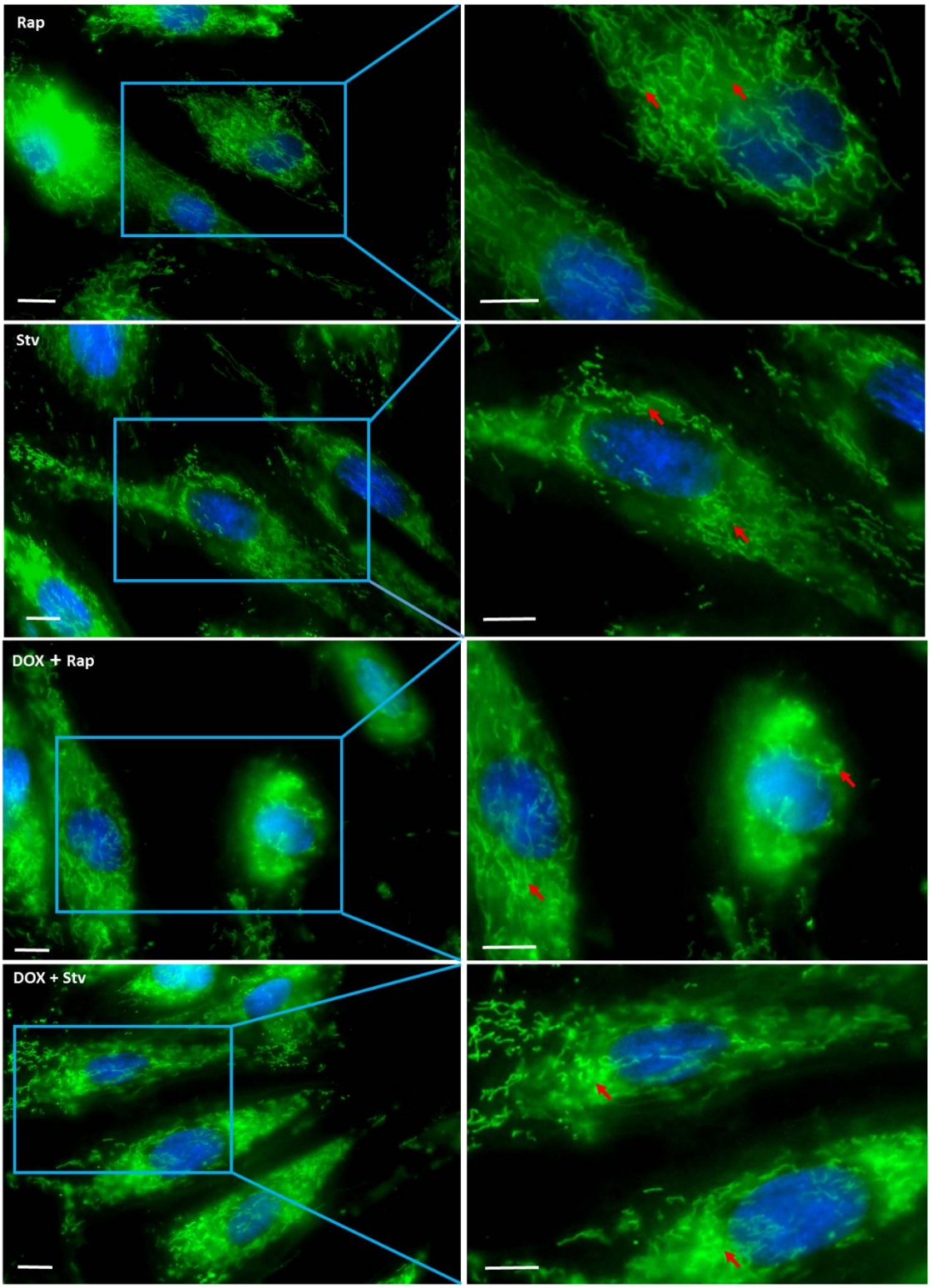

Figure 3.10: Mitochondrial morphology following autophagy induction and chronic DOX treatment. Autophagy was induced using rapamycin (25 nM) and starvation (50% amino acid reduction). Cells were treated daily with 0.2 µM DOX daily, for 5 days (1 µM cumulative dose) (N=3). Red arrows indicate mitochondrial networks. **Green**: mitochondrial network. **Blue**: nuclei. Abbreviations: **Con**: Control, **DOX**: Doxorubicin, **Rap**: Rapamycin; **Stv**: starvation. Magnification = 60x. Scale bar = 20 µm.

3.4.2 Mitochondrial lipid peroxidation as an indicator of oxidative stress

Oxidative stress plays a key role in the damaging effects of DOX, particularly in the myocardium. As the mitochondria are the main contributors of ROS production in a cell, they are often the first structures to get damaged. Damaged mitochondria induce even more ROS, resulting in a vicious cycle. Therefore to determine oxidative stress, mitochondrial lipid peroxidation was investigated using the ratiometric fluorescent probe, MitoPerOX.

Chronic DOX treatment significantly increased lipid peroxidation (149±7.5%, P<0.001) versus the control (100.0±4.2%) group (Fig. 3.11). Autophagy stimulation through the use of starvation reduced (87.7±6.5%, p<0.05) the levels of damaged mitochondria. Although no difference were observed between the DOX-Rap and DOX groups, the starvation combination substantially lowered oxidative damage (111.5±10.1%, p<0.01) when compared to the DOX only group.

A)

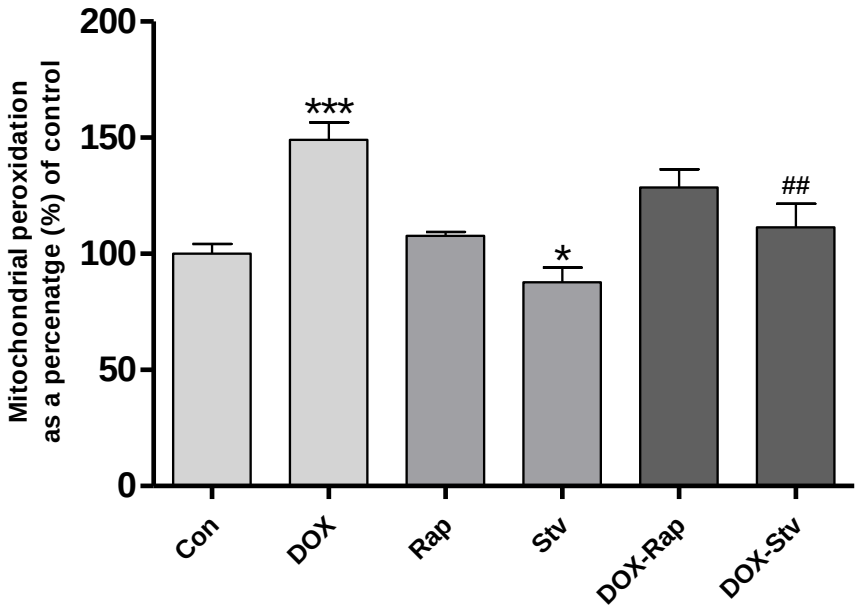

B)

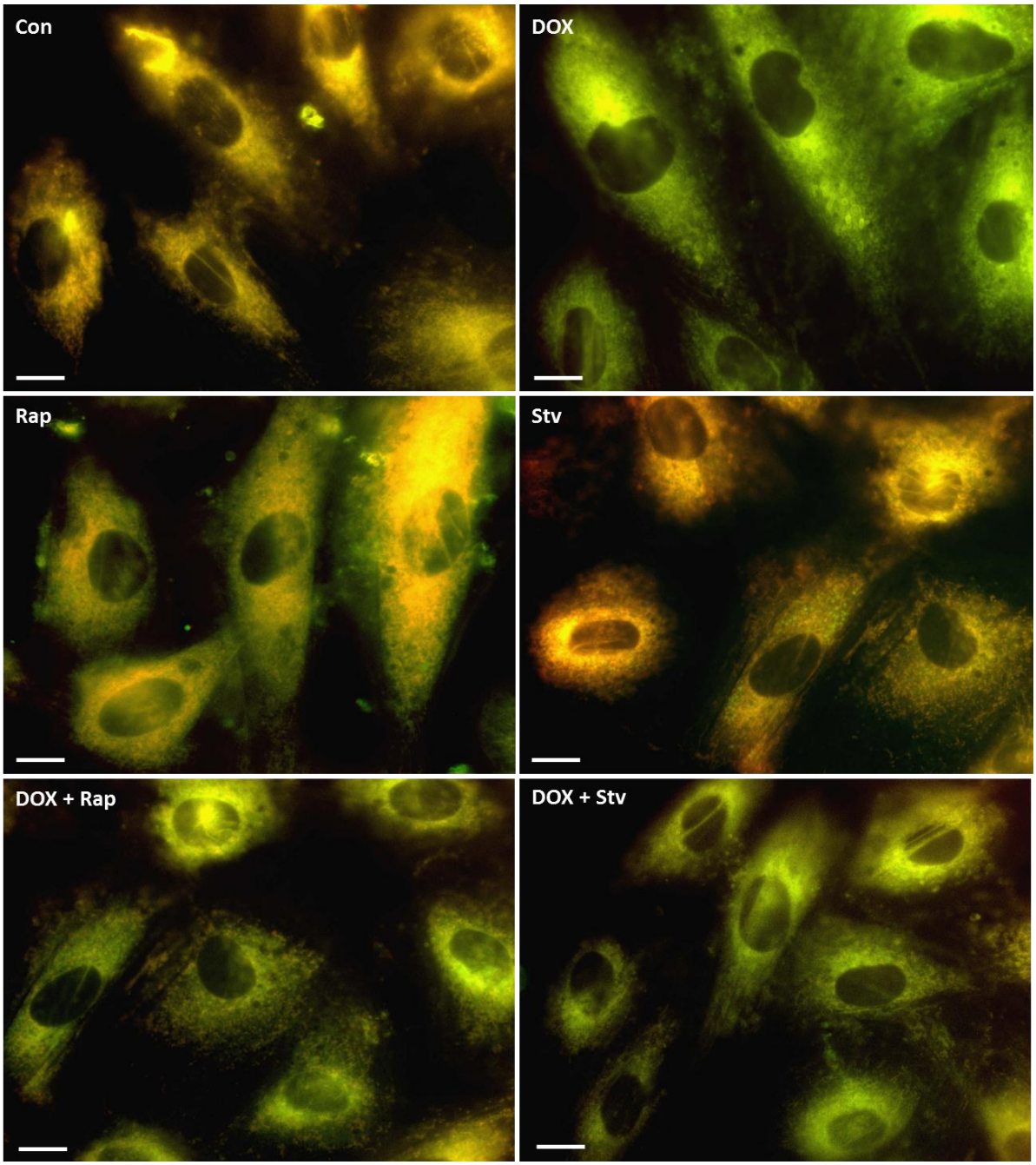

Figure 3.11: Mitochondrial lipid peroxidation assessment. Autophagy was induced using rapamycin (25 nM) and starvation (50% amino acid reduction). Cells were treated daily with 0.2 µM DOX daily, for 5 days (1 µM cumulative dose) (N=3). Bar Graph **(A)** and representative images **(B)** for mitochondrial lipid peroxidation. **Yellow**: low lipid peroxidation levels **Green**: elevated lipid peroxidation levels. Result presented as mean ± SEM (N=3). ***P < 0.001; *P < 0.05 vs control. $^{\#\#}$P < 0.01 vs DOX. Abbreviations: **Con**: Control, **DOX**: Doxorubicin, **Rap**: Rapamycin; **Stv**: starvation: Magnification = 60x. Scale bar = 20 µm.

3.4.3 Assessment of mitochondrial function

To further substantiate the results already obtained in section 3.4.1 and 3.4.2, this study thought it fitting to also investigate mitochondrial function using the popular ratiometric fluorescent probe, JC-1. When mitochondria are hyperpolarized, JC-1 forms orange/reddish adducts, compared to the green colour when mitochondria become depolarized.

Results obtained indicate that DOX treatment reduces (84.3±2.5%, $p<0.01$) mitochondrial function when compared to the control, whereas starvation alone or in combination with DOX and the DOX-Rap groups substantially improved mitochondrial function. These results mimic those observed when mitochondrial morphology was assessed in section. 3.4.1.

A)

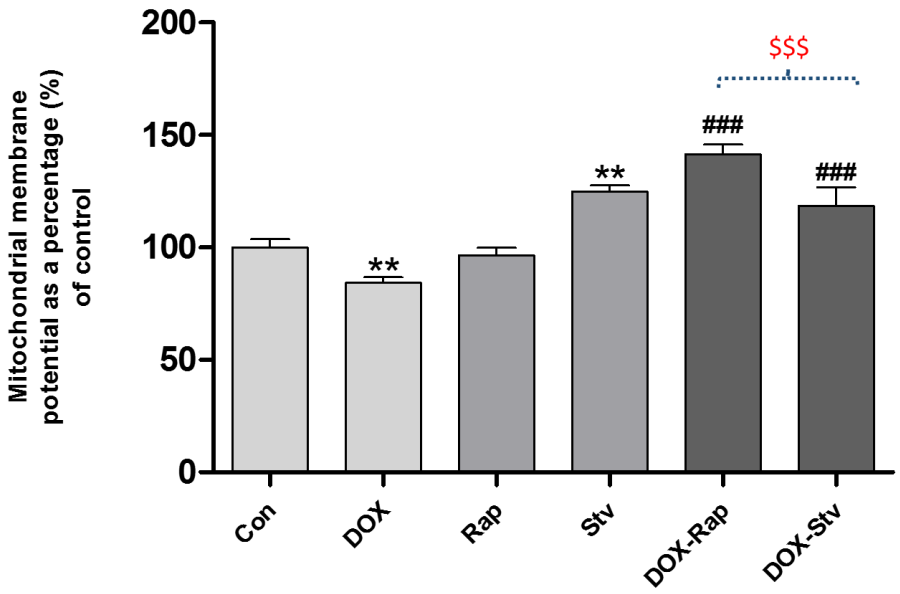

B)

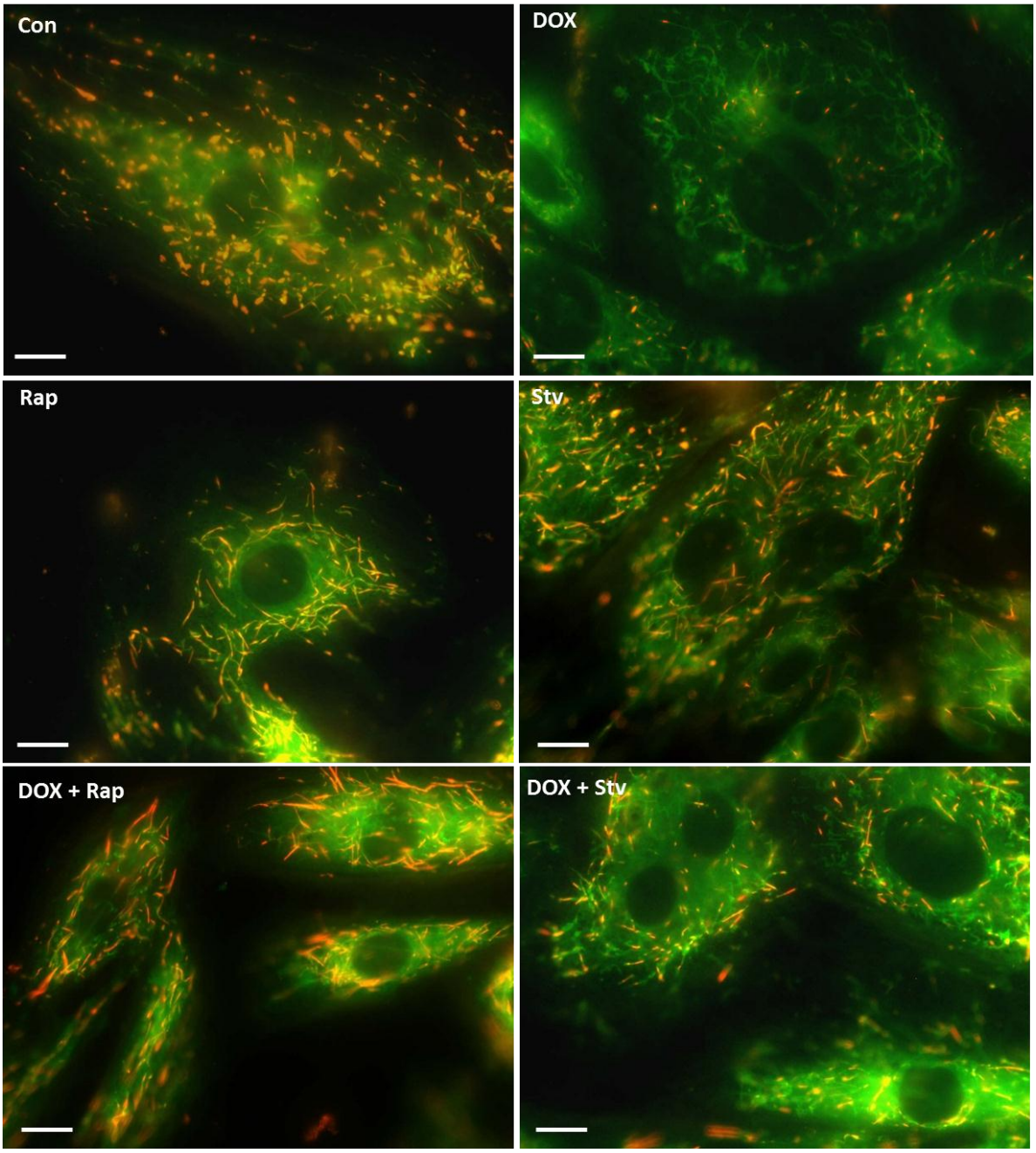

Figure 3.12: The assessment of mitochondrial membrane potential using JC-1. Autophagy was induced using rapamycin (25 nM) and starvation (50% amino acid reduction). Cells were treated daily with 0.2 µM DOX daily, for 5 days (1 µM cumulative dose) (N=3). Bar Graph **(A)** and representative images **(B)** for mitochondrial membrane potential. **Red/orange**: Hyperpolarized mitochondria. **Green**: depolarized mitochondria. Result presented as mean ± SEM (N=3). **P < 0.001 vs control. $^{###}$P < 0.01 vs DOX. Abbreviations: **Con**: Control, **DOX**: Doxorubicin, **Rap**: Rapamycin; **Stv**: starvation: Magnification = 60x. Scale bar = 20 µm.

3.4.4 DOX accumulation

Since DOX is auto-fluorescent, this study took advantage of this characteristic and measured the mean fluorescence intensity, and used it as an indicator of DOX accumulation in these cells. As indicated in the figure and images below, both the DOX-Rap (85.0±2.9%, $p<0.001$) and DOX-Stv (25.9±0.6%, $p<0.001$) groups significantly decreased DOX accumulation when compared to the DOX only group (100±2.3%). Furthermore, autophagy induction by starvation has a greater capacity to reduce DOX accumulation in cells when compared to rapamycin induced autophagy. This possibility suggests that autophagy has the ability to remove DOX molecules inside the cells, potentially utilizing the autophagic vacuoles. Therefore, based on all the results presented in this chapter, it is quite evident that chronic DOX treatment induces its detrimental effects by down-regulating autophagy amongst other mechanisms. Thus, by stimulating autophagic activity before DOX administration, this promoted survival by counteracting DOX's detrimental effects.

A)

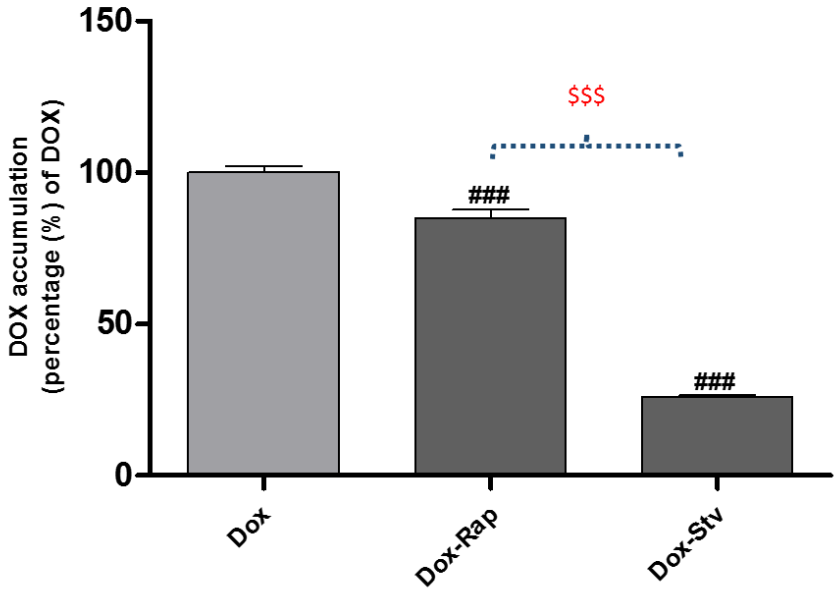

B)

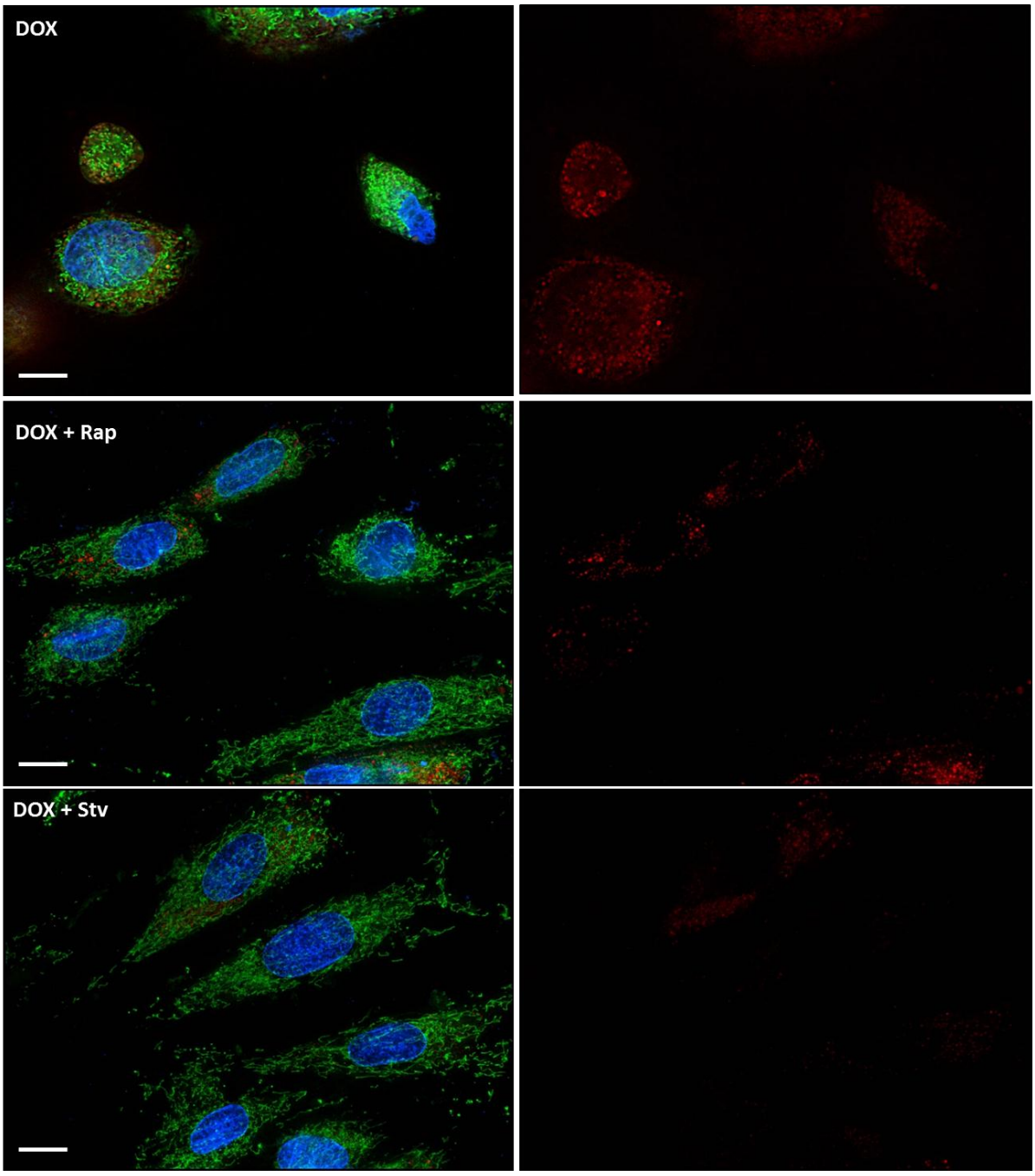

Figure 3.13: Assessment of DOX accumulation. Autophagy was induced using rapamycin (25 nM) and starvation (50% amino acid reduction). Cells were treated daily with 0.2 µM DOX daily, for 5 days (1 µM cumulative dose) (N=3). Bar Graph **(A)** and representative images **(B)** for DOX accumulation in cells. **Red**: DOX. **Green**: mitochondria. **Blue**: nuclei. Result presented as mean ± SEM (N=3). $^{###}$P < 0.01 vs DOX. $^{\$\$\$}$P < 0.001 vs DOX-Rap. Abbreviations: **DOX**: Doxorubicin, **Rap**: Rapamycin; **Stv**: starvation: Magnification = 60x. Scale bar = 20 µm.

4 CHAPTER 4: DISCUSSION

A limited number of cardiomyoblast differentiate during retinoic acid and serum reduction treatment

H9c2 cardiomyoblasts are a commonly used cardiac cell model, however, current literature has criticized their validity and compatibility as an appropriate *in vitro* model versus cardiomyocytes (Comelli *et al*., 2011). These cardiomyoblasts are morphologically and metabolically different from cardiomyocytes, as they do not express cardiac specific proteins such as MLC and cTnT in significant amounts. Moreover, H9c2 cardiomyoblast anti-oxidant capacity is significantly lower than that of cardiomyocytes and they rely on glucose rather than fatty acids as their substrate preference. These differences have previously been reported to affect H9c2 susceptibility to drugs such as DOX and isoprentanol (Branco *et al*., 2012). To overcome this limitation this study induced differentiation by either reducing the serum only or by reducing serum and supplementing with retinoic acid. Numerous studies have previously been able to demonstrate that serum reduction is an effective way to induce cell differentiation particularly in skeletal cells such as C2C12s (Fujita *et al*., 2010). In H9c2, serum reduction allows cardiomyotubes to form and induces the expression of myosin heavy chain (MHC) and MLC (Pereira *et al*., 2011), whereas the addition of RA promotes multinucleated cardiomyotube formation and cardiac troponin expression as observed in this study (Fig. 3.2). RA promotes cardiomyotube formation by activating primary differentiation genes. Activating genes that encode transcriptional factors such as sex determining region Y-box 9 and HomeoBOX A1. These factors modify gene expression during differentiation (Gudas & Wagner, 2011). A number of other key differentiation pathways are also activated by RA, these include the oestrogen and WNT signalling pathways (Osei-Sarfo & Gudas., 2014).

It was evident by day six that there is a clear difference between inducing differentiation by serum reduction only, and daily supplementation with RA in addition to reducing serum. Although RA played a significant role in the expression of cardiac proteins early in the treatment protocol, this effect was lost as the treatment progressed. Interestingly time played more of a significant role in the expression of cardiac markers when serum was reduced, since more expression was observed as the treatment progressed. These results are supported by Comelli and colleagues (2012) who demonstrated a time-dependent effect in cardiac troponin expression. In an effort to increase the differentiation rate, higher concentrations of RA (1 µM) have been used, however, little or no improvement was observed compared to lower concentrations (10 nM) (Branco *et al*., 2012). The advantage of an extended treatment protocol

is evident in the formation of mitochondrial networks and an increase in mitochondrial mass that resembles that of cardiomyocytes (Comelli *et al*., 2012).

This study also showed that although serum reduction alone increased respiration rate, this effect was more pronounced in the presence of RA (Fig. 3.4). Peroxisome proliferator-activated receptor gamma co-activator 1 alpha (PGC-1α) protein expression and greater mitochondrial ATPase synthase activity possibly contributed to this improvement as suggested by Comelli *et al*., (2012). Therefore, although RA in the presence of reduced serum induced H9c2 myoblast differentiation towards a cardiomyotube phenotype, this protocol is hampered by its limited differentiation capacity thus other avenues of H9c2 cardiomyoblast differentiation are necessary or longer differentiation times should be employed. Furthermore, future studies should also consider assessing the fatty acid metabolism profile of mitochondria in differentiated cells as this may be a good indicator of the metabolic switch from glycolysis to oxidative phosphorylation as mitochondria are abundant within myocardial cells.

Rapamycin and starvation treatment prevents DOX inhibition of autophagy

Autophagy is a well characterized and conserved cytoprotective pathway for cellular degradation. Under normal baseline conditions, it represents a vital homeostatic mechanism for maintenance of cardiovascular function, however, in excess it can induce cardiomyopathy by functioning as a death pathway (Nikoletopoulou *et al*., 2013). Although successful therapeutic approaches that have regulated autophagy have been reported, literature has been quite controversial with the context of DOX-induced cardiotoxicity (Dirk-Naylor, 2013). As such, this study utilized numerous mechanisms to upregulate autophagy in order to determine its beneficial effects. It is clear from this study that DOX inhibits autophagic activity in the chronic setting (Fig. 3.7-3.9). This phenomenon has previously been demonstrated by this group, albeit being a short-term study (Sishi *et al*., 2013). Therefore by upregulating autophagy before DOX treatment, this mechanism appears to maintain a certain level of autophagy that is not detrimental to the cells. The mechanism of how DOX inhibits autophagy is poorly understood. However, DOX treatment has been show to downregulate the expression of 5' AMP-activated protein kinase (AMPK), an energy sensing enzyme that inhibits mTOR and induces autophagy under low energy conditions. DOX also downregulates the expression of ULK1 complex, a complex involved in autophagy activation (Kawaguchi *et al*., 2012). The starvation treatment potentially prevented DOX inhibition of autophagy by activating the Rag

GTPase complex, an amino acid sensing complex that inhibits mTOR upon low amino acid concentrations (Russell *et al*., 2014). Furthermore, starvation reduces the overall energy content in cells. The reduction in energy promotes AMPK activation and potentially prevents inhibition of autophagy (Viollet *et al*., 2010). Likewise, rapamycin treatment also achieved similar results. Rapamycin is known to interact with the rapamycin binding domain of FKBP12, a protein that modulates the mTOR complex (Hoeffer *et al*., 2008). This process inhibits mTOR by inducing a conformational change to the complex (Shimobayashi & Hall, 2014), resulting in autophagy upregulation in this context.

Chronic DOX treatment induces apoptosis and decreases cell viability

Autophagy is a naturally occurring process that is responsible for maintaining cellular homeostasis. This is achieved by degrading damaged organelles and proteins and giving a platform for new healthy organelles to be synthesized (Mizushima, 2007). The inhibition of this process has previously been shown to be extremely detrimental in the DOX context (Sishi *et al*., 2013). Likewise, this study showed that autophagy inhibition by bafilomycin treatment reduced cell viability (Fig. 3.5) and promoted cell death (Fig. 3.6). This is, however, expected considering that autophagy inhibition leads to a build-up of damaged proteins and organelles as they cannot be degraded by the autophagic machinery (Zhang, 2013) .This process is further augmented by DOX, as one of the mechanism it uses to induce cytotoxicity is through damaging organelles or promoting protein degradation (Lim *et al*., 2004). Autophagy inhibition by bafilomycin also leads to an accumulation of autophagic vacuoles, a process also previously shown to be detrimental to cell health (Geng *et al*., 2010).

Another mechanism of modulating autophagy is through silencing mTOR using siRNA molecules. The autophagy modulator, siRNA (mTOR) significantly decreased cell viability (Fig 3.6) and increased cell death (Fig 3.5) in this study. A number of studies employing various cancer models have also reported on the detrimental effects of silencing mTOR (Matsubara *et al*., 2012; Liu *et al*., 2011). The differences in the mechanisms of autophagy induction by siRNA (mTOR) versus other inducers is key to understanding why mTOR silencing is not beneficial in this context. siRNA (mTOR) decreases overall mTOR content by targeting and degrading mTOR ribonucleic acid. Whereas rapamycin and starvation inhibit mTOR function, and the process is reversible (Iwamaru *et al*., 2007). Therefore, the degradation of mTOR is detrimental because this complex is responsible for a number of processes except autophagy.

These include cell growth, protein translation and ribosome biogenesis (Watanabe *et al.*, 2011). In the context of this study, inhibition of these key survival processes is detrimental because they are responsible for normal H9c2 myoblast function (Comelli *et al*., 2011). In *in vivo* models, mTOR knockdown animals do not survive the full gestation period, further highlighting the detrimental nature of completely knocking down this protein (Murakami *et al*., 2004; Gangloff *et al*., 2004).

The induction of autophagy by rapamycin or starvation attenuated apoptosis and improved cell viability in this current study. These findings have previously been reported by Sishi *et al*., (2013) and Kawaguchi *et al*., (2012). The mechanisms responsible for the protective nature of autophagy upregulation in this context are not well characterized. However, rapamycin pre-treatment has been reported to reduce the susceptibility of cells to apoptosis that is mediated by opening of the MPT pore (Maiuri *et al*., 2007). It is suggested that autophagy upregulation achieves this by preventing translocation of the pro-apoptotic protein BAX to the mitochondria were it would initiate MPT pore opening, release of cytochrome c and subsequent apoptosis (Deniaud *et al.*, 2008). This is supported by Hamacher-Brady *et al*., 2006 who showed that beclin-1, an autophagy protein inhibits BAX activation. Another known cause of cellular apoptosis in the DOX context is ER stress as it leads to an accumulation of misfolded proteins within the ER lumen (Lu *et al*., 2011). A study by Sen *et al*., 2011 showed that autophagy induction by rapamycin significantly decreased ER stress in hearts subjected to hemodynamic stress, thus suggesting that autophagy upregulation in our context possibly decreased apoptosis by attenuating DOX-induced ER stress. Recent studies using diabetic (Kapuy *et al*., 2014) and cancer (Bachar-Wikstrom *et al*., 2013) models have also reported the reduction of ER stress following autophagy upregulation. The exact mechanism responsible for such beneficial effect is still poorly understood, although a study by Bernales *et al*., 2006 has shown that the selective uptake of damaged ER by autophagy (ER-phagy) is a possible mechanism responsible for this beneficial effects. In actual fact a recent study by Khaminets *et al*., (2015) has reported on the importance of autophagy in maintaining ER turnover, whereby the inability to do this is extremely detrimental as it results in the development of diseases such as sensory neuropathy in neuronal cells (Kurth *et al*., 2009). It is known that DOX also mediates apoptosis by inducing DNA damage. Literature suggests that autophagy induction potentially delays apoptotic signals from DOX-induced DNA damage (Kang *et al*., 2009). Studies have shown that in response to DNA damage, p53 induces transcriptional activation of tuberous sclerosis complex 2 (TSC2) which leads to mTOR inhibition, autophagy induction and ultimately energy production. The

energy produced by autophagy is then used for DNA repair by ATP-dependent DNA; this process attenuates the apoptotic signals from damaged DNA (Kang *et al*., 2009; Martin & MacNeil, 2002). Alexander *et al*., 2010 showed that following DNA breakage, Forkhead box O3 (FOXO3), a transcriptional modulator detaches from the damaged DNA material and activates ATM kinase, an enzyme known to directly control cell cycle and DNA repair. ATM then upregulates autophagy by downregulating mTOR and activating AMPK. Likewise, the energy produced by autophagy is then used by ATM for DNA repair as a means to prevent apoptosis and improve cell viability.

Autophagy upregulation preserves mitochondrial health

The chemotherapeutic drug DOX localizes in the mitochondria because of its high affinity for cardiolipin, an abundant protein in these structures (Volkova *et al*., 2011). Once in the mitochondria it causes morphological changes of these organelles (Sishi *et al*., 2013). Mitochondria become shortened, clustered together and the mitochondrial network is disrupted (Fig. 3.10). These changes in mitochondrial morphology are due to the excessive fragmentation of the mitochondrial filaments which are responsible for maintaining normal mitochondrial structure (Sardao *et a*l., 2009). The excessive accumulation of DOX also leads to mitochondrial oxidative stress, mitochondrial leakage via the MPT pore, loss in mitochondrial function and increased mitochondrial fission (Marechal *et al*., 2011; Lu *et al*., 2009). These factors have been reported to affect mitochondrial morphology, although the exact mechanisms remain unclear (Pyakurel *et al*., 2015). This suggests that autophagy possibly preserved mitochondrial morphology by preventing the detrimental effects of DOX. These include reducing DOX accumulation, mitochondrial oxidative stress and preserving mitochondrial function as demonstrated by this study. Furthermore, the ability of autophagy to prevent opening of the MPT pore as previously described is also a possible mechanism in which mitochondrial morphology was preserved.

Apart from preserving the morphology of mitochondrial, autophagy upregulation also decreased mitochondrial lipid peroxidation (Fig. 3.11). However, it is not clear how autophagy achieves this, although selective uptake of mitochondria by the autophagic machinery (mitophagy) has been proposed as a possible mechanism (Li *et al*., 2013). Mitochondria are the main source of ROS in the DOX cytotoxicity setting, and ROS itself is the main mechanism of mitochondrial damage. It is therefore hypothesized that removal of damaged mitochondria

attenuates ROS production and subsequently reduces mitochondrial lipid peroxidation (Bin-Umer *et al.*, 2014). A recent study by Li *et al.*, 2014 reported that rapamycin treatment reduced mitochondrial damage by activating mitophagy. This was confirmed by increased expression of LC3, beclin-1 and p62 in mitochondrial fractions versus the cytosolic fractions. p62 mediates mitophagy by binding to the ubiquitin molecules found on the surface of damaged mitochondria. LC3 which is located on the outer surface of the autophagosome then attaches to p62, allowing the mitochondria to be engulfed by the autophagic machinery (Kubli & Gustafsson., 2012). A study by Bin-Umer *et al.*, 2014 also concluded that cell starvation increased mitophagy and reduced mitochondrial oxidative stress. This further corroborates the notion that mitophagy is a possible mechanism responsible for decreasing mitochondrial lipid peroxidation following autophagy upregulation in the chronic DOX setting. In our current study, autophagy upregulation also improved mitochondrial function (Fig. 3.12), and this is attributed to the decrease in mitochondrial oxidative stress as shown by the lipid peroxidation results. Other studies have also reported on the improvement of mitochondrial function in cells that received rapamycin or starvation pre-treatment before DOX administration (Kawaguchi *et al.*, 2012; Sishi *et al.*, 2013). As mentioned previously, the autophagy protein beclin-1 inhibits BAX localization to the mitochondria. Inhibition of this process preserves mitochondrial function because BAX directly affects it by promoting opening of the MPT pore (Deniaud *et al.*, 2008).

Except the mitochondria, DOX also localizes in the nucleus, ER and cytosol. Hence chronic DOX treatment lead to an accumulation of DOX in the cells (Fig. 3.13). DOX accumulation in the organelles is detrimental, leading to an accumulation of maladaptive mitochondria and ER (Geng *et al.*, 2010). These maladaptive organelles are sequestered and degraded by the autophagic machinery following rapamycin or starvation treatment (Okamoto, 2014). Therefore during this process, the DOX bound to these organelles is also taken up by the autophagic machinery and possibly degraded, reducing DOX accumulation in the cells as seen in this study. Autophagy also sequestrates cytosolic cargo in a non-specific manner (Mizushima, 2007). Therefore, the DOX located in the cytosol is also taken up by autophagy, contributing to the low levels of DOX following rapamycin or starvation treatment.

5 CHAPTER 5: CONCLUSION

Chronic DOX cardiotoxicity remains a life threating side effect of DOX chemotherapy treatment. A number of adjuvant therapies such as anti-oxidants and iron chelators have been proposed as potential chemotherapeutic interventions. However, these therapies have had limited success clinically. Autophagy, a well-known cellular degradative process responsible for maintaining cellular homeostasis is gaining momentum as potential adjuvant therapy for DOX cardiotoxicity. There is, however, controversy as to whether autophagy inhibition or induction is beneficial in treating this condition.

In order to address this problem, this study assessed the effects of autophagy inhibition or induction in a chronic DOX cytotoxicity model. We have shown that autophagy inhibition by bafilomycin is not beneficial, as it does not prevent the detrimental effects of DOX. In actual fact, this process augments DOX induced cell death. Likewise, we have also shown that the silencing of mTOR is not an ideal therapeutic intervention because of the importance of mTOR signalling in normal cell function.

Our study has also shown that autophagy upregulation by rapamycin, a FDA approved chemotherapeutic drug successfully prevents the detrimental effects of DOX cytotoxicity. This is achieved by preventing DOX from inhibiting autophagy or damaging the mitochondria. However, rapamycin disturbs insulin signalling and promotes insulin resistance and is therefore not ideal for diabetic patients that may also have cancer. It is also for this reason this study investigated whether starvation can be used as a potential adjuvant therapy for DOX cytotoxicity. We have shown that starvation prior to chemotherapy with DOX prevents the detrimental effects associated with DOX. Clinically, starvation has previously been used to sensitize cancers cells to chemotherapeutic treatments, and promising results have been obtained (Safdie *et al*., 2009). However, there is no clinical data available for the effects that starvation may have on chronic DOX cardiotoxicity although short term in vivo studies have demonstrated beneficial effects. This therefore leaves many unanswered questions such as:

- When should starvation be induced in patients (before or during chemotherapy) and for how long?
- The frequency of the starvation (moderate or intermitted, short or long term)?
- Should the starvation period be maintained considering that chronic DOX cardiotoxicity occurs months/years/decades following chemotherapy?
- Would the starvation regimen interfere with DOX's antitumor activity?

- If starvation is found to be protective within this context, which mechanism/s would be responsible for the beneficial effects observed?

Therefore, based on the above, further studies, both preclinical and clinical, should be able to demonstrate the optimal regimen of fasting, confirmation that this regimen does not interfere with the antitumor properties of DOX, as well as the underlying mechanisms exerting the cardioprotective effects.

The main limitation of our study still remains the fact that we were not able to differentiate enough H9c2 cardiomyoblasts into cardiomyotubes. However, this is an ongoing study and the *in vitro* section served as a proof of concept to assess if autophagy induction or inhibition is beneficial in a chronic DOX setting. Therefore the next step in this project is to assess the effects of autophagy upregulation by rapamycin and starvation *in vivo*. We potentially also want to further assess a number of mitochondrial parameters in the *in vivo* model, because mitochondria were implicated as a key factor determining cell fate in this current study. The findings from this study and the future animal study will contribute immensely to the process of trying to find adjuvant therapies against chronic DOX cardiotoxicity.

6 REFERENCES

Alexander, A., Kim, J. & Walker, C.L. 2010. ATM engages the TSC2/mTORC1 signalling node to regulate autophagy. *Autophagy*. 6(5): 672–673

Alexieva, B., Sainova, I., Pavlova, V., Markova, T.Z., Valkova, I. & Nikolova, E. 2014. Insights into Mechanisms of Doxorubicin Cardiotoxicity. J*ournal of physiology and pharmacology advances*. 4(3): 342-348

Ambrosy, P.A., Fonarow, G.C, Butler, J., Chioncel, O., Greene, S.J., Vaduganathan, M., Nodari, S., Lam, C.S., Sato, N., Shah, A.N. & Gheorghiade, M. 2014. The global health and economic burden of hospitalizations for heart failure: lessons learned from hospitalized heart failure registries. *American journal of cardiology*. 63(12): 1123-1133

Arai, M., Yoguchi, A., Takizawa, T., Yokoyama, T., Kanda, T., Kurabayashi, M. & Nagai, R. 2000. Mechanism of DOX-induced inhibition of sarcoplasmic reticulum Ca^{2+}-ATPase gene transcription. *Circulatory research*. 86(1): 8–14.

Bachar-Wikstrom, E., Wikstrom, J.D., Ariav, Y., Tirosh, B., Kaiser, N., Cerasi, E. & Leibowitz, G. 2013. Stimulation of autophagy improves endoplasmic reticulum stress-induced diabetes**.** *Diabetes.* 62(4): 1227-1237

Bae, S., Ma. K., Kim. H.T., Lee, E.S., Oh, K.T., Park, E.S., Lee, K.C. & Youn, Y.S. 2012. Doxorubicin-loaded human serum albumin nanoparticles surface-modified with TNF-related apoptosis-inducing ligand and transferrin for targeting multiple tumor types. *Biomaterials.* 33(5): 1536-1546

Bennet, M.R. 2002, Apoptosis in the cardiovascular system. *Heart*. 87(5): 480-487

Bernales, S., McDonald, K.L. & Walter, P. 2006. Autophagy counterbalances endoplasmic reticulum expansion during the unfolded protein response. *PLoS biology*. 4(12): e423

Berthiaume, J.M., Oliveira, P.J., Fariss, M.W. & Wallace, K.B. 2005. Dietary vitamin E decreases doxorubicin-induced oxidative stress without preventing mitochondrial dysfunction. *Cardiovascular toxicology*. 5(3): 257-267

Bertin, P.A., Smith, D. & Nguyen, S.T. 2005. High-density doxorubicin-conjugated polymeric nanoparticles via ring-opening metathesis polymerization. *Chemical communications.* 14 (30): 3793-3795

Bin-Umer M.A., McLaughlin, J.E., Butterly, M.S., McCormick, S. & Tumer, N.E. 2014. Elimination of damaged mitochondria through mitophagy reduces mitochondrial oxidative stress and increases tolerance to trichothecenes. *Proceedings of the national academy of sciences*. 111(32): 11798-11803

Boucek, R.J. 1998. Mechanism for anthracycline induced cardiomyopathy: clinical and laboratory correlations. *Progress in paediatric cardiology.* 8(2): 59-70

Branco, A.F., Sampaio, S.F., Moreira, A.C., Holy, J., Wallace, K.B., Baldeiras, I., Oliveira, P.J. & Sardão, V.A. 2012. Differentiation-dependent doxorubicin toxicity on H9c2 cardiomyoblasts. *Cardiovascular toxicology*. 12(4): 326-340

Brigger, I., Dubernet, C. & Couvreur.P. 2002. Nanoparticles in cancer therapy and diagnosis. *Advanced drug delivery reviews*. 54(3): 631–651

Bristow, M. R., Mason, J. W., Billingham, M. E. & Daniels, J. R. 1978. Doxorubicin cardiomyopathy: evaluation of phonocardiography, endomyocardial biopsy, and cardiac catheterization. *Annals of internal medicines*. 88(2): 168-175.

Cairo, G. & Pietrangelo, A. 2000. Iron regulatory proteins in pathobiology. *Biochemical journal*. 352(2): 241–250

Carafoli, E. 1985. The homeostasis of calcium in heart cells. *Journal of Molecular and Cellular Cardiology*. 17(3): 203–212

Carreira, R.S., Monteiro, P., Gon Alves, L.M & Providencia, L.A. 2006. Carvedilol: Just another beta blocker or a powerful cardioprotector. *Cardiovascular and haematological disorders-drug target*. 6(4): 257-266

Castro-Ferreira, R., Fontes-Carvalho, R., Falcão-Pires, I. & Leite-Moreira A.F. 2011. The role of titin in the modulation of cardiac function and its pathophysiological implications. *Arquivos brasileiros de cardiologia*. 96(4): 332-339

Chatterjee, K., Zhang, J., Honbo, N. & Karlinerb, J.S. 2010. Doxorubicin Cardiomyopathy. *Cardiology*. 115(2): 155–162

Chen, K., Xu, X., Kobayashi, S., Timm, D., Jepperson, T. & Liang, Q. 2011. Caloric restriction mimetic 2-deoxyglucose antagonizes doxorubicin-induced cardiomyocyte death by multiple mechanisms. *Journal of biological chemistry*. 286(25): 1993–2006

Chinnaiyan, A. M., O'Rourke, K., Yu, G. L., Lyons, R. H., Garg, M., Duan, D. R., Xing, L., Gentz, R., Ni, J. & Dixit, V.M. 1996. Signal transduction by DR3, a death domain-containing receptor related to TNFR-1 and CD95. *Science.* 274(5289): 990–992

Comelli, M., Domenis, R., Bisetto, E., Contin, M., Marchini, M., Ortolani, F., Tomasetig, L. & Mavelli, I. 2011. Cardiac differentiation promotes mitochondria development and ameliorates oxidative capacity in H9c2 cardiomyoblasts. *Mitochondrion*. 11(2): 315-326

Communal, C., Sumandea. M., de Tombe, P., Narula, J., Solaro, R.J. & Hajjar, R.J. 2002. Functional consequences of caspase activation in cardiac myocytes. *Proceeding of national academy of science*. 99(9): 6252-6256

Cross, A.R. & Jones, O. T. 1991. Enzymatic mechanisms of superoxide production. *Biochima et biophysica acta*. 1057(3): 281-298

Davies, K.J. & Doroshow, J.H. 1986. Redox cycling of anthracycline by cardiac mitochondria. I. Anthracycline radical formation by NADH dehydrogenase. *Journal of biological chemistry*. 261(7): 3060-3067

Davis, M.E. 2009. The first targeted delivery of siRNA in humans via a self-assembling cyclodextrin polymer-based nanoparticle: from concept to clinic. *Molecular pharmaceutics*. 6(3): 659-668

Deniaud, A., Sharaf el dein, O., Maillier, E., Poncet, D., Kroemer, G., Lemaire, C. & Brenner C. 2008. Endoplasmic reticulum stress induces calcium-dependent permeability transition, mitochondrial outer membrane permeabilization and apoptosis. *Oncogene*. 27(3): 285–299.

Dimitrakis, P., Romay-Ogando, M.I., Timolati, F., Suter, T.M. & Zuppinger, C. 2012. Effects of doxorubicin cancer therapy on autophagy and the ubiquitin-proteasome system in long-term cultured adult rat cardiomyocytes. *Cell tissue research*. 350(2): 361–372

Dirks-Naylor, A.J. 2013. The role of autophagy in doxorubicin-induced cardiotoxicity. *Life sciences*. 93(13): 913–916

Edinger, A. L. & Thompson, C. B. 2004. Death by design: apoptosis, necrosis and autophagy. *Current opinion in cell biology*. 16(6): 663–669

Eisenberg-Lerner, A., Bialik, S., Simon, H.U. & Kimchi, A. 2009. Life and death partners: apoptosis, autophagy and the cross-talk between them. *Cell death and differentiation*. 16(7). 966–975

Firuzi, O., Miri, R., Tavakkoli, M. & Saso, L. 2011. Antioxidant Therapy: Current Status and Future Prospects. *Current medicinal chemistry*. 18(25): 3871-3888

Follis, A.V. Chipuk, J.E., Fisher, J.C. Yun, M., Grace, C.R., Nourse, A., Baran, K., Ou, L., Min. L., White, S.W., Green, D.R. & Kriwacki, R.W. 2013. PUMA binding induces partial unfolding within BCL-xL to disrupt p53 binding and promote apoptosis. *Nature chemical biology*. 9(3): 163-168

Forrest, G. L., Akman, S., Doroshow, J., Rivera, H. & Kaplan, W. D. 1991. Genomic sequence and expression of a cloned human carbonyl reductase gene with daunorubicin reductase activity. *Molecular pharmacolo*gy. 40(4): 502-507

Frishman, W. H., Sung, H. M., Yee, H. C., Linda, L., Keefe, D., Einzig, A.L. & Dutcher, J. 1997. Cardiovascular toxicity with cancer chemotherapy. *Current problems in cancer*. 21(6): 301- 360

Fujita, H, Endo, A., Shimizu, K. & Nagamori, E. 2010. Evaluation of serum-free differentiation conditions for C2C12 myoblast cells assessed as to active tension generation capability, *Biotechnology and bioengineering*. 107(5): 894-901

Gangloff, Y.G., Mueller, M., Dann, S.G., Svoboda, P., Sticker, M., Spetz, J.F., Um, S.H., Brown, E.J., Cereghini, S., Thomas, G. & Kozma, S.C. 2004. Disruption of the mouse mTOR gene leads to early postimplantation lethality and prohibits embryonic stem cell development. *Molecular cell biology*. 24(21): 9508–9516

Geng,Y,, Kohli, L., Klocke, B.J. & Roth, K.A. 2010. Chloroquine-induced autophagic vacuole accumulation and cell death in glioma cells is p53 independent. *Neuro-oncology*. 12(5): 473-481

Gharib, M. & Burnett, A.K. 2002. Chemotherapy-induced cardiotoxicity: current practice and prospects of prophylaxis. *European journal of heart failure*. 4(3): 235-42.

Giergiel, M. & Kankoff. M. 2015. Age and sex related changes in superoxide dismutase activity in bovine tissues. *Czech journal of animal science*. 60(8): 367-374

Glick, D., Barth, S. & Macleod, KF. 2010. Autophagy: cellular and molecular mechanisms. *Journal of pathology*. 221(1): 3–12

Goorin, A.M., Chauvenet, A.R., Perez-Atayde, A.R., Cruz, J., McKone, R. & Lipshultz, S.E. 1999. Initial congestive heart failure, six to ten years after doxorubicin chemotherapy for childhood cancer. *Clinical and laboratory observations.* 116(1): 145-147

Goormaghtigh, E., Huart, P., Praet, M., Brasseur, R. & Ruysschaert, J.M. 1990. Structure of the adriamycin-cardiolipin complex. Role in mitochondrial toxicity. *Biophysical chemistry*. 35(2): 247-257.

Green, D. & Kroemer, G. 1998. The central executioners of apoptosis: caspase or mitochondria. *Trends in cell biology*. 8(7): 267-271

Greene, R.F., Collins, J.M., Jenkins, J.F., Speyer, J.L. & Myers, C.E. 1983. Plasma pharmacokinetics of adriamycin and adriamycinol: implications for the design of in vitro experiments and treatment protocols. *Cancer Research* 43:3417–3421

Greiner, M.A. & Lipschultz, S.E. 1998. Epidemiology of anthracycline cardiotoxicity in children and adults. *Seminar oncology.* 25(10):72–85

Gudas, L.J & Wagner, J.A. 2011. Retinoids regulate stem cell differentiation. *Journal of cell physiology*. 226(2): 322-330

Halliwell, B. & Gutteridge, J. (2007). Free Radicals in Biology and Medicine. Oxford university press, ISBN978-0-19-856869-8, London, U.K.

Hamacher-Brady, A., Brady, N.R. & Gottlieb, R.A. 2006. Enhancing macroautophagy protects against ischemia/reperfusion injury in cardiac myocytes *Journal of biological chemistry*. 281(40): 29776–29787

Harake, D., Franco, V.I., Henkel, J.M., Miller, T.L. & Lipshultz, S.E. 2012. Cardiotoxicity in childhood cancer survivors: strategies for prevention and management. *Future cardiology*. 8(4): 647-670

Harris, L., Batist, G., Belt, R., Rovira, D., Navari, R., Azarnia, N., Welles, L. & Winer, E. 2002. Liposome-encapsulated doxorubicin compared with conventional doxorubicin in a randomized multicenter trial as first-line therapy of metastatic breast carcinoma. *Cancer*. 94(1): 25-36.

Hein. S., Arnon. E., Kostin, S., Schönburg, M., Elsässer, A., Polyakova, V., Bauer, E.P., Klövekorn, W.P & Schaper, J. 2003. Progression from compensated hypertrophy to failure in the pressure-overloaded human heart: structural deterioration and compensatory mechanisms. *Circulation*. 107(7): 984–991.

Hoeffer, C.A., Tang, W., Wong, H., Santillan, A., Patterson, R.J., Martinez, L.A., Tejada-Simon, M.V., Paylor, R., Hamilton, S.L. & Klann, E. 2008. Removal of FKBP12 enhances mTOR-Raptor interactions, LTP, memory, and perseverative/repetitive behaviour. *Neuron*. 60(5): 832-845

Hydock, D.S., Karen, Y. Wonders, K.Y. Schneider, C.M. & Hayward, R. 2009. Voluntary Wheel Running in Rats Receiving Doxorubicin: Effects on Running Activity and Cardiac Myosin Heavy Chain. *Anticancer research*. 29(11): 4401-4407.

Ichikawa, Y., Ghanefar, M., Bayeva1, M., Wu, R., Khechaduri, A., R, Sathyamangla, V., Prasad, N., Mutharasan, R.K., Naik, TJ & Ardehali, H. 2014. Cardiotoxicity of doxorubicin is mediated through mitochondrial iron accumulation. *Journal of clinical investigation*. 124(2): 617–630

Immordino, M.A., Dosio, F. & Cattel. L. Stealth liposomes: review of the basic science, rationale, and clinical applications, existing and potential. *International journal of nanomedicine*. 1(3): 297–315

Indu, R., Azhar, T.S., Nair, A. & Nair, C.K. 2014. Amelioration of doxorubicin induced cardio and hepato-toxicity by carotenoids. *Journal of clinical research*. 10(1): 62-67

Itakura, E. & Mizushima, N. 2011. p62 targeting to the autophagosome formation site requires self-oligomerization but not LC3 binding. *Journal of cell biology*. 192(1): 17-27

Iwamaru, A., Kondo, Y., Iwado, E., Aoki, H., Fujiwara, K., Yokoyama, T., Mills, G.B & Kondo, S. 2007. Silencing mammalian target of rapamycin signaling by small interfering RNA enhances rapamycin-induced autophagy in malignant glioma cells. *Oncogene*. 26(13): 1840-1851

Janes, K.A., Fresneau, M.P. Marazuela, A., Fabra, A & Alonso, M.J. 2011. *Journal of controlled release* .Chitosan nanoparticles as delivery systems for doxorubicin. 73 (2): 255-267

Jang, Y.M., Kendaiah, S., Drew, B., Phillips, T., Selman, C., Julian, D & .Leeuwenburgh, C. 2004. DOX treatment in vivo activates caspase-12 mediated cardiac apoptosis in both male and female rats. *FEBS letter*. 577(3): 483-490

Kalay, N. Basar, E., Ozdogru, I., Er, O., Cetinkaya, Y., Dogan, A., Inanc, T., Oguzhan, A., Eryol, N.K., Topsakal, R. & Ergin, A. Protective effects of carvedilol against anthracycline-induced cardiomyopathy. *Journal of american college of cardiology*. 48(11): 2258-2262

Kang, K.B., Zhu, C., Yong, S.K., Gao, Q. & Wong, M.C. 2009. Enhanced sensitivity of celecoxib in human glioblastoma cells: Induction of DNA damage leading to p53-dependent G1 cell cycle arrest and autophagy. *Molecular cancer research*. 25(8): 66-82

Kanter, P.M. Bullard, G.A. Ginsberg, R.A., Pilkiewicz, F.G., Mayer, L.D., Cullis, P.R. & Pavelic. Z.P. 1993. Comparison of the cardiotoxic effects of liposomal doxorubicin (TLC D-99) versus free doxorubicin in beagle dogs. *In vivo.* 7(1):17-26

Kapuy, O., Vinod, P.K. & Bánhegyi, G. 2014. mTOR inhibition increases cell viability via autophagy induction during endoplasmic reticulum stress - An experimental and modelling study. *FEBS open bio*. 4(1): 704-13

Kawaguchi, T., Takemura, G., Kanamori, H., Takeyama, T., Watanabe, T., Morishita, K., Morishita, K., Ogino, A., Tsujimoto,A Goto, K., Maruyama,R., Kawasaki, M., Mikami,A., Fujiwara, T., Hisayoshi., Fujiwara, H. & Minatoguchi. S. 2012. Prior starvation mitigates acute DOX cardiotoxicity through restoration of autophagy in affected cardiomyocytes. *Cardiovascular research*. 96(3): 456-465.

Khaminets, A., Heinrich, T., Mari, M., Grumati, P., Huebner, A.K., Akutsu, M., Liebmann, L., Stolz, A., Nietzsche, S., Koch, N., Mauthe, M., Katona, I., Qualmann, B., Weis, J., Reggiori, F., Kurth, I., Hübner, C.A. & Dikic, I. Regulation of endoplasmic reticulum turnover by selective autophagy. *Nature*. 522(7556): 354-368

Kiyomiya, K., Matsuo, S. & Kurebe, M. 2001. Mechanism of specific nuclear transport of adriamycin: the mode of nuclear translocation of adriamycin-proteasome complex. *Cancer research.* 61(6): 2467-2471

Kobayashi, S., Volden, P., Timm, D. Mao, K., Xu. X. & Liang, Q. 2010. Transcription factor GATA4 inhibits doxorubicin-induced autophagy and cardiomyocyte death. *The journal of biological chemistry*. 285(1): 793-804

Kolwicz, S.C., Purohit, S. & Tian, R. 2013. Cardiac Metabolism and its Interactions with Contraction, Growth, and Survival of Cardiomyocytes. *Circulation research*. 113(5): 603-616

Kubli, D.A. & Gustafsson, A.B. 2012. Mitochondria and Mitophagy: The Yin and Yang of Cell Death Control. *Circulation Research*. 111 (9): 1208-1221

Kurth, I., Pamminger, T., Hennings, J.C., Soehendra, D., Huebner, A.K., Rotthier, A., Baets, J., Senderek, J., Topaloglu, H., Farrell, S.A., Nürnberg, G., Nürnberg, P., De Jonghe,

P., Gal, A., Kaether, C., Timmerman, V. & Hübner, C.A. 2009. Mutations in FAM134B, encoding a newly identified Golgi protein, cause severe sensory and autonomic neuropathy. *Nature genetics.* 41(11): 1179–1181

Kwiatkowskia, D.J. & Wagle, N. 2015. mTOR Inhibitors in Cancer: What Can We Learn from Exceptional Responses. *E-biomedicine*. 2(1): 2-4

Ky, B., Putt, M., Sawaya, H., French, B., Januzzi, J.L., Sebag, I.A., Plana, J.C., Cohen, V., Banchs, J., Carver, J.R., Wiegers, S.E., Martin, R.P., Picard, M.H., Gerszten, R.E., Halpern, E.F., Passeri, J., Kuter, I. & Scherrer-Crosbie, M. 2014. Early increases in multiple biomarkers predict subsequent cardiotoxicity in patients with breast cancer treated with doxorubicin, taxanes, and trastuzumab. *Journal of the american college of cardiology*. 63(8): 809-816

Langer, S.W. 2014. Dexrazoxane for the treatment of chemotherapy related side effects. *Cancer management research*. 6(1): 357–363.

Laplante, M. & Sabatini, D.M. 2009. mTOR signalling at a glance. *Journal of cell science*. 122(20): 3589-3594

Lebrecht, D. & Walker U.A. 2007. Role of mtDNA lesions in anthracycline cardiotoxicity. *Cardiovascular Toxicology*. 7(2): 108–113

Lefrak, E. A., Pitha, J., Rosenheim, S. & Gottlieb, J. A. 1973. A clinicopathologic analysis of Adriamycin cardiotoxicity. *Cancer*. 32(2): 302–314

Li, B., Kim do, S., Yadav, R.K., Kim, H.R. & Chae, H.J. 2015. Sulforaphane prevents doxorubicin-induced oxidative stress and cell death in rat H9c2 cells. *International journal of molecular medicine*. 36(1):53-64

Li, L., Chen, Y. & Gibson, S.B. 2013. Starvation-induced autophagy is regulated by mitochondrial reactive oxygen species leading to AMPK activation *Cell signalling*. 25(1): 50-65

Li, Q., Zhang, T., Wang, J., Zhang, Z., Zhai, Y., Yang, G.Y. & Sun, X. 2014. Rapamycin attenuates mitochondrial dysfunction via activation of mitophagy in experimental ischemic stroke. *Biochemical and biophysical research communications*. 444(2):182-188

Li, T., Danelisen, I., Belló-Klein, A. & Singal, P.K. 2000. Effects of probucol on changes of antioxidant enzymes in adriamycin-induced cardiomyopathy in rats. Cardiovascular research. 46(3):523-30

Li, T., Danelisen, I. & Singal, P.K. 2002. Early changes in myocardial antioxidant enzymes in rats treated with adriamycin. *Molecular and cellular biochemistry*. 232(1): 19-26

Lien, Y., Lin, M., Nithipongvanitch, R., Oberley, T.D., Noel, T., Zhao, Q., Daosukho, C. & St Clair, D.K. 2006. Tumor necrosis factor receptor deficiency exacerbated adriamycin-

induced cardiomyocytes apoptosis: an insight into the fas connection. *Molecular cancer therapeutics*. 5(2): 261-269

Lim, C.C., Zuppinger, C., Guo, X., Kuster, G.M., Helmes, M., Eppenger, H.M., Suter, T.M., Liao, R. & Sawyer, D.B. 2004. Anthracyclines induce calpain-dependent titin proteolysis and necrosis in cardiomyocytes. *The journal of biological chemistry*. 279(9): 8290-8299

Liu, J., Zheng, H., Tang, M., Ryu, Y.-C. & Wang, X. 2008. A therapeutic dose of doxorubicin activates ubiquitin-proteasome system-mediated proteolysis by acting on both the ubiquitination apparatus and proteasome. *American Journal of Physiology-Heart and Circulatory Physiology*. 295(1): 2541-2550

Lin, Y., Vatner, D.E., Kim, S.J., Ge, H., Masurekar, M., Massover, W.H., Yang, G., Matsui, Y., Sadoshima, J. & Vatne, S.F. 2005. Autophagy in chronically ischemic myocardium. *Proceedings of the national academy of sciences of the United States of America*. 102 (39): 13807–13812.

Lipshultz, S.E., Alvarez, J.A. & Scully, R.E. 2008. Anthracycline associated cardiotoxicity in survivors of childhood cancer. *Heart*. 94(4): 525-33.

Lipshultz, S.E., Lipsitz, S.R., Mone, S.M., Goorin, A.M., Sallan, S.E., Sanders, S.P., Orav, E.J., Gelber, R.D. & Colan, S.D. 1995. Female sex and drug dose as risk factors for late cardiotoxic effects of doxorubicin therapy for childhood cancer. *The New England journal of medicine*. 332(26): 1738-1743.

Liu, M.Y., Hou, G.Q., Zhang, Y., Bei, W.J., Yan, A.H. 2011. Effects of mTOR siRNA on mTOR/p70S6K signaling pathway in esophageal squamous cell carcinoma cells and the growth of transplanted tumor in nude mice. *Zhonghua zhong liu za zhi*. 33(5): 334-339

Lopaschuk, G. D., Spafford, M. A. & Marsh, D. R. 1991.Glycolysis is predominant source of myocardial ATP production immediately after birth. *American journal of physiology*, 261(6): 1698–1705

Lopaschuk, G.D. & Jaswal, J. S. 2010. Energy metabolic phenotype of the cardiomyocyte during development, differentiation, and postnatal maturation. *Journal of cardiovascular pharmacology*. 56(2): 130–140.

Lorusso, D., Di Stefano. A., Carone, V., Fagotti, A., Pisconti, S. & Scambia, G. 2007. Pegylated liposomal doxorubicin-related palmar-plantar erythrodysesthesia (‘hand-foot’ syndrome). *Annals of oncology*. 18(7): 1159–1164

Lotrionte, M., Palazzoni, G., Abbate, A., Marco, E., Mezzaroma, E., Di Persio, S., Frati, G., Loperfido, F. & Biondi-Zoccai, G. 2013. Cardiotoxicity of a non-pegylated liposomal doxorubicin-based regimen versus an epirubicin-based regimen for breast cancer: The LITE (Liposomal doxorubicin–Investigational chemotherapy–Tissue Doppler imaging

Evaluation) randomized pilot study. *International journal of cardiology*.167(3): 1055-1057.

Lu, L., Wu, W., Yan, J., Li, X., Yu, H. & Yu, X. 2009. Adriamycin-induced autophagic cardiomyocyte death plays a pathogenic role in a rat model of heart failure. *International journal of cardiology*. 134(1): 82-90.

Lu, M., Merali, S., Gordon, R., Jiang, J., Li, Y., Mandeli, J., Duan, X., Fallon, J. & Holland, J.F. 2011. Prevention of Doxorubicin cardiopathic changes by a benzyl styryl sulfone in mice. *Genes cancer*. 2(10): 985-992

Maiuri, M.C., Zalckvar, E., Kimchi, A. & Kroemer, G. 2007. Self-eating and self-killing: crosstalk between autophagy and apoptosis. *Nature reviews molecular cell biology*. 8(9): 741-752

Marechal, X., Montaigne, D., Marciniak, C., Marchetti, P., Hassoun, S.M., Beauvillain, J.C., Lancel, S. & Neviere, R. 2011. Doxorubicin-induced cardiac dysfunction is attenuated by ciclosporin treatment in mice through improvements in mitochondrial bioenergetics. *Clinical science*. 121(9): 405-413

Martin, I.V. MacNeill, S.A. 2002. ATP-dependent DNA ligases. *Genome biology*. 3(4): 351-357

Matsubara, H., Sakakibara, K., Kunimitsu, T., Matsuoka, H., Kato, K., Oyachi, N., Dobashi, Y. & Matsumoto, M. 2012. Non-small cell lung carcinoma therapy using mTOR-siRNA. International *Journal of clinical and experimental pathology*. 5(2): 119-125

Minotti, G., Menna, P., Salvatorelli, E., Cairo, G. & Gianni, L. 2004. Anthracyclines: Molecular advances and pharmacologic developments in antitumor activity and cardiotoxicity. *The american society for pharmacology and experimental therapeutics.* 56(2): 185-229

Minotti, G., Recalcati, S., Liberi, G., Calafiore, A. M., Mancuso, C., Preziosi, P. & Cairo, G. 1998. The secondary alcohol metabolite of DOX irreversibly inactivates aconitase/iron regulatory protein-1 in cytosolic fractions of human myocardium. *FASEB journal*. 12(7): 541–551

Minotti, G., Ronchi, R., Salvatorelli, E., Menna, P. & Cairo, G. 2001. Doxorubicin irreversibly inactivates iron regulatory proteins 1 and 2 in cardiomyocytes: evidence for distinct metabolic pathways and implications for iron-mediated cardiotoxicity of antitumor therapy. *Cancer research*. 61(23): 8422-8428

Mizushima, N. 2007. Autophagy: process and function. *Genes and development*. 21(22): 2861-2873

Mozaffarian, D., Benjamin, E.J., Go, A.S., Arnett, D.K., Blaha, M.J, Cushman, M., de Ferranti, S., Després, J.P., Fullerton, H.J., Howard, V.J., Huffman, M.D., Judd, S.E., Kissela, B.M., Lackland, D.T., Lichtman, J.H., Lisabeth, L.D., Liu, S., Mackey, R.H.,

Matchar, D.B., McGuire, D.K., Mohler, E.R., Moy, C.S., Muntner, P., Mussolino, M,E., Nasir, K., Neumar, R.W., Nichol, G., Palaniappan, L., Pandey, D.K., Reeves, M.J., Rodriguez, C.J., Sorlie, P.D., Stein, J., Towfighi, A., Turan, T.N., Virani, S.S., Willey, J.Z., Woo, D., Yeh, R.W & Turner, M.B. 2015. American Heart Association Statistics Committee and Stroke Statistics Subcommittee. Heart Disease and Stroke Statistics—2015 Update. A Report from the American Heart Association. *Circulation*. 131(4): 29-322

Mross, K., Maessen, P., van der Vijgh, W.J., Gall, H., Boven, E. & Pinedo, H.M. 1988. Pharmacokinetics and metabolism of epidoxorubicin and doxorubicin in humans. *Journal of clinical oncology* 6(1): 517–526

Murakami, M., Ichisaka, T., Maeda, M., Oshiro, N., Hara, K., Edenhofer, F., Kiyama, H., Yonezawa, K. & Yamanaka, S. 2004. mTOR is essential for growth and proliferation in early mouse embryos and embryonic stem cells. *Molecular and cellular biology*. 24 (15): 6710–6718

Nakamura, T., Ueda, Y., Juan, Y., Katsuda, S., Takahashi, H & Koh, E. 2000. Fas mediated apoptosis in Adriamycin induced cardiomyopathy in rats: in vivo study. *Circulation*. 102(5): 572-578

Nakayama, H., Chen, X., Baines, C.P., Klevitsky, R., Zhang, X., Zhang, H., Jaleel, N., Chua, B.H., Hewett, T.E., Robbins, J., Houser, S.R. & Molkentin J.D. 2007. Ca^{2+} and mitochondrial-dependent cardiomyocyte necrosis as a primary mediator of heart failure. *Journal of clinical investigation*. 117(9): 2431-2444.

Nikoletopoulou, V., Markaki, M., Palikaras, K. & Tavernarakis, N. 2013. Crosstalk between apoptosis, necrosis and autophagy. *Biochim biophys acta*. 1833(12): 3448-3459

O'Brien, M.E., Wigler, N., Inbar, M., Rosso, R., Grischke, E., Santoro, A., Catane, R., Kieback, D.G., Tomczak, P., Ackland, S.P., Orlandi, F., Mellars, L., Alland, L. & Tendler, C. 2004. CAELYX Breast Cancer Study Group.Reduced cardiotoxicity and comparable efficacy in a phase III trial of pegylated liposomal doxorubicin HCl (CAELYX™/Doxil) versus conventional doxorubicin for first-line treatment of metastatic breast cancer. *Annals of oncology*. 15(3): 440-449.

Octavia, Y., Tocchetti, C.G., Gabrielson, K.L., Janssens, S., Crijns, H.J. & Moens A.L., 2012. Doxorubicin-induced cardiomyopathy: from molecular mechanisms to therapeutic strategies. *Journal of molecular and cellular cardiology*. 52(6): 1213-1225.

Okamoto, K. 2014. Organellophagy: eliminating cellular building blocks via selective autophagy. *Journal of cell biology*. 205(4): 435-445

Oliveira, P.J. Bjork, J.A., Santos, M.S., Leino, R.L., Froberg, M.K., Moreno, A.J. & Wallace K.B. 2004. Carvedilol-mediated antioxidant protection against doxorubicin-induced cardiac mitochondrial toxicity. *Toxicology and applied pharmacology*. 200(2): 159-168.

Osei-Sarfo, K. & Gudas, L.J. 2014. Retinoic acid suppresses the canonical Wnt signaling pathway in embryonic stem cells and activates the noncanonical Wnt signaling pathway. *Stem cells*. 32(8): 2061-2071

Park, J., Fong, P.M. & Lu, J. 2009. PEGylated PLGA nanoparticles for the improved delivery of doxorubicin. *Nanomedicine: nanotechnology, biology, and medicine.* 5(4): 410–418

Pereira, S.L., Ramalho-Santos, J., Branco, A.F., Sardão, V.A., Oliveira, P.J. & Carvalho R.A. 2011. Metabolic remodelling during H9c2 myoblast differentiation: relevance for in vitro toxicity studies. *Cardiovascular toxicology*. 11(2): 180-90

Petrelli, F., Borgonovo, K. & Barni, S. 2010. Targeted delivery for breast cancer therapy: the history of nanoparticle-albumin-bound paclitaxel. *Expert opinion on pharmacotherapy*. 11(8):1413-1432.

Pfeffer, B., Tziros, C. & Katz, R.J. 2009. Current concepts of anthracycline cardiotoxicity: pathogenesis, diagnosis and prevention. *The british journal of cardiology*. 16(2): 85-89

Prezioso, L. Tanzi, S., Galaverna, F., Frati, C., Testa, B., Savi, M., Graiani, G., Lagrasta, C., Cavalli, S., Galati, S., Madeddu, D., Lodi Rizzini, E., Ferraro, F., Musso, E., Stilli, D., Urbanek, K., Piegari, E., De Angelis, A., Maseri, A., Rossi, F., Quaini, E & Quaini F. 2010. Cancer Treatment-Induced Cardiotoxicity: a Cardiac Stem Cell Disease. *Cardiovascular & hematological agents in medicinal chemistry*. 8(1): 55-75.

Pyakurel, A., Savoia, C., Hess, D. & Scorrano, L. 2015. Extracellular regulated kinase phosphorylates mitofusin 1 to control mitochondrial morphology and apoptosis. *Molecular cell*. 58(2): 244-254

Rossini, L., Monti, E., Cova, D., & Piccinini, F. 1986. Determination of doxorubicin and doxorubicin-3-ol in rat heart. *Archives of Toxicology*. *Supplement* 9: 474–478.

Rubinstein, A. D., Eisenstein, M., Ber, Y., Bialik, S. & Kimchi, A. 2011. The autophagy protein Atg12 associates with anti-apoptotic Bcl-2 family members to promote mitochondrial apoptosis. *Mol. cell.* 44(5): 698-709.

Russell, R.C., Yuan, H.X. & Guan, K.L. 2014. Autophagy regulation by nutrient signalling. *Cell Research*. 24(1): 42-57

Ryu, H.S., Chang, K.H., Chang, S.J., Kim, M.S., Joo, H.J. & Oh, K.S. Expression of TRAIL (TNF-related apoptosis-inducing ligand) receptors in cervical cancer. *International journal of gynaecological cancer*. 10(5): 417-424

Safdie, F.M., Dorff, T., Quinn, D., Fontana, L., Wei, M., Lee, C., Cohen, P. & Longo, V.D. 2009. Fasting and cancer treatment in humans: A case series report. *Aging*. 1(12): 988-1007

Sardão, V.A., Oliveira, P.J., Holy, J., Oliveira, C.R. & Wallace, K.B. 2009. Morphological alterations induced by doxorubicin on H9c2 myoblasts: nuclear, mitochondrial, and cytoskeletal targets. *Cell biology and toxicology*. 25(3): 227-243

Sen, S., Guthrie, P. & Taegtmeyer, H. 2011. Rapamycin Relieves ER Stress and Improves Function in Hearts Subjected to High Workload. *Federation of american societies for experimental biology*. 25 (2011): 1907-1918

Shi, Y., Moon, M., Dawood, S., McManus, B.A. & Liu, P.P. 2011. Mechanisms and management of doxorubicin cardiotoxicity. *Herz.* 36(6): 296–305

Shimobayashi, M. & Hall, M.N. 2014. Making new contacts: the mTOR network in metabolism and signalling crosstalk. *Nature reviews molecular cell biology.* 15(3): 155-162

Shimomura. H., Terasaki, F., Hayashi, T., Kitaura, Y., Isomura, T. & Suma. H., 2001. Autophagic degeneration as a possible mechanism of myocardial cell death in dilated cardiomyopathy. *Japanese circulation journal*. 65(1): 965–968.

Šimùnek, T., Štìrba, M., Popelová, O., Adamcová, M., Hrdina, R. & Geršl, V. 2009. Anthracycline-induced cardiotoxicity: Overview of studies examining the roles of oxidative stress and free cellular iron. *Pharmacological reports.* 61(1): 154–171

Singal, P.K., Siveski-Iliskovic, N., Hill, M., Thomas, P.T & Li, T. 1995. Combination therapy with probucol prevents Adriamycin-induced cardiomyopathy. *The Journal of Molecular and cellular cardiology*. 27(4): 1055–1063.

Sishi, B.J.N. Loos, B., van Rooyen, J. & Engelbrecht, A. 2013. Autophagy upregulation promotes survival and attenuates DOX-induced cardiotoxicity. *Biochemical pharmacology.* 85(1): 124-134

Smuder, A.J., Kavazis, A.N., Min, K. & Powers, S.K. 2013. Doxorubicin-induced markers of myocardial autophagic signalling in sedentary and exercise trained animals. *Journal of applied physiology.* 115(2): 176–185

Speyer, J. L., Green, M. D., Zeleniuch-Jacquotte, A., Wernz, J. C., Rey, M., Sanger,J., Kramer, E., Ferrans, V., Hochster, H., Meyers, M., Blum, R. H., Feit, F., Attubato, M.,Burrows, W. & Muggia, F. M. 1992. ICRF-187 permits longer treatment with doxorubicin in women with breast cancer. *Journal of clincal Oncology*. 10(1): 117-127

Steven, R. & Steinhubl, M.D. 2008. Why have antioxidants failed in clinical trials. *American journal of cardiology*. 101(10): 14-19

Su, M., Mei, Y & Sinha, S. 2013. Role of the crosstalk between autophagy and apoptosis in cancer. *Journal of oncology*. 2013 (2013): 1-14

Swain, S. M., Whaley, F. S. & Ewer, M. S. 2003. Congestive heart failure in patients treated with doxorubicin. A retrospective analysis of three trials. *Cancer*. 97(11): 2869-79

Swain, S. M., Whaley, F. S., Gerber, M.C., Weisberg, S., York, M., Spicer, D., Jones, S. E., Wadler, S., Desai, A., Vogel, C., Speyer, J., Mittelman, A., Reddy, S., Pendergrass, K., Velez-Garcia, E., Ewer, M.S. & Bianchine, J.R, Gams RA (1997a) Cardioprotection with dexrazoxane for doxorubicin-containing therapy in advanced breast cancer. *Journal of clinical oncology*. 15(4): 1318–1322

Swain, S.M., Whaley, F. S., Gerber, M.C., Ewer, M.S., Bianchine, J. R. & Gams, R. A. (1997b). Delayed administration of dexrazoxane provides cardioprotection for patients with advanced breast cancer treated with doxorubicin-containing therapy. *Journal of clinical oncology*. 15(4): 1333–1340

Swarnakar, N.K., Thanki, K. & Jain, S. 2014.Enhanced antitumor efficacy and counterfeited cardiotoxicity of combinatorial oral therapy using Doxorubicin- and Coenzyme Q10-liquid crystalline nanoparticles in comparison with intravenous Adriamycin. *Nanomedicine*. 10(6): 1231-1241

Tacar, O., Sriamornsak, P. & Dass, C.R. 2013. Doxorubicin: an update on anticancer molecular action, toxicity and novel drug delivery systems. *Journal of pharmacy and pharmacology*. 65(2): 157-170

Takemura, G. & Fujiwara, H. 2007. Doxorubicin-Induced Cardiomyopathy: From the Cardiotoxic Mechanisms to Management. *Progress in cardiovascular diseases.* 49(5): 330–352

Tebbi, C.K., London, W.B., Friedman, D., Villaluna, D., De Alarcon, P.A., Constine, L.S., Mendenhall, N.P., Sposto, R., Chauvenet, A. & Schwartz, C.L. 2007. Dexrazoxane-associated risk for acute myeloid leukemia/myelodysplastic syndrome and other secondary malignancies in pediatric Hodgkin's disease. *Journal clinical oncology.* 25(5): 493–500.

Torres, V.M. & Simic, V.D. 2012. Doxorubicin-induced oxidative injury of cardiomyocytes do we have right strategies for prevention. *Cardiotoxicity of oncologic treatment.* Prof. Manuela Fiuza (Ed.), ISBN: 978-953-51-0273-1.

Vergely, C., Delemasure, S., Cottin, Y. & Rochette, L. 2006. Preventing the cardiotoxic effects of anthracyclines: from basic concepts to clinical data. *Ann cardiol angeiol*. 55(2): 104-12

Viollet B., Horman, S., Leclerc, J., Lantier, L., Foretz, M., Billaud, M., Giri, S. & Andreelli. 2010. AMPK inhibition in health and disease. *Critical reviews in biochemistry and molecular biology*. 45(4): 276-295

Viswanatha-Swamy, A.H., Wangikar, U., Koti, B.C., Thippeswamy, A.H., Ronad, P.M. & Manjula, D.V. 2011. Cardioprotective effect of ascorbic acid on doxorubicin-induced myocardial toxicity in rats. *Indian journal of pharmacology*. 43(5): 507-511

Volkova, M. & Russell, RI. 2011. Anthracycline Cardiotoxicity: Prevalence, Pathogenesis and Treatment. *Current cardiology reviews*. 7(4): 214–220.

Von Hoff, D.D., Layard, M.W., Basa, P., Davis, H.L, Von Hoff, A.L., Rozencweig, M. & Muggia, F.M: 1979. Risk factors for doxorubicin-induced congestive heart failure. *Annals of internal medicine*. 91(5): 710-717

Wahab, M.H., Akoul, E.S. & Abdel-Aziz, A.A. 2000. Modulatory effects of melatonin and vitamin E on doxorubicin-induced cardiotoxicity in Ehrlich ascites carcinoma-bearing mice. *Tumori*. 86(2): 157-162.

Wallace K.B. 2007. Adriamycin-induced interference with cardiac mitochondrial calcium homeostasis. *Cardiovascular toxicology*. 7(2):101–107.

Wang, J. & Pantopoulos, K. Regulation of cellular iron metabolism. *Biochemical journal*. 2011. 434(3): 365-381

Wang, X., Wang, X., Chen, H., Wu, D., Chen J.X., Wang, X.X., Li, R.L., He, J.H., Mo, L., Cen, X., Wei, Y.Q. & Jiang, W. 2014. Ghrelin inhibits doxorubicin cardiotoxicity by inhibiting excessive autophagy through AMPK and p38-MAPK. *Biochemical pharmacology*.88 (3): 334–350

Wanga, B., Yingxin, M., Konga, X., Ding, X., Gu, H., Chu, T. & Ying, W. 2004. NAD+ administration decreases doxorubicin-induced liver damage of mice by enhancing anti-oxidant capacity and decreasing DNA damage. *Chemico-biological interactions*. 5(212): 65-71

Watanabe, R., Wei, L. & Huang, J. 2011. mTOR signalling, function, novel inhibitors, and therapeutic targets. *Journal of nuclear medicine*. 52(4): 497-500

Xu, X., Chen, K., Kobayashi, S., Timm, D. & Liang, Q. 2012. Resveratrol attenuates doxorubicin-induced cardiomyocyte death via inhibition of p70 S6 kinase 1-mediated autophagy. *Journal of pharmacology and experimental therapeutics*. 341(1): 183–195

Xu, X., Sutak, R. & Richardson, D.R. 2008. Iron chelation by clinically relevant anthracyclines: alteration in expression of iron regulated genes and atypical changes in intracellular iron distribution and trafficking. *Molecular pharmacology*. 73(3): 833-844

Yacoub, T.J., Reddy, A.S. & Szleifer, I. 2011. Structural effects and translocation of doxorubicin in a DPPC/Chol bilayer: the role of cholesterol. *Biophysical journal*. 101(2): 378-385

Yen, H.C., Oberley, T.D., Vichitbandha, S., Ho, Y.S & St Clair D.K. 1996. The protective role of manganese superoxide dismutase against adriamycin-induced acute cardiac toxicity in transgenic mice. *Journal of clinical investigation*. 98(5): 1253–1260.

Yoshida, M., Shiojima, I., Ikeda, H. & Komuro. I., 2009. Chronic doxorubicin cardiotoxicity is mediated by oxidative DNA damage-ATM-p53-apoptosis pathway and attenuated by pitavastatin through the inhibition of Rac1 activity. *Journal of molecular and cellular cardiology*. 47(4): 698–705

Young, B., Lowe, J.S., Stevens, A & Heath, W.J. 2006. Wheather's functional histology: A text and colour atlas 5th edition. Philadelphia. churchill livingstone

Yu, M.K., Park, J. & Jon, S. 2012. Targeting Strategies for Multifunctional Nanoparticles in Cancer Imaging and Therapy. *Theranostics*. 2(1): 34-44

Yuan, A., Wu, J., Song, C., Tang, X., Qiao, Q., Zhao, L., Gong, G. & Hu, Y., A novel self-assembly albumin nanocarrier for reducing DOX mediated cardiotoxicity. 2012. *Journal of pharmaceutical sciences*.102(5): 1626-35

Zhang, J. 2013. Autophagy and Mitophagy in Cellular Damage Control. *Redox biology*. 1(1): 19-23

Zhang, Y., Shi, J., Li, Y. & Wei. L. 2009. Cardiomyocyte death in doxorubicin induced cardiotoxicity. *Archivum immunologiae et therapia experimentalis*. 57(6): 435-445

Zou, H., Henzel, W.J., Liu, X., Lutschg, A. & Wang, A. 1997. Apaf-1, a human protein homologous to *C. elegans* CED-4, participates in cytochrome c-dependent activation of caspase-3. *Cell*. 90(3): 405-413

7 APPENDICES

APPENDIX A: SUPPLEMENTARY DATA

A.1. Rapamycin preserves cell viability during DOX cytotoxicity

This study performed a dose response using two dose of rapamycin (Rap 1: 50 nM and Rap 2: 25 nM) previously used by our group to determine if rapamycin treatment could preserved cell viability during DOX cytotoxicity. The cells were treated as previously described in section 2.2.2.

Both rapamycin treatments had no effect on cell viability when compared to control (Fig. A.1.1). However, in combination, both these treatments significantly preserved cell viability to similar extents when compared to the DOX group (75.6±2.4%).

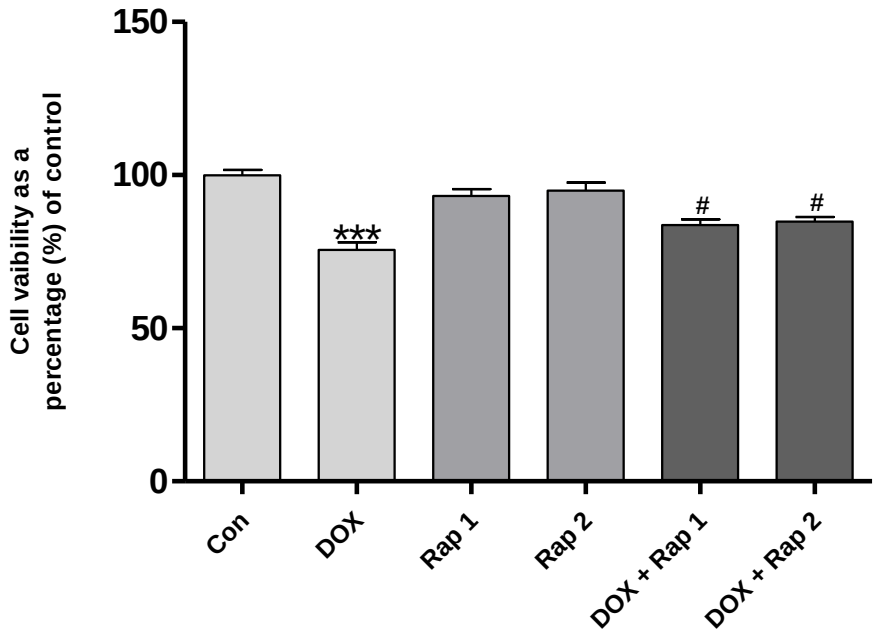

Fig. A.1.1: Cell viability analysis following autophagy upregulation by rapamycin: Autophagy was induced by treating cells with rapamycin. Additionally, cells were treated daily for 5 days with 0.2 µM DOX (1 µM cumulative dose). Result presented as mean ± SEM (N=3). ***P < 0.001 vs control. #P < 0.05 vs DOX. Abbreviations: **Con**: Control, **DOX**: doxorubicin, **Rap 1**: 50 nM rapamycin and **Rap 2**: 25 nM rapamycin.

A.1.2. Starvation treatments protects cells against DOX cytotoxicity in a dose-dependent manner

To determine if autophagy upregulation by starvation could preserve cell viability in the presence of DOX, we performed a dose response using three starvation conditions. These include: starvation 1(Stv 1): 90% amino acid reduction medium, starvation 2 (Stv 2): 50% amino acid reduction medium and starvation 3 (Stv 3): 10% amino acid reduction medium. The treatment protocol was performed as previously described in section 2.2.3.

DOX and Stv 1 treatment significantly reduced cell viability, whereas the other two starvation conditions had no significant effect on viability when compared to control (100.0±1.7) (Fig. A.1.2). In combination, only the Stv 2 and Stv 3 improved cell viability whereas the Stv 1 condition did very little to improve viability when compared to the DOX group only.

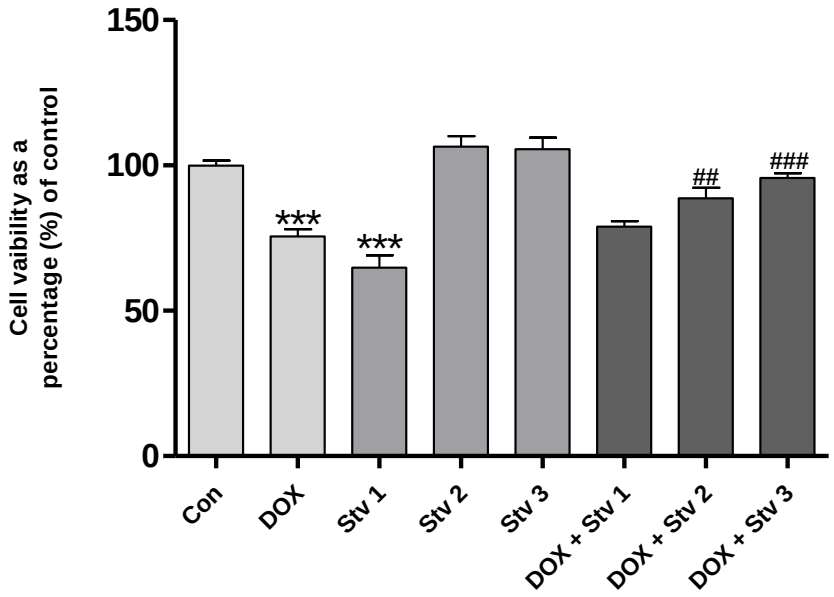

Fig. A.1.2: Cell viability analysis following autophagy upregulation by starvation: Autophagy was induced by treating cells with starvation medium. Additionally, cells were treated daily for 5 days with a 0.2 µM DOX (1 µM cumulative dose). Result presented as mean ± SEM (N=3). ***P < 0.001 vs control. ###P < 0.001, ##P < 0.01 vs DOX. Abbreviations: **Con**: Control, **DOX**: doxorubicin, **Stv 1**: 90% amino acid reduction, **Stv 2**: 50% amino acid reduction, **Stv 3**: 10% amino acid reduction.

A.1.3. Silencing of mammalian target of rapamycin is detrimental

The genetic knock-down of mTOR by siRNA (mTOR) is commonly used in the literature for therapeutic purposes. In this study, we aimed to activate and maintain upregulated autophagy by silencing mTOR and then assessing the effects of this upregulation on DOX cytotoxicity. Silencing was performed either performed at day 1 (1 siRNA), or at days 1 and 3 (2 siRNA), or at days 1, 3 and 5 (3 siRNA). Silencing with the scrambler siRNA (ConS) was performed at days 1, 3 and 5. DOX was administered as described in section 2.2.1

The 3 and 2 siRNA treatments significantly reduced viability whereas the 1 siRNA and the scrambler siRNA did not affect it when compared to control (Fig. A.1.3). In the presence of DOX the 3 siRNA (44.7±3.2, $p< 0.001$) and 2 siRNA (50.8±6.0, $p< 0.01$) treatments significantly reduced viability, highlighting the detrimental nature of continued mTOR silencing. The 1 siRNA had no effect viability when compared to the DOX group.

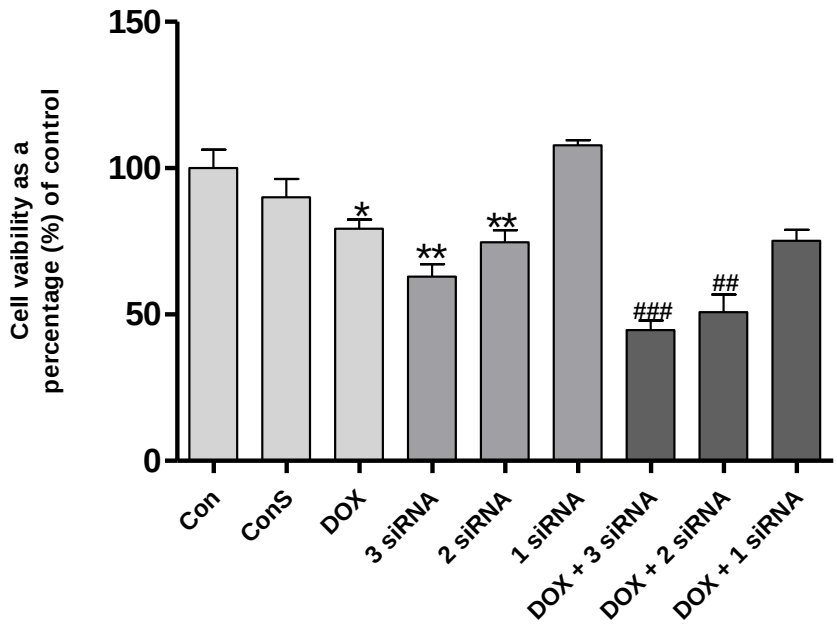

Fig. A.1.3: Cell viability analysis following autophagy upregulation by siRNA (mTOR): Autophagy was induced by siRNA (mTOR). Additionally, cells were treated daily for 5 days with a 0.2 µM DOX (1 µM cumulative dose). Result presented as mean ± SEM (N=3). **P < 0.01, *P < 0.05 vs control. ###P < 0.001, ##P < 0.01 vs DOX. Abbreviations: **Con**: Control, **ConS**: scrambler sequence, DOX: doxorubicin, **3 siRNA**: 3 times silencing of mTOR, **2 siRNA**: 2 times silencing of mTOR and **1 siRNA**: 1 time silencing of mTOR.

A.1.4. Bafilomycin severely reduce cell viability

The well-known autophagy inhibitor mTOR was used to assess if autophagy inhibition is beneficial in the DOX context. Autophagy was inhibited as previously described in section 2.2.5. The cells also received DOX treatment as explain in section 2.2.1

Both bafilomycin treatments significantly reduced cell viability by more than 60% when compared to control (Fig. A.1.4). In combination with DOX there was no further reduction in cell viability, although viability was still lower than the DOX only group.

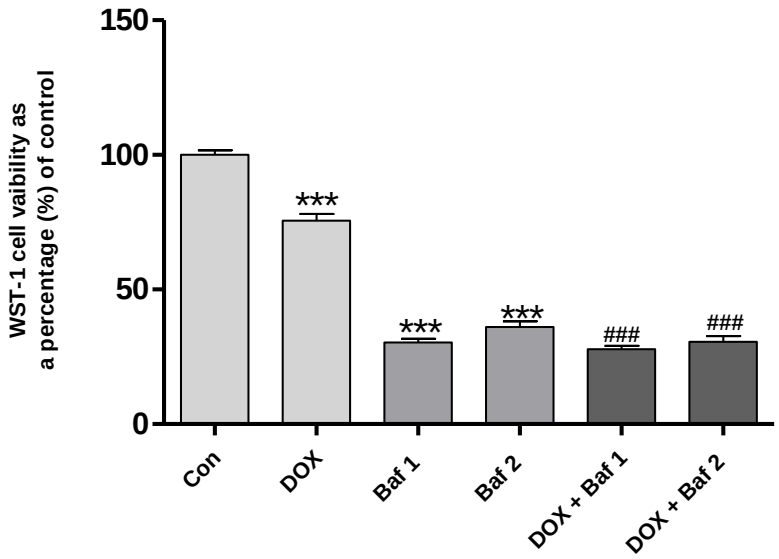

Fig. A.1.4: Cell viability analysis following autophagy inhibition by bafilomycin: Autophagy was inhibited via bafilomycin treatment. The cells were treated daily with a 0.2 µM dose of DOX for 5 days (1 µM cumulative dose). Result presented as mean ± SEM (N=3). ***P < 0.001 vs control. ###P < 0.001, vs DOX. Abbreviations: **Con**: Control, **DOX**: doxorubicin, **Baf 1**: 5 nM bafilomycin and **Baf 2**: 1 nM bafilomycin.

A.2. DOSE RESPONSE: APOPTOSIS

A.2.1. Rapamycin treatment counteracts apoptosis during DOX cytotoxicity

Autophagy can induces or prevent apoptosis in different contexts. In some cases, it also facilitates the apoptotic process. To understand the function of autophagy in our context, a caspase-glo assay was used to assess apoptosis. Autophagy upregulation by rapamycin significantly reduced apoptosis when compared to control (100±6.2%) (Fig. A2.1). DOX treatment significantly induced apoptosis and both rapamycin treatments were able to prevent this from occurring.

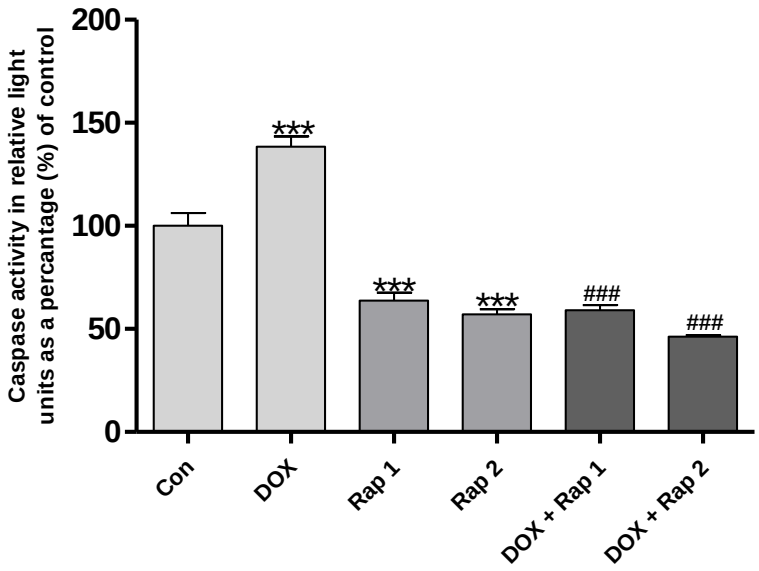

Fig. A.2.1: Caspase activity analysis following autophagy upregulation by rapamycin: Autophagy was induced by treating cells with rapamycin. Additionally, cells were treated daily for 5 days with a 0.2 µM DOX (1 µM cumulative dose). Result presented as mean ± SEM (N=3). ***P < 0.001 vs control. ###P < 0.05 vs DOX. Abbreviations: **Con**: Control, **DOX**: doxorubicin, **Rap 1**: 50 nM rapamycin and **Rap 2**: 25 nM rapamycin.

A.2.2. Starvation treatment successfully prevent DOX-induced apoptosis

The DOX treatment as reported previously continued to induce apoptosis. Similar results were also observed in the Stv1 group (130.7±2.6, p<0.01) when compared to control (100.0±6.2) (Fig. A.2.2). The other two starvation treatments had no effect on apoptotic activity. Interestingly, all three starvation treatments were able to decrease apoptotic activity in the

presence of DOX. What was even more noteworthy was the fact that all these treatment had a similar capacity to prevent DOX-induced apoptosis.

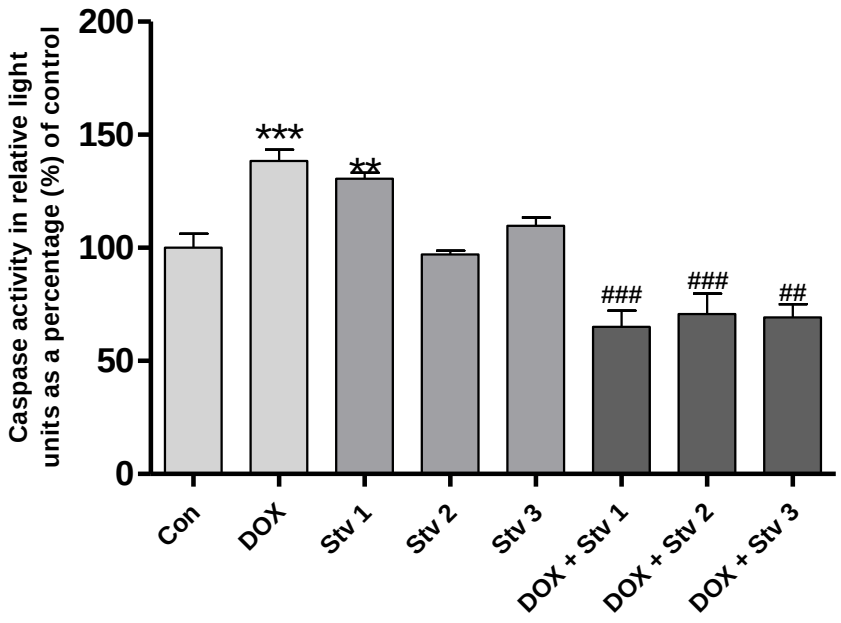

Fig. A.2.2: Analysis of caspase activity following autophagy upregulation by starvation: Autophagy was induced by treating cells with starvation medium. Additionally, cells were treated daily for 5 days with a 0.2 µM DOX (1 µM cumulative dose). Result presented as mean ± SEM (N=3). ***P < 0.001, **P < 0.01 vs control. $^{###}$P < 0.001, $^{##}$P < 0.01 vs DOX. Abbreviations: **Con**: Control, **DOX**: doxorubicin, **Stv 1**: 90% amino acid reduction medium, **Stv 2**: 50% amino acid reduction medium, **Stv 3**: 10% amino acid reduction medium.

A.2.3. Silencing of mammalian target of rapamycin (mTOR) augments DOX induced apoptosis

The silencing of mTOR proved to be largely detrimental. Two of the mTOR siRNA treatments (3 and 2 siRNA) significantly induced apoptosis, whereas the 1 mTOR siRNA showed no significant difference when compared to control (100±6.2%) (Fig. A.2.3). The two detrimental siRNA treatments augmented DOX-induced apoptosis, whereas the 1 siRNA had no significant effect on it when compared to the DOX group.

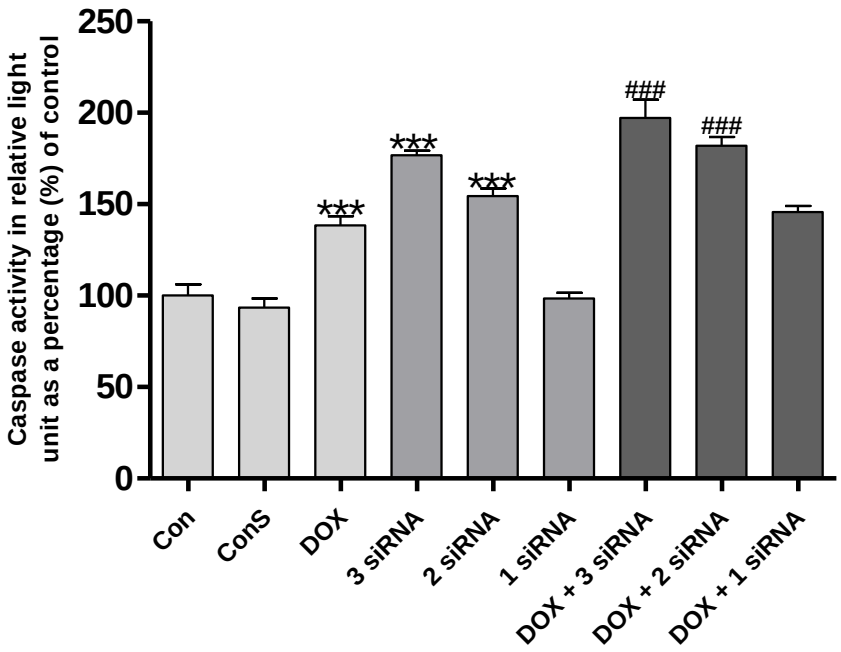

Fig. A.2.3. Analysis of caspase activity following autophagy modulation by siRNA (mTOR): Autophagy was induced by siRNA (mTOR) as follows. Additionally, cells were treated daily for 5 days with a 0.2 µM DOX (1 µM cumulative dose). Result presented as mean ± SEM (N=3). ***P < 0.001, **P < 0.01 and *P < 0.05 vs control. ###P < 0.001 vs DOX. Abbreviations: **Con**: Control, **ConS**: scrambler sequence **DOX**: doxorubicin, **3 siRNA**: 3 times silencing of mTOR, **2 siRNA**: 2 times silencing of mTOR and **1 siRNA**: 1 time silencing of mTOR.

A.2.4. Bafilomycin treatment induces apoptosis

Interestingly, autophagy inhibition by both bafilomycin treatments significantly reduced apoptosis when compared to control (100±3.6%) (Fig A.2.4a). These treatments further counteracted DOX-induced apoptosis. However, when carefully assessing the cell density we saw that the reduction in apoptosis was the result of excessive cell death as can be observed in the images provided below (Fig. A2.4b). Based on this findings, autophagy inhibition by bafilomycin was discontinued as it severely detrimental in this study.

A)

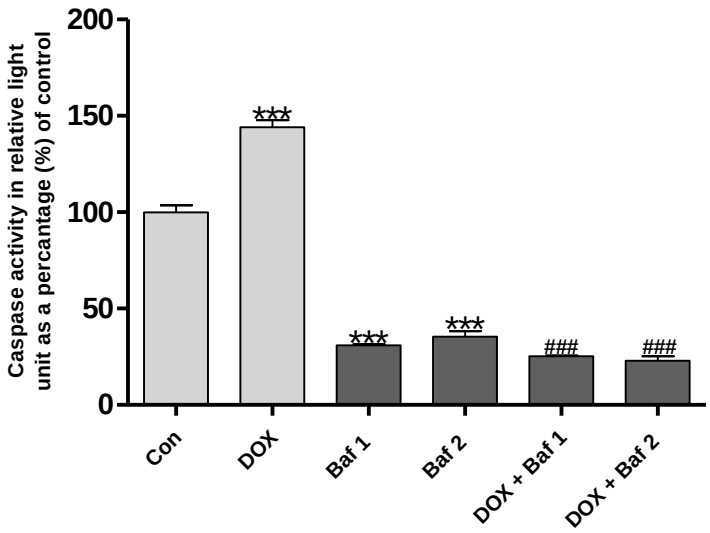

B)

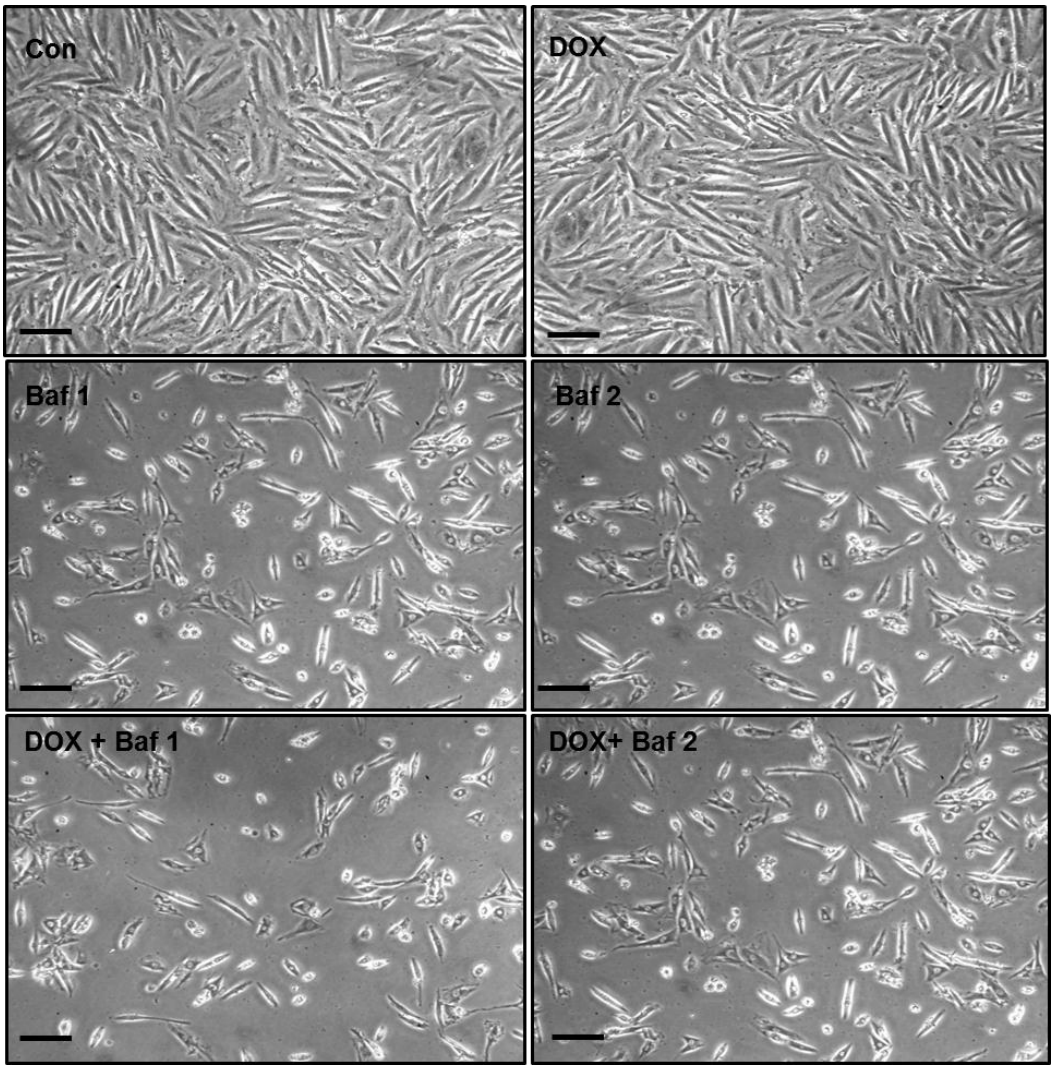

Fig. A.2.4: Analysis of caspase activity following autophagy modulation by bafilomycin: The cells were treated daily with a 0.2 µM dose of DOX for 5 days (1 µM cumulative dose). Autophagy was inhibited by bafilomycin. Graph (A) and image (B) representation following bafilomycin treatment. Result presented as mean ± SEM (N=3). ***P < 0.001 vs control. $^{###}$P < 0.001, vs DOX. Abbreviations: **Con**: Control, **DOX**: doxorubicin, **Baf 1**: 5 nM bafilomycin and **Baf 2**: 1 nM bafilomycin.

A.3. PROTEIN EXPRESSION ASSESSMENT

A.3.1. Rapamycin treatment prevents DOX inhibition of autophagy

- mTOR expression

It is not clear in the literature if DOX inhibits or induces autophagy. To answer this question, we employed western blotting to assess the effect of chronic DOX treatment on autophagy in the context of our study. Three autophagic marker were employed, namely mTOR, an upstream inhibitor of autophagy that is downregulated during increased autophagic function. p62 which is an LC3 anchor protein that is degraded by the autophagic machinery during high autophagic activity. Lastly LC3, which is converted from LC3-I to LC3-II during increased autophagy.

Chronic DOX treatment lead to a significant reduction in the expression of mTOR. Likewise autophagy induction by 50 nM (66.7±3.0, $p<0.001$) and 25 nM (48.8±2.4, $p<0.001$) rapamycin treatments also reduced mTOR expression, albeit to a greater extend when compared to control (100.0±2.8) (Fig. A.3.1.). The 50 nM rapamycin combination treatment had no effect on mTOR expression whereas the 25 nM rapamycin treatment significantly decreased mTOR expression when compared to the DOX group.

A)

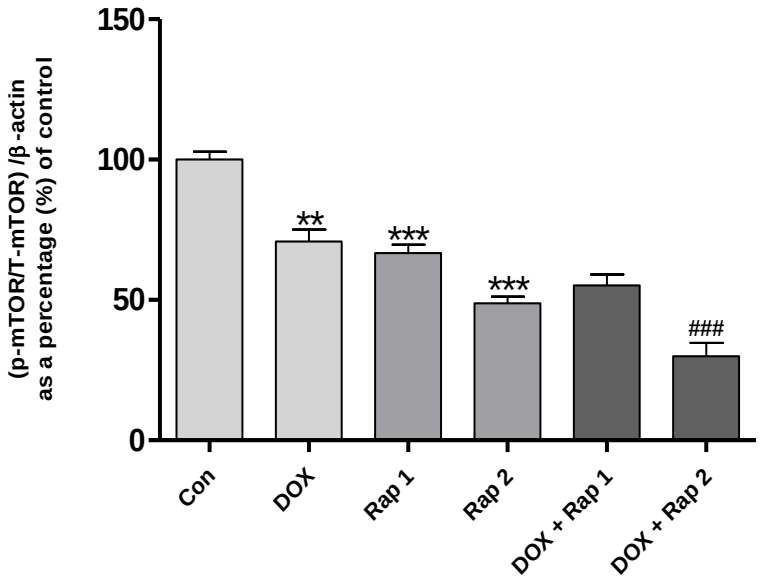

B)

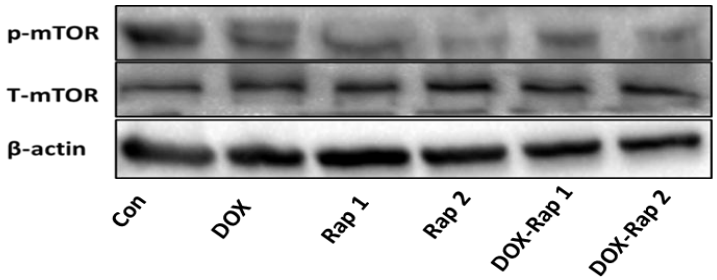

Fig. A. 3.4. The expression of mTOR protein phosphorylation following autophagy induction during chronic DOX treatment. Autophagy was induced by treating cells with rapamycin. Additionally, cells were treated daily for 5 days with a 0.2 µM DOX (1 µM cumulative dose). **(A)** Bar graph and **(B)** Western blot representation of mTOR expression. All blots were normalized to beta actin loading control. Result presented as mean ± SEM (N=3). ***P < 0.001, **P < 0.01 vs control. $^{###}$P < 0.001 vs DOX. Abbreviations: **Con**: Control, **DOX**: doxorubicin, **Rap 1**: 50 nM rapamycin and **Rap 2**: 25 nM rapamycin

- p62 expression

DOX treatment (133.6±3.9%, p<0.001) lead to a substantial accumulation of p62 whereas the 50 nM rapamycin (42.7±3.1%, p<0.001) and 25 nM rapamycin (26.0±2.1%, p<0.001) treatments promoted degradation of this protein when compared to control (100±4.9) (Fig.

A.3.5). The rapamycin combinations treatments also induced a significant degradation of p62 in comparison to the DOX group.

A)

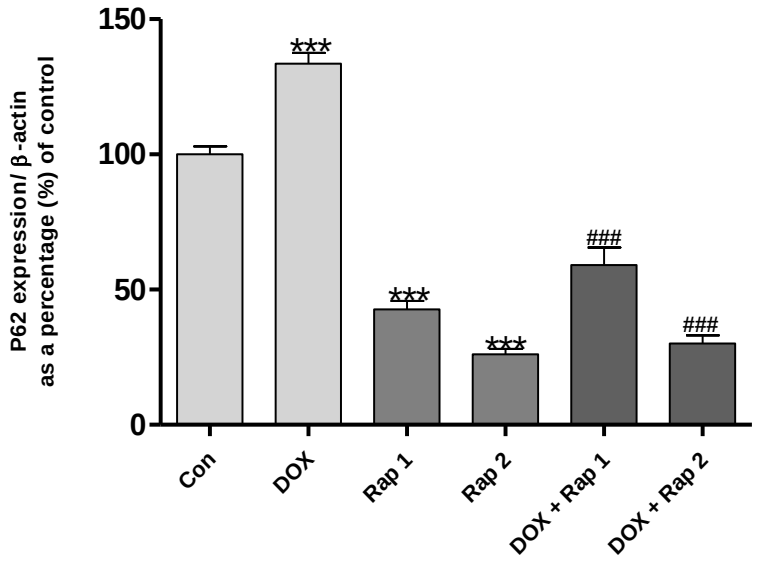

B)

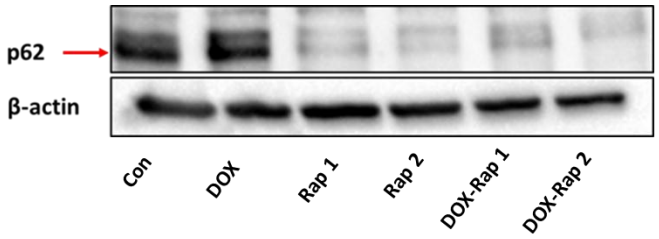

Fig. A. 3.5. The expression of p62 following autophagy induction during chronic DOX treatment. Autophagy was induced by treating cells rapamycin. Additionally, cells were treated daily for 5 days with a 0.2 µM DOX (1 µM cumulative dose). **(A)** Bar graph and **(B)** Western blot representation of p62 expression. All blots were normalized to beta actin loading control. Result presented as mean ± SEM (N=3). ***P < 0.001, vs control. ###P < 0.001 vs DOX. Abbreviations: **Con**: Control, **DOX**: doxorubicin, **Rap 1**: 50 nM rapamycin and **Rap 2**: 25 nM rapamycin

When assessing the graph, it appears that the expression of LC3 was significantly increased by DOX treatment (246.2±10.9%, $p<0.05$) when compared to control (100±4.7) (Fig. A.3.6.), suggesting an increase in the conversion of LC3-I to LC3-II. However, the blots clearly show that the increase in LC3 expression is the result of an accumulation of LC3-I and LC3-II and

not the conversion of the latter. Both rapamycin treatments increased autophagy activity as seen by the conversion of LC3-I to LC3-II on the image. Some conversion occurred in the combination groups, although it was limited. In summary the 25 nM rapamycin dose was chosen as it successfully preserved cell viability and it showed a greater capacity in preventing DOX induced apoptosis and DOX inhibition of autophagy.

A)

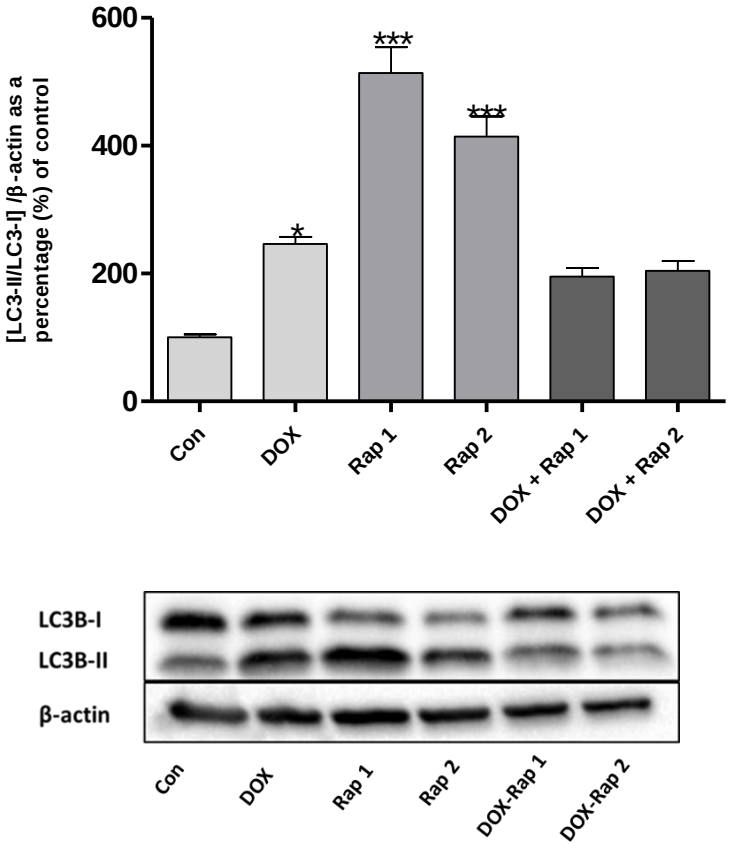

Fig. A. 3.6. The expression of LC3 following autophagy induction during chronic DOX treatment. Autophagy was induced by treating cells with 25 nM or 50 nM of rapamycin. Additionally, cells were treated daily for 5 days with a 0.2 µM DOX (1 µM cumulative dose). **(A)** Bar graph and **(B)** Western blot representation of LC3 expression. All blots were normalized to beta actin loading control. Result presented as mean ± SEM (N=3). ***P < 0.001, *P < 0.05 vs control. Abbreviations: **Con**: Control, **DOX**: doxorubicin, **Rap 1**: 50 nM rapamycin: **Rap 2**: 25 nM rapamycin.

A.3.2. Starvation treatment counteract autophagy inhibition during DOX cytotoxicity.

- mTOR

Starvation is an inducer of autophagy because of its inhibitory effect on mTOR. All three starvation treatments significantly reduced mTOR expression when compared to control (100±1.0%). In combination, these treatments further downregulated mTOR expression to similar extends.

A)

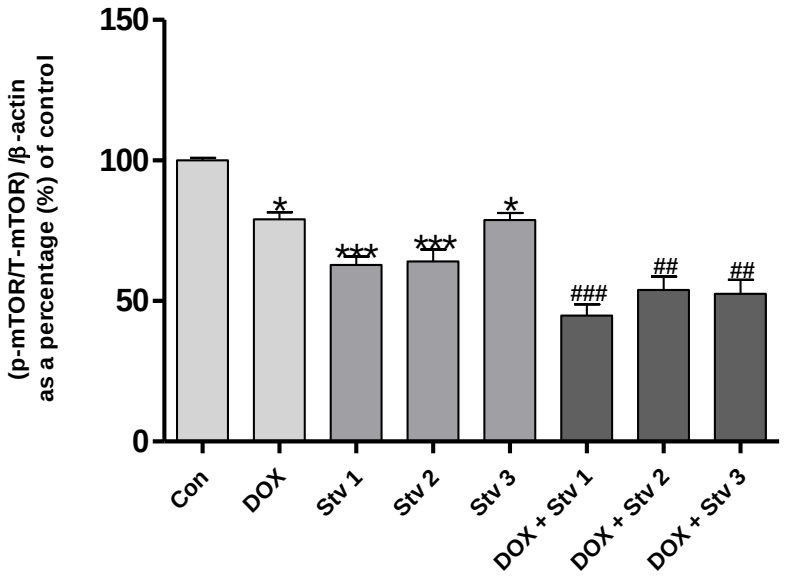

B)

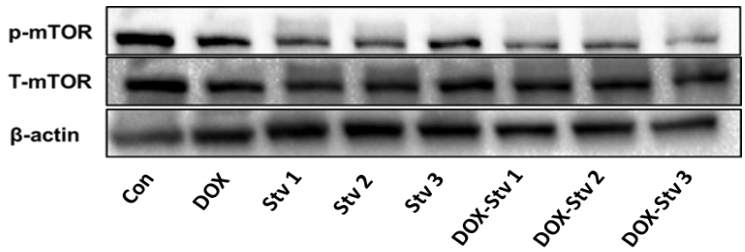

Fig. A. 3.1. The expression of mTOR protein phosphorylation following autophagy induction during chronic DOX treatment. Autophagy was induced by treating cells with starvation medium. Additionally, cells were treated daily for 5 days with a 0.2 µM DOX (1 µM cumulative dose). **(A)** Bar graph and **(B)** Western blot representation of mTOR expression. All blots were normalized to beta actin loading control. Result presented as mean ± SEM (N=3). ***P < 0.001, *P < 0.05 vs control. $^{###}$P < 0.001, $^{##}$P < 0.01 vs DOX. Abbreviations: **Con**:

Control, **DOX**: doxorubicin, **Stv 1**: 90% amino acid reduction medium, **Stv 2**: 50% amino acid reduction medium, **Stv 3**: 10% amino acid reduction medium.

- p62

DOX treatment significantly induced p62 accumulation (156.2±2.125%, $p<0.01$). The starvation treatments promoted considerably degradation of p62 when compared to the control (100.7±2.7). The Stv treatment showed the greatest capacity in degrading p62. In combination with DOX, there was a dose-dependent increase in the degradative capacity of these starvation treatments. However, all treatments successfully induced significant p62 degradation when compared to the DOX group.

A)

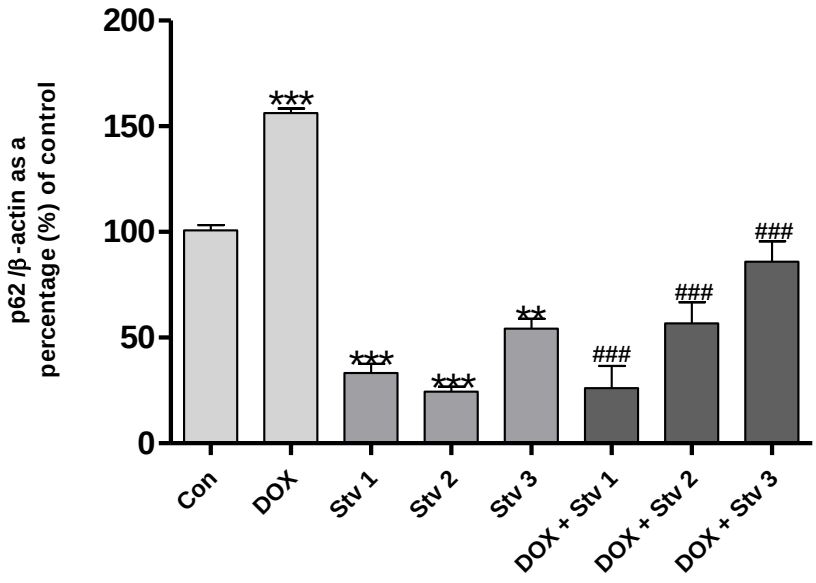

B)

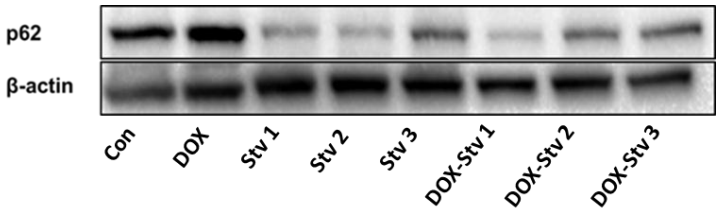

Fig. A.3.2. The expression of p62 following autophagy induction during chronic DOX treatment. Autophagy was induced by treating cells with starvation medium. Additionally, cells were treated daily for 5 days with a 0.2 µM DOX (1 µM cumulative dose). **(A)** Bar graph and **(B)** Western blot representation of p62 expression. All blots were normalized to beta actin loading control. Result presented as mean ± SEM (N=3). ***P < 0.001, **P < 0.01 vs control. $^{###}$P < 0.001 vs DOX. Abbreviations: **Con**: Control, **DOX**: doxorubicin, **Stv 1**: 90% amino acid reduction medium, **Stv 2**: 50% amino acid reduction medium, **Stv 3**: 10% amino acid reduction medium

- LC3

When assessing the graph, DOX treatment appears to have increased (210.8±12.9%, p<0.01) LC3 conversion when compared to control (100±7.661%) (Fig. A.3.3). When one assess the blot image, it is clear that there is limited LC3-I to LC3-II conversion occurring. The Stv 1 and Stv 2 treatments showed some LC3 conversion although there was excessive LC3-I expression in in the Stv2 condition. The Stv 3 showed limited conversion when compared to the control. When assessing the three starvation treatments in the combination treatment, a dose-dependent loss in LC3-I conversion to LC3-II is observed. Taking all the cell viability, apoptosis and autophagy data into consideration, we decided to make use of the Stv 2 treatment. This dose significantly preserved cell viability and prevented apoptosis during chronic DOX treatment. The Stv 3 condition also achieved this, however, it the Stv 2 treatment showed a greater capacity to induce autophagy, hence it was chosen over the latter treatment.

A)

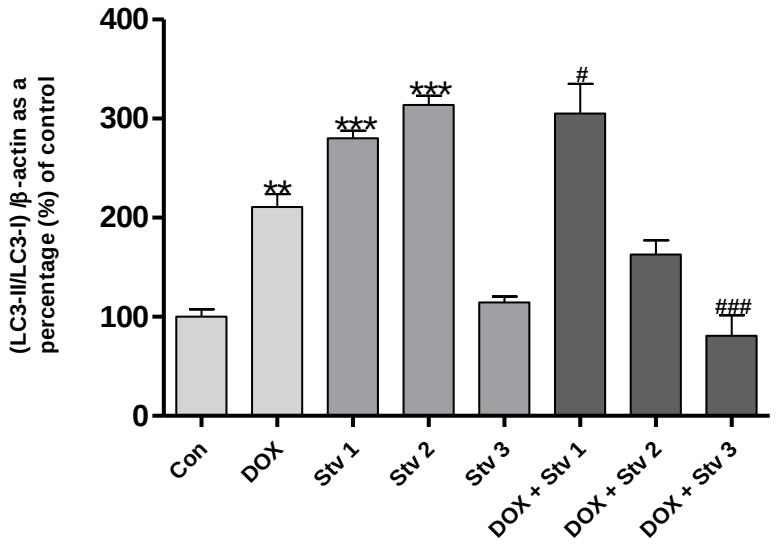

B)

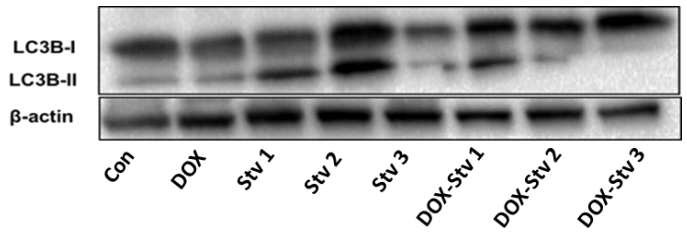

Fig. A. 3.3. The expression of LC3 following autophagy induction during chronic DOX treatment. Autophagy was induced by treating cells with starvation medium. Additionally, cells were treated daily for 5 days with a 0.2 µM DOX (1 µM cumulative dose). **(A)** Bar graph and **(B)** Western blot representation of LC3 expression. All blots were normalized to beta actin loading control. Result presented as mean ± SEM (N=3). ***P < 0.001, **P < 0.01 vs control. $^{###}$P < 0.001, $^{#}$P < 0.05 vs DOX. Abbreviations: **Con**: Control, **DOX**: doxorubicin, **Stv 1**: 90% amino acid reduction medium, **Stv 2**: 50% amino acid reduction medium, **Stv 3**: 10% amino acid reduction medium.

A.3.3. silencing of mTOR challenges autophagy inhibition by DOX treatment

- mTOR

The silencing of mTOR is another mechanism of inducing autophagy. DOX treatment (74.8±2.0%, p<0.01) significantly decreased mTOR expression when compared to control (100.0±1.7%) (Fig. A.3.7). All siRNA treatments reduced mTOR expression when compared

to the latter. In combination, two of the siRNA treatments (3 and 2 siRNA) continued to reduce mTOR expression whereas the 1 siRNA treatment had no effect on mTOR expression when compared to the DOX group.

A)

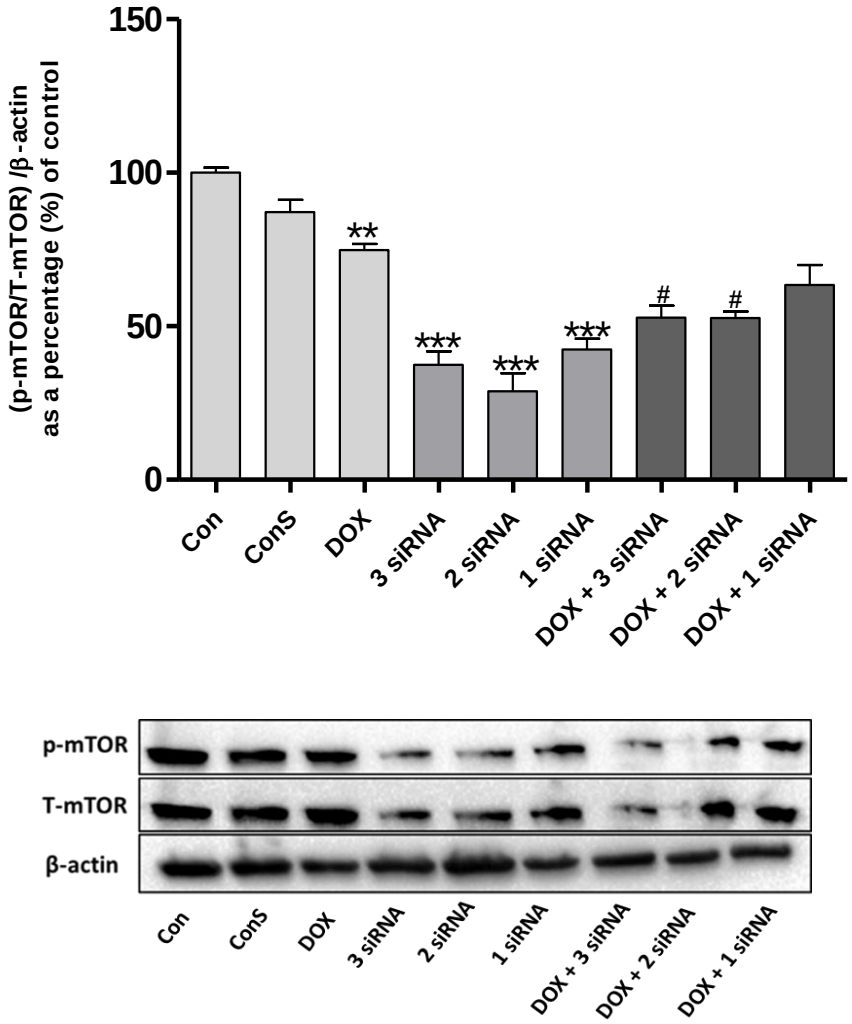

Fig. A. 3.7. The expression of mTOR protein phosphorylation following autophagy induction during chronic DOX treatment. Autophagy was induced by siRNA (mTOR). Additionally, cells were treated daily for 5 days with a 0.2 µM DOX (1 µM cumulative dose). **(A)** Bar graph and **(B)** Western blot representation of mTOR expression. All blots were normalized to beta actin loading control. Result presented as mean ± SEM (N=3). ***P < 0.001, **P < 0.01 vs control. #P < 0.05 vs DOX. Abbreviations: **Con**: Control, **ConS**: scrambler sequence **DOX**: doxorubicin, **3 siRNA**: 3 times silencing of mTOR, **2 mTOR**: 2 times silencing of mTOR and **1 siRNA**: 1 time silencing of mTOR.

- p62

Long term treatment with DOX-induced accumulation (128.30±3.076%, p< 0.01) of p62 when compared to control (102.2±1.982%) (Fig. A.3.8). Surprisingly the 3 siRNA treatment did not affect p62 expression, the 2 siRNA (134.8±9.1%, p<0.001) treatment induced its accumulation while the 1 siRNA (68.8±2.0%, p<0.001) treatment resulted in a significant degradation of it. However, in combination, these treatments successfully reduced p62 degradation when compared to DOX group.

A)

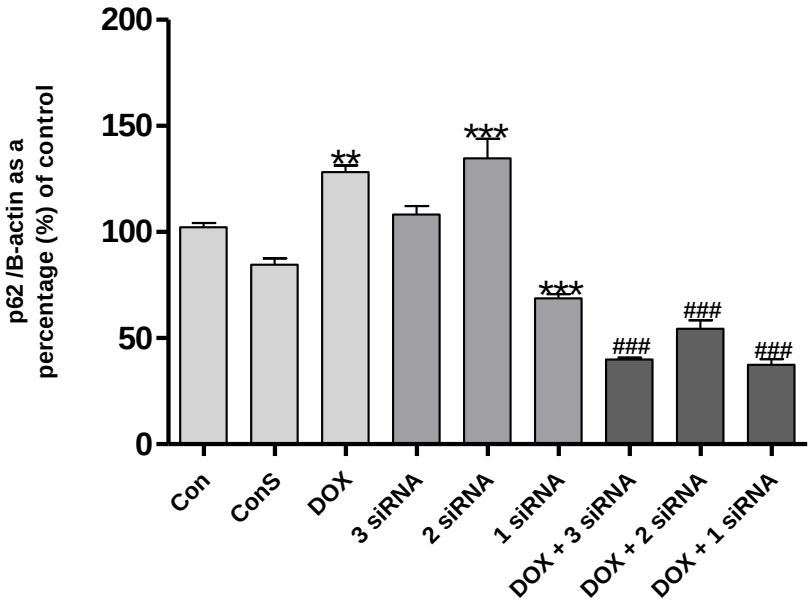

B)

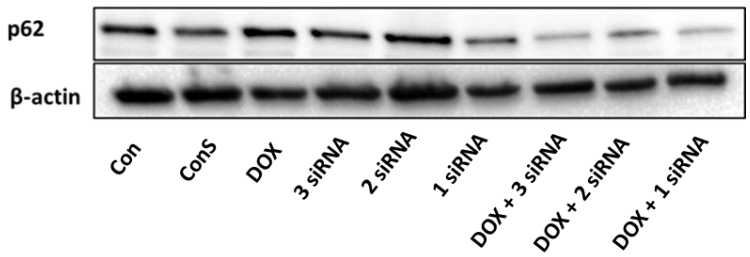

Fig. A. 3.7. The expression of p62 following autophagy induction during chronic DOX treatment. Autophagy was induced by siRNA (mTOR). Additionally, cells were treated daily for 5 days with a 0.2 µM DOX (1 µM cumulative dose). **(A)** Bar graph and **(B)** Western blot representation of p62 expression. All blots were normalized to beta actin loading control. Result presented as mean ± SEM (N=3). ***P < 0.001, **P < 0.01 vs control. $^{###}$P < 0.001 vs DOX. Abbreviations: **Con**: Control, **ConS**: scrambler sequence, **DOX**: doxorubicin, **3 siRNA**: 3 times silencing of mTOR, **2 siRNA**: 2 times silencing of mTOR and **1 siRNA**: 1 time silencing of mTOR.

- LC3

Chronic treatment with DOX lead to a limited conversion of LC3-I to LC3-II as previously reported in other sections (Fig. A.3.9). The siRNA treatments induced significant conversion of LC3, furthermore this change occurred in a dose-dependent manner. Likewise this dose-dependent change was also observed in the combination treatment, however, no significant conversion occurred in the 1 siRNA group. In summary, the siRNA (mTOR) group was discontinued as it failed to prevent DOX-induced apoptosis or preserve cell viability.

A)

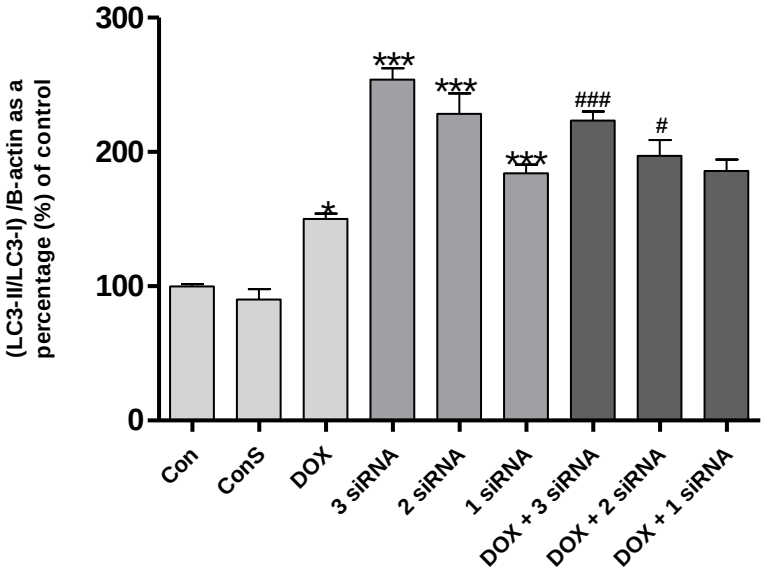

B)

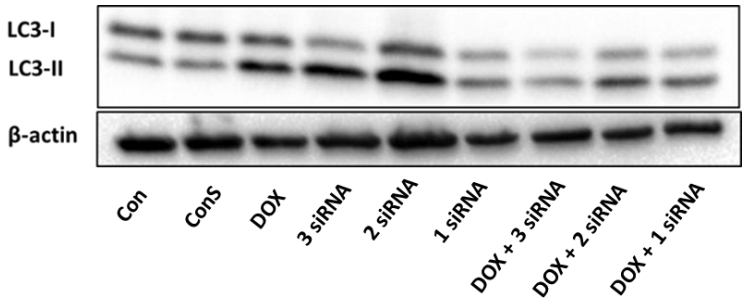

Fig. A. 3.9. The expression of LC3 following autophagy induction during chronic DOX treatment. Autophagy was induced by siRNA (mTOR). Additionally, cells were treated daily for 5 days with a 0.2 µM DOX (1 µM cumulative dose). All blots were normalized to beta actin loading control. **(A)** Bar graph and **(B)** Western blot representation of LC3 expression. Result presented as mean ± SEM (N=3). ***P < 0.001, *P < 0.05 vs control. ###P < 0.001, #P < 0.05 vs DOX. Abbreviations: **Con**: Control, **ConS**: scrambler sequence **DOX**: doxorubicin, **3 siRNA**: 3 times silencing of mTOR, **2 siRNA**: 2 times silencing of mTOR and **1 siRNA**: 1 time silencing of mTOR.

APPENDIX B: PROTOCOLS

1. Tissue culture hood cleaning

- All cell culturing processes were performed in a sterile, uv decontaminated tissue culturing hood
- The hood was sprayed and wiped down with damp ethanol towel before use
- All pipets, pipet tips and pipet bouys were sterilized and sprayed with ethanol before being placed in the tissue culture hood

2. Culturing of H9c2 myoblast

- Frozen H9c2 myoblast were removed from nitrogen tank and thawed
- Cell were then plated in a T25 flask and supplemented with 4 ml of warm DMEM culture medium
- Medium was changed the following day, and then every 3 days after that
- Cells were culture until the reach 80%-90% confluence
- Cells were then trypisinized by addition of 4ml of trypsin. The trypisinization process was performed in a shaking incubator for 3 minutes at 37^{o}C
- 4 ml of warm medium was added to the T25 flask to stop trypsin activity
- Cells were then centrifuged at 1500 rpm for 3 minutes
- The supernatant was discarded and the pellet was resuspended in 4ml of fresh warm medium
- Equal volumes of this cell mixture was transferred in to 2 T175 containing 10 ml of warm culture medium, grown to confluence and then seeded as per the requirement of each experiment

3. Cell Counting

- A hemocytometer was cleaned with 70% ethanol
- Resuspended cells were vortexed and 15 µL of this mixture was transferred on the hemocytometer
- 4 blocks (A-D) containing cells were counted and cell number was determined as follows:

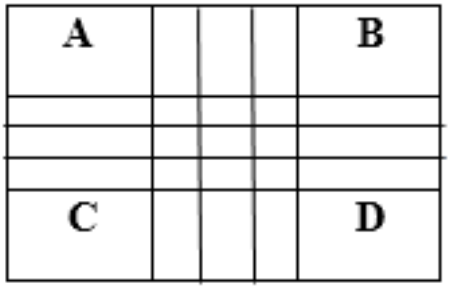

$$Total\ cell\ number: \frac{number\ of\ total\ cells\ in\ all\ 4\ blocks}{4}\ x\ 10000\ x\ volume\ resuspended\ in$$

- From here onwards the appropriate seeding was number was plated as per experiment

4. **Freezing of cells**

- 1 million cells were transferred into a separate 15 ml falcon tube
- Cells were centrifuged as described before and supernatant discarded
- The cells were than resuspended in a 1ml of freezing medium which is made up of 990 µL of FBS + 10 µl of DMSO
- The entire mixture containing 1 million cells were then transferred into freezing microfuge tubes
- The cells were then place in a -20^{o}C freezer for an hour and then at -80^{o}C overnight
- The following morning the cells were transferred into a nitrogen tank until they would be needed again

5. **Immunocytochemistry**

- 100 000 cells were seeded on a cover slip and treated as per expirement
- Cells were transferred on ice and then fixation was performed for 10 minutes with cold 4% paraformaldehyde
- The paraformaldehyde was removed and cells were washed 3 times with PBS
- Cell membrane permeation was performed for 6 minutes with 0.1% triton (Dissolved in dH_2O)

- This was followed by blocking with 1% BSA for 30 minutes
- Cell were then incubated overnight at -4^{o}C with primary cTnT anti-body (1: 100)
- 3x Washing with cold PBS was performed the following morning
- Cell were then incubated for 1 hour with fluorescent secondary Alexa flour anti-body (1: 400). **All work from here onwards was done in the dark**
- 3x Washing with PBS was performed and cells were then incubated with cold Hoechst stain (1:8000) for 5 minutes
- Cell were then washed again as described before and left to air dry for 10 minutes
- A drop of mounting medium was placed on slide and the cover slip was mounted facing the mounting medium
- Slides were then covered with foil and left to air dry in a dark room overnight.
- A fluorescent microscope was used to analyses the images

6. **Oxigraph assessments:**

Oxigraph preparation and calibration

- The oxigraph's electrodes and chamber were washed with distilled water prior to and after use
- Calibration was performed with 1ml of Hadley's intracellular buffer
- The buffer was removed and fresh buffer (500µl) was added into the oxygen chamber

Running of oxigraph

- Cells were grown, treated and harvested as described before
- They were then resuspended in 129µl of Hedley's intracellular buffer and then transferred into chamber contain 500µL of buffer
- Additionally, 20µl of saponin and 1µl of succinate was added to the chamber and cells were allowed to respire in this condition for 5 minutes
- 350µl of ADP was then added and respiration rate was measure for 1 hour
- After 1 hour 10µl of carbonyl cyanide-p-trifluoro-methoxy-phenylhydazone (FCCP) was added to terminate the experiment and confirm that mitochondria were still actively respiring prior to termination of the experiment

7. **Western blot: Cell harvesting**
    - Medium was removed and cells were washed 3 times with cold PBS. The entire process was performed on ice at all time
    - Cold 1ml of RIPA buffer was supplemented with: 1µl of aprotonin, 1µl of leupeptin, 5µl Na_3VO4, NaF, benzamidine, PMSF and 10µl pepstatin was prepared beforehand
    - 60 µl of RIPA was added 6 well tissue culture plates
    - Cells were then scrapped using a cell scrapper and transferred into clean 2 ml microfuge tube
    - This was followed by a 4 seconds sonication process at an amplitude of 4
    - Cell were then placed on ice to allow cell contents to settle
    - Then cells were then pelleted at 8000 rpm for 10 at -20 ^oC and the lysate (Supernantant) was transferred into a clean microfuge tube
    - The lysate was stored at -80 ^oC until needed

8. **Western blot: Bradford protein concentration determination**
    - Cell lysate was thawed on ice
    - 5µl of sample was transferred into clean 2 ml microfuge tube.
    - 95µl of water + 900µl of Bradford was added to each sample eppie
    - A Bradford standard was made up accounting to this table below:

BSA (µl)	**dH_2O (µl)**	**Protein concentration (µg)**
0	100	Blank
10	90	2
20	80	4
40	60	8
60	40	12
80µl	20µl	16µg
100µl	0µl	20µg

    - 900µl of Bradford was added to the Bradford standard and the samples
    - The sample were vortexed and absorbance was measure at a wavelength of 595

- Absorbance for the sample was plotted against a standard curve to determine the protein concentration of the sample

9. **Western blot: Protein separation and band analysis**
    - Appropriate volumes of samples were transferred into clean 0.5 ml microfuge tubes
    - The appropriate volume of loading buffer was also added to each sample
    - The samples and protein ladder was then loaded into the wells of the gel
    - The samples were ran at 100 mV for 10 minutes to let it migrate through the stacking gel
    - From there the samples were ran at 180mV till the front line reach the end of the gel
    - Once the run was completed, the gel activated on the Chemi Doc™ XRS system and then transferred to PDVF membrane
    - The transfer was performed for 15 minutes at a 25 V and a current of 1.3 mA.
    - The PDVF membrane was then placed in methanol for 30 seconds, dried and then washed 3 times for 5 minutes in TBST
    - This was followed by blocking in 5% fat free milk for 1 hours
    - The membrane was washed 3 times in TBST again for 10 minutes and then transferred in primary anti-body (1:1000) overnight at 4^{o}C
    - Another washed process was performed 3 times the following morning for 10 minutes
    - The membrane was then probed with secondary anti-body (1:5000) at room temperature for 1 hour and this was followed by another wash process with TBST as described before
    - The membrane was exposed to ECL (1:1) for 2 minutes. Then it was exposed on the Chemi Doc™ XRS system

10. **Membrane stripping protocol**
    - Membrane was washed two times with dH2O for 5 minutes and the stripped with a 0.2 M NaOH solution at room temp for 5 min on shaker
    - The membrane was washed again 2 time for 5 minutes with dH2O followed by a 1 hour blocking process in 5% milk in TBS-T
    - Then washed 3 times for 5 minutes in TBS-T

- This was the followed by normal propping with 1^{o} anti-body overnight and then 2^{o} anti-body for 1 hour at room temperature

11. **Preparation of starvation medium**

Starvation medium (%)	**Amino acid free medium (%)**	**Culture medium (%)**
Stv 1	90	10
Stv 2	50	50
Stv 3	10	90

12. **Caspase-glo 3/7 assay**

- 20 000 were seeded on 96 well plates and grown to 70% -80% confluence.
- Medium was removed and 100µl of fresh medium was added to each well
- The caspase-Glo assay was prepared according to the manufacture's protocol and 100µl of the assay mixture was added to each well
- The plate was then covered in foil and mixed in an incubator for 1 hour.
- The mixture was then allowed to equilibrate to room temperature for 30 minutes
- Luminescence was then read using a luminometer
- The luminescence from the blank well was subtracted from the sample luminescence to rule out any background noise

13. **JC-1**: Mitochondrial potential assessment

- Cell were grown in T25 flasks to 70% -80% confluence.
- This was followed by cell trypisinization for 5 minutes in 4ml of trypsin
- The cells were then resuspended in 1ml of PBS
- JC-1 (5 µM) was then added to the PBS suspended cells and then incubated for 15 minutes
- Analysis was performed using the BD FACSAria I flow cytometer. A minimum of 10 000 cells per event were collected using a 488nm laser and collected

between 515-545 and 575-625. The geometric mean of the intensity histogram was used to measure fluorescent intensity

14. **MitoPerOX:** mitochondrial lipid peroxidation
    - Cells were seeded and grown to 70%-80 confluence
    - Medium was removed and cells were washed 3 times with PBS and then trypisinized
    - Cells were then resuspended in PBS and 5µM of MitoPerOX added to the PBS cells suspension
    - Cells were incubated for 15 minutes before being submitted to flow cytometry.
    - A minimum of 10 000 cells per event were collected using a 488nm laser and collected between 515-545 and 575-625.The geometric mean of the intensity histogram was used to measure fluorescent intensity

15. **Mitotracker green:** mitochondrial morphology
    - Medium was removed and cells were resuspened in 200µl of fresh medium
    - Mitotracker (25µM) was then added to each well and cells were incubated for 15 minutes
    - An olympus fluorescent microscope was then used to analyse mitochondrial morphology

APPENDIX C: PREPARATION OF REAGENTS

1. Cell culture medium preparation

- 500ml of FBS and 150ml of pen/strep was thawed at 37^{o}C in a bead bath incubator
- 50 ml of FBS and 5ml of pen/strep was added to 500ml of DMEM culture medium
- The medium was then aliquoted into 50ml falcon tube and refrigerated at 4^{o}C until needed

2. Retinoic acid medium

- 3mg of retinoic acid was dissolved in 1ml of DMSO to make a 3mM stock solution which was frozen
- The 10nM treatment medium was made by making serial dilution of the 1mM stock
- The 10nM treatment medium was made fresh every day
- The retinoic acid stock and the serial dilutions were thawed once and were not kept for longer than 2 weeks

3. Hedley's intracellular respiration buffer

- 0.25M Sucrose (8.56g / 100ml)
- 2mM KH_2PO_4 (0.027g/ 100ml)
- 5mM $MgCl_2$ (0.1g/ 100ml)
- 1mM EDTA: (0.036g/ 100ml)
- 20mM MOPS (1.672/ 100ml)
- 0.1% BSA (0.1g/ 100 ml)
- 1mM ADP: (0.048/ 100ml): Added separately and prepared fresh.
- pH 7.4

4. RIPA Buffer

- 790 mg Tris base and 900 mg NaCl was added to 75 ml of distilled H2O.
- The solution was then stared and until all the solids were dissolved and then the pH was adjusted to 7.4
- 10 ml of 10% NP-40, 2.5 ml of 10% Na-deoxycholate and 1 ml of 100 mM EDTA was added and solution was stirred until it became clear
- The volume was then adjusted to 100 ml and the RIPA aliquots were stored at 2-8°C.

- The following inhibitors were added on the day of cell harvesting: 1µl of aprotonin, 1µl of leupeptin, 5µl Na_3VO4, NaF, benzamidine, PMSF (added just before cell harvesting) and 10µl pepstatin

5. Bradford

- 500mg of Coommasive brilliant blue G250 was mixed with 250ml of 95% ethanol
- 500ml of phosphoric acid was then added to this solution
- The stock solution was covered in foil the filtered 3 times using a double layer of filter paper
- 200ml of the stock was then diluted with 800ml of water and this filtered 3 times to make a working solution
- The working solution covered with foil and was stored at room temperature.
- The stock was stored at 4^{o}C

6. Laemmli's loading buffer

dH_2O	3.8 ml
0.5MTris-HCl, pH 6.8	1.0 ml
Glycerol	0.8 ml
10%(w/v) SDS	1.6 ml
0.05% (w/v) Bromophenol blue	0.4 ml

7. Western blot gel preparation

- The stacking gel and the 10% and 15% resolving gels in this study was prepared according to the following table:

8. 10x TBS

- 24.23g Tris-base
- 87.66g NaCl

9. 1x TBS-T

- 200ml of 10x was transferred into 1800mL of dh_2O followed by addition of 2ml of TWEEN to make a 1x TBST working solution.

10. Stripping buffer (0.2 M NaOH)

$$mass = C\ x\ v\ x\ M$$

$$mass = 0.2M\ x\ 1L\ x\ 39.997g/mol$$

Mass = 7.9994g

- 8g of NaOH was dissolved in 1L of dh_2O to make a 0.2 M solution of NaOH

11. 1X PBS

- 16g NaCl
- 0.9g KCl
- 2.88g Na_2HPO_4
- 0.48g KH_2PO_4
- pH = 7.4

12. Rapamycin preparation

Rapamycin working solution for 50nM dose

$$V1 = \frac{C2\ x\ V2}{C1}$$

$$V1 = \frac{50nM\ x\ 10\ ml}{2.74mM}$$

V1= $0.182x10^{-6}$

0.182µL and 0.091µL was transferred into 10ml of culture medium to make a 50nM and 25nM working solution

13. Bafilomycin preparation

- *Making of 200µM stock*

$$mass = C\ x\ v\ x\ M$$

$$mass = 200mM\ x\ 1mL\ x\ 622.83$$

Mass = 0.125 mg

- 0.25mg of bafilomycin was dissolved in 1ml of DMSO to make a 200mM stock

- *Bafilomycin working volume*

$$V1 = \frac{C2\ x\ V2}{C1}$$

$$V1 = \frac{5\mu M\ x\ 50ml}{200mM}$$

V1= 1.75 µL

- 1.25 µl was transferred into a 50ml of culture medium to make a 5nM working solution.

14. Saponin

- 1mg of saponin was dissolved in 1ml of 70% ethanol
- 20µl of this solution was then transferred into oxigraph chamber to permeate cells

15. Carbonyl cyanide-p-trifluoro-methoxy-phenylhydrazone (FCCP)

- *Preparation of 1mM stock solution*

$$mass = C\ x\ v\ x\ M$$

$$mass = 1mM\ x\ 1mL\ x\ 254.17$$

Mass = 0.25mg

- 0.25mg of FCCP was dissolved in 1ml of DMSO to make a 1ml stock solution

- *Working FCCP volume*

$$V1 = \frac{C2\ x\ V2}{C1}$$

$$V1 = \frac{10\mu M\ x\ 1\ ml}{1mM}$$

V1= 10µL

- 10µl of FCCP was transferred into oxigraph chamber to depolarise mitochondria as a means to assess normal mitochondrial function following oxigraph analysis

16. MitoPerOX

- *Preparation of 1mM stock solution*

$$C = \frac{m}{M} / V$$

$$mass = \frac{1mg}{504.4255} / 1mL$$

C = 1.982mM

- 1mg of MitoPerOX was dissolved in 1ml of 100% ethanol to make a 1.982mM of stock

- *Working MitoPerOX volume*

$$V1 = \frac{C2\ x\ V2}{C1}$$

$$V1 = \frac{5\mu M\ x\ 1\ ml}{1.982mM}$$

V1= 2.5µL

- 2.5µl of MitoPerOX was transferred into each 1ml of cell suspension before be submitted to flow analysis

APPENDIX D: REAGENTS

CHEMICALS	COMPANY	CATALOG NUMBER
2-isopropanol	Merck	1-09634-2500
ADP	Sigma	01905
Amino acid free medium (Serum free, Hanks balanced salt solution)	ThermoFisher Scientific	24020-117
Ammonium persulphate (APS)	Sigma	A3678
Aprotonin	Sigma	A1153
Bafilomycin	LKT laboratories	BOO25
Benzamidine	Sigma	B6506
Bio rad 10x tris/glycine buffer	Bio-Rad	1610771
Bovine serum albumin	Roche	10735078001
Caspase-Glo 3/7 assay	Promega	G8091
Coomassie brilliant blue G250	Merck	42655
Cyanide-p-trifluoro-phenylhydazone (FCCP)	Sigma	C2920
Dako fluorescent mounting medium	Diagnostech	S302380
Disodium hydrogen phosphate (Na_2HPO_4)	Sigma	S3264
DMEM	ThermoFisher Scientific	41965-039
DMSO	Sigma	D2650
Doxorubicin	Sigma	D1515
ECL	Bio-Rad	170-5061
EDTA	EDS	Sigma
Fetal bovine serum	Biocom Biotech	FBS-G1-12A
Hiperfect transfection reagent	Qiagen	301705

Hoechst	Sigma	B2261
Isobutanol	Merck	UN1212
JC-1	ThermoFisher Scientific	T3168
Leupeptin	Sigma	L2884
Magnesium chloride ($MgCl_2$)	SARchem	4123000
MitoPerOX	ThermoFisher Scientific	D3861
Mitotracker	ThermoFisher Scientific	M7514
Monopotassium phosphate (KH_2PO_4)	AnalaR	BB102034B
MOPS	Sigma	M1254
mTOR siRNA	Cell Signalling	6381
Na-deoxycholate	Sigma	D6750
NP-40	Sigma	7438S
Paraformaldehyde	Sigma	158127
Pen/strep	ThermoFisher Scientific	15140-122
Pepstatin A	Sigma	P5318
Phosphoric acid	Merck	P5811
PMSF	Roche	10 837 091 011
Potassium Chloride (KCL)	Merck	K310 3036 944
Precision plus protein "Dual colour standard"	Bio-Rad	161-0374
Rapamycin	Sigma	R8781
Retinoic acid	Sigma	R2625
Saponin	Sigma	47036
Signal Silence Control siRNA	Cell Signalling	6201S
Sodium Chloride (NaCl)	Sigma	S7653
Sodium Dodecyl Sulphate (SDS)	Sigma	L3771
Sodium fluoride	Sigma	S7920

Sodium orthivanadate (Na_3VO_4)	Sigma	S6508
Succinic acid	Sigma	S3674
Sucrose	Sigma	S0389
TEMED	Sigma	T9281
Tris-base	Merck	648310
Triton	Sigma	X-100
Trypsin-EDTA	ThermoFisher Scientific	25200-072
WST-1	Abcam	Ab155902

ANTI-BODIES	**COMPANY**	**CATALOG NUMBER**
Alexa flour 488-goat anti-mouse secondary anti-body	ThermoFisher Scientific	A11029
Anti-rabbit HRP secondary anti-body	Cell Signalling	70745
Cardiac troponin T	Abcam	11C11
Caspase-3	Cell Signalling	96645S
GAPDH	Cell signalling	S1745
LC3	Cell Signalling	41085
p-mTOR	Cell Signalling	7C10
mTOR	Cell Signalling	2983S
Myosin Light chain	Cell signalling	D5I1C
p62	Abcam	Ab91526
p-mTOR	Cell Signalling	S2448

HARDWARE	COMPANY	CATALOG NUMBER
15 ml Falcon tubes	Biocom biotech	50015
24 well plates	White Scientific	500021
48 well plates	Biocom biotech	30048
50 ml Falcon tubes	Biocom biotech	50050
6 well plates	Biocom Biotech	30006
Cell Scrappers	LASEC	PGRE541070
Coverslips	Sigma	S1815
Histology slides	Sigma	S8400
T175 culture flasks	White Scientific	500031
T25 culture flasks	White Scientific	500033
T75 culture flasks	White Scientific	TPP-90075
PDVF transfer packs	Bio-Rad	170-4156